Fall 12-2010

# Microvariability of the Blazar 3C279

Hannah M. Clemmons
*Georgia State University*

] [] (D. Michael Crenshaw) (Ben Q. McGimsey)

# Microvariability of the Blazar 3C279

A Thesis

Submitted in Partial Fulfillment of Requirements for the Degree of

Master of Science

in the College of Arts and Sciences

Georgia State University

2010

by

Hannah Marine Clemmons

Committee:

---

Dr. H. Richard Miller, Chair

---

Dr. Ben Q. McGimsey, Member

---

Dr. D. Michael Crenshaw, Member

---

Date

---

Dr. H. Richard Miller, Chair
Department of Physics & Astronomy

# Microvariability of the Blazar 3C279

by

Hannah Marine Clemmons

Under the Direction of H. Richard Miller

## Abstract

Active Galactic Nuclei (AGN) are some of the most extreme objects in the universe. They output copious amounts of energy spanning the entire electromagnetic spectrum. There are many different subclasses of AGN depending on your viewing angle. Blazars, viewing down the relativistic jet, are the most variable class of AGN known. They exhibit extreme variability in all wavelengths on timescales as short as minutes. In this thesis I will consider the extreme faintness of 3C279 with respect to the long-term light curve as well as recent observations of microvariability. I am able to confirm small amplitude events using simultaneous observations from two telescopes and cross correlation analysis. Transitory quasi-periodic oscillations are observed during two of the nights with confirmed microvariability.

INDEX WORDS: Active galactic nuclei, Blazars, 3C279, Microvariability

# Microvariability of the Blazar 3C279

by

Hannah Marine Clemmons

A Thesis Submitted in Partial Fulfillment of Requirements for the Degree of

Master of Science

in the College of Arts and Sciences

Georgia State University

2010

# Microvariability of the Blazar 3C279

by

Hannah Marine Clemmons

| | |
|---|---|
| Committee Chair: | H. Richard Miller |
| Committee: | Ben Q. McGimsey |
| | D. Michael Crenshaw |

Electronic Version Approved:

Office of Graduate Studies

College of Arts & Sciences

Georgia State University

December 2010

To my mother

Thank you for being my hero.

# Acknowledgments

This process is one of long nights squinting at the computer, and at times, trying to figure out which way is up. I would like to thank my husband, Jimmy, for being right beside me many of those long nights. You reminded me to eat when it had been more than 12 hours and always kept my cup full of coffee. Without complaint, you have stood behind me pushing me along and picking me up when I fell. Thank you is not enough for all that you have done.

Thank you to my advisor, Dick Miller, for setting me on this task. This began as an ordinary research project and has blossomed into an extrodinary experience. Thank you to my committee, Mike Crenshaw and Ben McGimsey, for your suggestions, attention to detail, and patience. The various data for this thesis were gathered by my fellow PEGAns. Thank you Joe and Jeremy for getting me into this mess! You guys got me started on this path by showing me the ropes. A special thank you to Rob Parks for helping me survive graduate school. Your insight and advice saved me hours of frustration and disappointment.

Since middle school, there has been one friend who has never left my side. Mallory, your courage and spirit inspire me to reach for things I have never believed possible. You have repeatedly refused to let me fail. You are my dream bearer.

For the 24 years before Jimmy, there was my family, my personal cheerleading squad. You knew I could do it and did not let me quit. Every time I came to a bump in the road, your love and support carried me across. I know you will always be there.

# Table of Contents

Acknowledgments . . . . . **v**

List of Tables . . . . . **viii**

List of Figures . . . . . **ix**

Abbreviations and Acronyms . . . . . **xi**

**1 Introduction . . . . . 1**

1.1 Active Galactic Nuclei . . . . . 1

1.1.1 Current Model . . . . . 1

1.1.2 AGN Taxonomy . . . . . 3

1.1.3 Radio Loud vs Radio Quiet . . . . . 5

1.2 Blazars . . . . . 5

1.2.1 Viewing Angle and Spectra . . . . . 5

1.2.2 Classification . . . . . 6

1.2.3 Spectral Energy Distribution . . . . . 6

1.2.4 Variability . . . . . 7

**2 Observations & Data Reduction . . . . . 9**

2.1 Observations . . . . . 9

2.1.1 Telescopes and Cameras . . . . . 9

2.1.2 Data Acquisition . . . . . 10

2.2 Data Reduction . . . . . 12

2.2.1 IRAF . . . . . 12

2.2.2 CCDPHOT . . . . . 13

2.2.3 Error Analysis . . . . . 14

2.3 The Dataset . . . . . 15

**3 Results & Analysis . . . . . 38**

3.1 Results . . . . . 38

3.1.1 Long-Term Light Curve . . . . . 39

3.1.2 Recent Light Curves . . . . . 40

3.2 Analysis . . . . . 51

3.2.1 Cross Correlation Function . . . . . 52

3.2.2 Possible Periodicity . . . . . 57

3.2.3 Color Variability . . . . . 72

**4 Conclusions & Future Work . . . . . 73**

4.1 Conclusions . . . . . 73

4.2 Future Work . . . . . 75

**References . . . . . 77**

**Appendices . . . . . 79**

**A Comparison Stars for 3C279. . . . . 80**

**B Light Curve for 14 April 2010. . . . . 82**

**C Light Curve for 15 April 2010. . . . . 87**

# List of Tables

1.1 AGN Structure Size and Velocity . . . . . 2

1.2 AGN Type and Orientation . . . . . 3

2.1 Telescope and CCD Specifications . . . . . 10

2.2 Long-Term Data for 3C279 in R-Filter . . . . . 16

2.3 Recent Data for 3C279 R-Filter . . . . . 20

2.4 Recent Data for 3C279 V-Filter . . . . . 30

A.1 Comparison Star Information . . . . . 80

# List of Figures


1.1 Geometry of AGN. . . . . 4

1.2 Typical Blazar SED . . . . . 7

1.3 SED of 3C279. . . . . 7

3.1 Long-Term Light Curve of 3C279 . . . . . 39

3.2 Light Curve for 10-15 April 2010 . . . . . 41

3.3 Observations from 10 April 2010 V-Filter. . . . . 43

3.4 Observations from 10 April 2010 R-Filter. . . . . 44

3.5 Observations from 11 April 2010 V-Filter. . . . . 46

3.6 Observations from 11 April 2010 R-Filter. . . . . 47

3.7 Observations from 12 April 2010 V-Filter. . . . . 49

3.8 Observations from 12 April 2010 R-Filter. . . . . 50

3.9 Cross Correlation for 10 April 2010. . . . . 53

3.10 Cross Correlation for Pieces of 10 April 2010. . . . . 54

3.11 Cross Correlation for 11 April 2010. . . . . 55

3.12 Cross Correlation for Pieces of 11 April 2010. . . . . 56

3.13 Cross Correlation for 12 April 2010. . . . . 58

3.14 Cross Correlation for Pieces of 12 April 2010. . . . . 59

3.15 Detrending for R-Filter Observations on 12 April 2010. . . . . 61

3.16 Periodigram for R-Filter Observations on 12 April 2010. . . . . 61

3.17 Phased Data for R-Filter Observations on 12 April 2010. . . . . 62

3.18 Detrending for V-Filter Observations on 12 April 2010. . . . . 63

3.19 Periodigram for V-Filter Observations on 12 April 2010. . . . . 63

3.20 Phased Data for V-Filter Observations on 12 April 2010. . . . . 64

3.21 Detrending for R-Filter Observations on 11 April 2010. . . . . 65
3.22 Detrended Data for R-Filter Observations on 11 April 2010. . . . . 65
3.23 Periodigram for all of the R-Filter Observations on 11 April 2010. . . . . 66
3.24 Periodigram for R-Filter Observations on 11 April 2010. . . . . 67
3.25 Phased Data for R-Filter Observations on 11 April 2010. . . . . 67
3.26 Detrending for V-Filter Observations on 11 April 2010. . . . . 68
3.27 Detrended Data for V-Filter Observations on 11 April 2010. . . . . 69
3.28 Periodigram for All of the V-Filter Observations on 11 April 2010. . . . . 70
3.29 Periodigram for Detrended V-Filter Observations on 11 April 2010. . . . . 70
3.30 Phased Data for V-Filter Observations on 11 April 2010. . . . . 71
3.31 Color Variability for 10-15 April. . . . . 72

4.1 Event Observed for 3C279 in High State 10 May 1989. . . . . 74

A.1 Finding Chart for 3C279. . . . . 81

B.1 Observations from 14 April 2010 V-Filter. . . . . 83
B.2 Observations from 14 April 2010 R-Filter. . . . . 84
B.3 Cross Correlation for 14 April 2010. . . . . 85
B.4 Cross Correlation for Pieces of 14 April 2010. . . . . 86

C.1 Observations from 15 April 2010 V-Filter. . . . . 88
C.2 Observations from 15 April 2010 R-Filter. . . . . 89
C.3 Cross Correlation for 15 April 2010. . . . . 90
C.4 Cross Correlation for Pieces of 15 April 2010. . . . . 91

## Abbreviations and Acronyms

| | |
|---|---|
| **ACF** | Auto Correlation Function |
| **AGN** | Active Galactic Nucleus |
| **CCD** | Charged Couple Device |
| **CCF** | Cross Correlation Function |
| **FAP** | False Alarm Probability |
| **FIR** | Far Infrared |
| **FITS** | Flexiable Image Transport System |
| **FR I** | Fanaroff-Riley Type I |
| **FR II** | Fanaroff-Riley Type II |
| **FWHM** | Full Width at Half Maximum |
| **GSU** | Georgia State University |
| **IDL** | Interactive Data Language |
| **IRAF** | Image Reduction and Analysis Facility |
| **JD** | Julian Date |
| **LNP** | Lomb Normalized Periodogram |
| **OVV** | Optically Violent Variable |
| **PEGA** | Program in Extragalactic Astronomy, Georgia State University |
| **PSD** | Power Spectral Density |
| $\mathbf{R}_s$ | Schwarzschild Radius |

| | |
|---|---|
| **SED** | Spectral Energy Distribution |
| **SMBH** | Supermassive Black Hole |
| **S/N** | Signal to Noise Ratio |

# – 1 –

# Introduction

## 1.1 Active Galactic Nuclei

When considering the most violent and variable objects in the universe, AGN would rank near the top of the list with sustained emission observable in every wavelength. Unfortunately, current technology is unable to resolve the inner core so we must rely on changes in brightness or spectral lines for hints as to what processes are occurring. There are several different types of AGN, but characteristics often include an optically stellar appearance, ultraviolet excess, continuum flux variability, broad emission lines, and large redshifts (Schmidt 1968).

### 1.1.1 Current Model

AGN are central to understanding the mysteries of cosmology, the early universe, and high-energy physics. Unfortunately, these objects are still quite mysterious. AGN are likely a phase galaxies go through as opposed to a permanent characteristic (Urry 2003). With varying intrinsic properties and orientations, these objects remain quite difficult to understand. They output enormous amounts of energy spanning the entire range of the electromagnetic spectrum. The inability to resolve the core leaves us piecing together the geometry from what can be observed.

The most accepted theory of the geometry of AGN is described in a paper by Holt et al. 1992. By observing AGN in wavelengths spanning the entire electromagnetic spectrum,

we have been able to construct a working model. The observed emission is believed to be originating from the vicinity of the supermassive black hole and its surrounding accretion disk. Gravitational potential energy is the driving force in the luminosity of the AGN. A dusty, optically thick, torus blocks the fast moving broad line clouds from most viewing angles. Farther out, the slower moving narrow line clouds reside. For radio-loud AGN, the torus and strong magnetic field lines help to collimate radio jets full of high-energy plasma, streaming out to large distances.

TABLE 1.1: AGN Structure Size and Velocity[a]

| **Component of AGN** | **Size** | **Velocity** |
|---|---|---|
| Black Hole | $10^{-7}$-$10^{-3}$ pc | ... |
| Accretion Disk | $10^{-3}$ pc | ... |
| Broad Line Region | Out to $\sim$1 pc | $\sim$5000 km s$^{-1}$ |
| Dusty Torus | 1-10 pc | ... |
| Narrow Line Region | $\gtrsim$100 pc | $\sim$500 km s$^{-1}$ |
| Jets (Radio Loud) | Formed w/in 100 R$s$ extending out to a Mpc | $\sim$0.995c |

[a] From Blandford (1990) and Peterson (1997)

### 1.1.2 AGN Taxonomy

It took several years from the discovery of AGN (in 1908 by E.A. Fath) for the astronomical community to believe all of these creatures could be the same monster (attempts to unify radio-loud and radio-quiet by Scheuer and Readhead in 1979). Observationally, they looked very different. Some galaxies had a much higher flux in the radio than others. Broad lines were seen in the spectra of Seyfert 1s, but not in Seyfert 2s. BL Lacs had no emission or absorption lines where OVVs had very broad ones. We now believe the observational differences result from the different possible viewing angles, not from intrinsic characteristics of the AGN. Figure 1.1 offers a visual representation of the geometry of AGN as well as a possible unification scheme.

TABLE 1.2: AGN Type and Orientation[a]

| **Radio Property** | **Orientation** | |
|---|---|---|
| | **Face-On** | **Edge-On** |
| Radio Loud | BL Lac | FR I |
| | Quasar/OVV | FR II |
| | BLRG | NLRG |
| Radio Quiet | Seyfert 1 | Seyfert 2 |
| | QSO | FIR Galaxy |

[a] From Peterson (1997). OVV- Optically Violent Quasar, FR I/II- Fanaroff Riley type 1/2, BLRG- Broad Line Radio Galaxy, NLRG- Narrow Line Radio Galaxy, QSO- Quasi-Stellar Object, FIR- Far Infrared.

Many different classes of AGN exist today and efforts are ongoing to create a unification model that will bring order to this galactic zoo. Table 1.2 groups the galaxies into a more readable form by orientation and radio loudness.

As part of the unification campaign, many studies have been done in the last decade attempting to relate black hole mass, AGN luminosity, radio loudness, and Eddington ratio (Urry 2004).

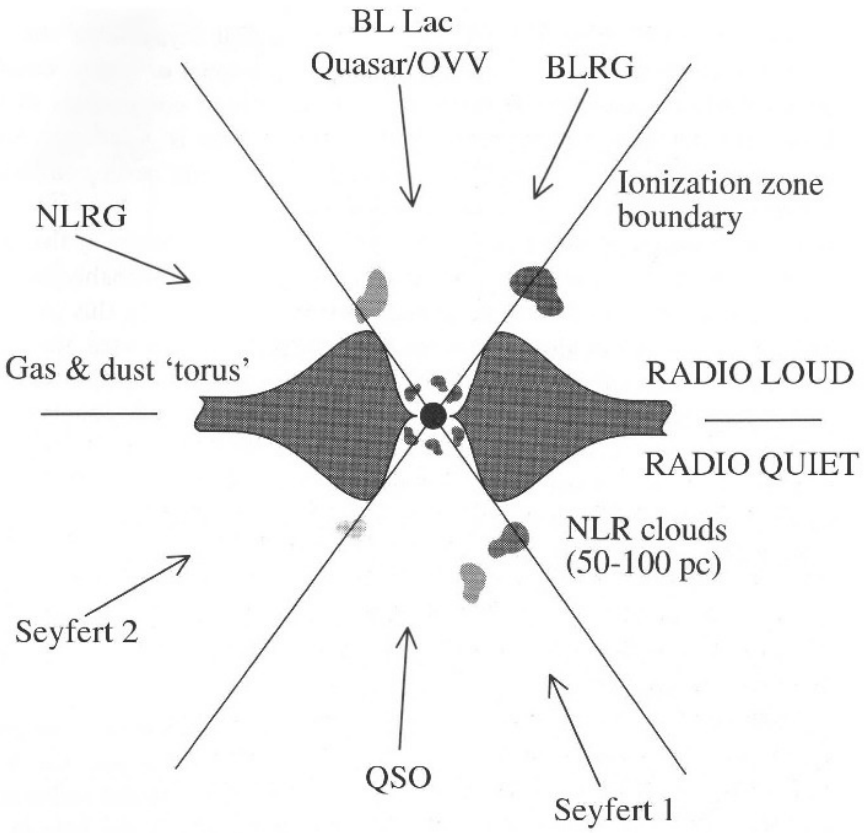


FIGURE 1.1: Illustration of the unified model of AGN (Urry & Padovani 1995). Figure adapted from McFarland (2005)

### 1.1.3 Radio Loud vs Radio Quiet

As seen above, radio loudness is one of the primary dividers of AGN that cannot be accounted for by viewing angle. Radio-loud is commonly defined as an AGN with the ratio of monochromatic flux at 5 GHz to that at 5000 Å as being greater than 10. Anything less is, therefore, radio-quiet.

What causes this seemingly intrinsic difference? There are two theories. One theory is that radio-loud and radio-quiet really are two different types of AGN with some real intrinsic difference. The other theory is they are the same type of object, but in the radio-quiet case, the jet is being suppressed. Jet power and host galaxy density are proposed reasons for the suppression (Urry 2004).

## 1.2 Blazars

Blazars are known to be the most violent and variable class of AGN. The large, rapid variations in flux help probe the complex workings of the central engine and put physical constraints on the source producing what we observe.

### 1.2.1 Viewing Angle and Spectra

Blazars are radio-loud AGN with the observer's line-of-sight aimed directly along, or within a few degrees of, the collimated jet. Generally, blazars have no significant emission or absorption features. The radiation from the relativistically boosted jet overpowers any features that might be present. A smooth, non-thermal continuum is observed with extreme variability in flux across all wavelengths. When compared to a star's continuum, a blazar exhibits

an infrared and ultraviolet (UV) excess. Another signature of a blazar is variability in the polarization, which can be high (up to ∼20%) (McFarland 2005).

One might be concerned about contamination of different sorts by the host galaxy. This is believed to pose no problem for the subject of this thesis, 3C279, being at z=0.536 with a lack of discernable stellar features.

### 1.2.2 Classification

Blazars can be further divided into two classes: OVV quasars and BL Lacs (named after the prototype, BL Lacertae). OVV quasars have very broad (equivalent width greater than 5 Å) emission lines in the low luminosity state (Urry 1999b). In a high luminosity state they are indistinguishable from BL Lacs.

Another approach to classifing blazars is using the shape of their Spectral Energy Distribution (SED). Radio selected (RBL) and x-ray selected (XBL) blazars differ by the wavelength in which the synchrotron bump occurs. This will be discussed more in Section 1.2.3.

### 1.2.3 Spectral Energy Distribution

The SED of blazars is double peaked. The first peak is synchrotron radiation from electrons spiraling around magnetic field lines. The second peak is due to inverse-Compton scattering. The seed photons for this process are unclear in origin. They could be from the same electrons involved in the synchrotron emission (synchrotron self-Compton) or they could be from UV/X-ray photons from the accretion disk (external Compton). For BL Lacs, the synchrotron self-Compton process is most likely the cause of the second bump (Urry 1999a).

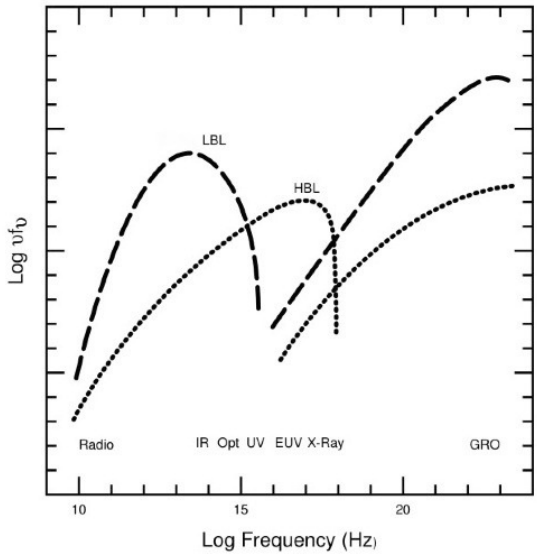


FIGURE 1.2: The SED of a typical blazar has two bumps. The location of these bumps varies depending on whether it is a LBL (low frequency peaked BL Lac), a.k.a "red" BL Lac (RBL), or a HBL (high frequency peaked BL Lac), a.k.a "blue" BL Lac (XBL). Figure from Urry (1999a)

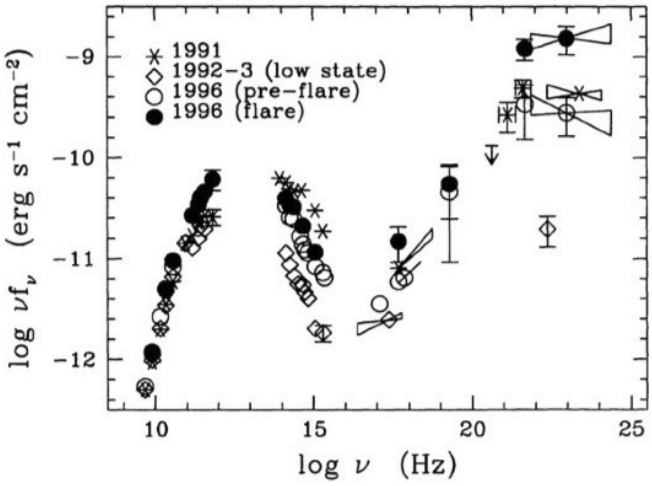


FIGURE 1.3: The SED of 3C279 in quiescent and flare states (Urry 1999a). It is clear the peaks of this blazar occur close in frequency to those of a LBL.

### 1.2.4 Variability

As previously stated, blazars vary on all timescales across the electromagnetic spectrum. In the optical regime, long-term lightcurves can show changes of ∼5 magnitudes (McFarland

2005). Carini (1990) noted microvariability can produce average changes of ∼0.01 magnitude in an hour. Therefore, for one object, an observing time of at least three hours must be obtained to detect intraday variability.

The most likely culprit for variability in blazars is fluctuations in the jet. This can be manifested in several different ways. Long-term variability is likely caused by a change in the internal energy of the jet flow or precession of the jet, both would cause shocks to propagate down the jet. Microvariability is likely caused by turbulence in the jet. This is not surprising considering the high flow velocity compared to the surrounding medium (Marscher 1996).

Relativistic motion is boosting all of these events, shortening the observed time of events and increasing the observed amplitude, acting as a magnifying glass. With all of these events happening simultaneously, it is no wonder lightcurves are difficult to analyze!

# – 2 –

# Observations & Data Reduction

## 2.1 Observations

Observations of blazar microvariabilty necessitate high temporal sampling and high photometric precision. This is especially difficult for ground based optical observations. Sampling frequency is constrained by scheduling, weather, and instrument failures/maintenance. Large trends can be seen over months to years, but confirmation of microvariabilty requires observations to be made on the time-scale of hours to minutes. The monitoring of 3C279 reported here spans 39 years, with, in some instances, a temporal resolution as short as minutes.

### 2.1.1 Telescopes and Cameras

The data for this thesis were acquired at Lowell Observatory using multiple telescopes. Lowell is home to the 1.8m (72") Perkins telescope, the 1.07m (42") Hall telescope, and the 0.79m (31") telescope. All three of these telescopes were utilized to make the long-term light curve shown in Figure 3.1.

All images were taken using direct CCD (Charged Coupled Device) imaging. The specifications of the CCD for each telescope are listed in Table 2.1.

TABLE 2.1: Telescope and CCD Specifications

| **Telescope** | **CCD** | **Chip Size** (Pixels) | **Gain** ($e^-$/ADU) | **Noise** ($e^-$) |
|---|---|---|---|---|
| Perkins 1.8m | Fairchild | 2048×2048 | 3.3 | 13 |
| Hall 1.07m | SITe | 2048×2048 | 3.9 | 11 |
| Lowell 0.79m | Thompson | 512×512 | 5.0 | 5.0 |

### 2.1.2 Data Acquisition

Ensuring a proper field of view is one of the most important steps to a productive observing run. Differential photometry requires the target of investigation and comparison stars to be located relatively close together in the sky. It is also important that the comparison stars cover the expected range in magnitude of variability for the object.

The target and comparison stars must fit in the same field of view of a CCD chip. The utilization of CCD's in the field of astronomy has significantly increased the precision of differential photometry. Even under non-photometric conditions, precise, reliable observations can be made. Since the field of view ($20' \times 20'$maximum) cuts through a small portion of the sky any type of variable extinction (ex. cloud cover) would affect the whole field, comparisons stars and target, equally. By increasing the integration time in these situations, the signal to noise can be kept at an acceptable level. Typical exposure times for this object in a very faint state (R=17.6) is 300 sec.

Ideally the magnitude of the comparision stars and the object would be nearly equal, making the error calculation straightforward. Suppose V is the magnitude of the target and C and K are the magnitudes of two comparison stars. If they are all equal in magnitude then the variance in the C-K light curve would also characterize the error in the V-C light curve. Unfortunately this senario is very rare. A second best situation would be if C and K could be chosen such that K is about equal to V and C is brighter than both V and K (K≈V>C). Howell et al. (1988) shows this arrangement gives a scaling factor ($\Gamma^2$) of approximately 1 and equal variance in the light curves of V-C and C-K. Again, this is an infrequent occurrence. The variance is the standard deviation squared and is defined as

$$\sigma^2_{V-C} = \sigma^2_{V-C}(VAR) + \sigma^2_{C-K}(INST) \tag{2.1}$$

where the first term indicates the variance arising from the variability of V and the second term includes the variance from all other sources. Howell et al. (1988) also demonstrates how to calculate $\Gamma^2$ when neither of the previously mentioned arrangements are possible. $\Gamma^2$ is defined as

$$\Gamma^2 = \frac{\sigma^2_{V-C}(INST)}{\sigma^2_{C-K}} \tag{2.2}$$

$\Gamma^2$ scales the variance in C-K to describe the variance in V-C. To do this the characteristics of the CCD chip, size of the aperature, and photon counts of V, C, K and sky must all be known. It is assumed that C and K have no intrinsic variability. The amount of variance in these light curves serves as a tool to analyze the photometric precision and presence of variability on all timescales.

For each night, multiple biases and flats in the filters of observations of the target must be taken. These basic images help to limit the effects of the instrumentation on the final data. The bias frame accounts for the overall charge level of the chip. The flat frame effectively maps the efficiency of each pixel and must be obtained in each filter for which the object will be observed. Darks were not taken since they are not necessary for the liquid nitrogen cooled CCD's at Lowell Observatory.

## 2.2 Data Reduction

The reduction process is the final step to having usable data. It is also the part of the process where mistakes are easily made. In the last 15 years, many scripts and programs have been written by various students in the Georgia State University (GSU) PEGA (Program in Extragalactic Astronomy) team to help reduce user errors and standardize the process.

### 2.2.1 IRAF

The raw data are fed into IRAF (Image Reduction and Analysis Facility) where the script, *pegaproc*, is performed on all of the images. This script begins by combining the multiple biases and flats from each night into a median bias and a median flat (one per filter). The overscan areas are trimmed and random, inconsistent pixel values are removed automatically during this step.

To process the object images for useful photometry they must be bias-subtracted and flat-fielded. Before this can be done the median flat image must be bias-subtracted so that bias error is not reintroduced when the object images are flat-fielded. Bias-subtraction is

exactly as sounds: the median bias is subtracted from the raw image, either median flat or the object image in this case.

After bias-subtracting the target images, they are flat-fielded. This is done by dividing the image by the bias-subtracted, median flat-field in the appropriate filter. Finally the images are cleaned of cosmic rays. The *pegaproc* script has taken the images from raw to processed form and are now ready for photometry.

### 2.2.2 CCDPHOT

Marc Buie of Lowell Observatory wrote CCDPHOT in IDL (Interactive Data Language) as a program to perform photometry on FITS (Flexiable Image Transport System) images. The program uses synthetic apertures and concentric annuli to mimic multi-aperture photometry. This setup allows photometry to be performed on multiple objects in the field of view. Magnitudes of comparison stars and targets are measured simultaneously correcting for the effects of airmass and extinction since the field of view intercepts only a small area of the sky. From frame to frame a centering algorithm is used, so reestablishing the anchor points is not necessary, making this program relatively expeditious. The output of CCDPHOT (.log file) lists each object on its own line containing: image number, image type, filter, Julian date, exposure time, aperture, full width at half maximum (FWHM), photon counts, and instrumental magnitude.

A comprehensive script, *lcgen*, was created by Jeremy Maune of GSU's PEGA team to format the information properly and create a light curve complete with error bars. This program is a much more robust composition of several smaller scripts written by McFarland

(2005), detailed descriptions of which can be found in his dissertation. Section 2.2.3 describes this process in more detail.

### 2.2.3 Error Analysis

The biggest obstacle for confirming microvariability is the over- or underestimation of error. Before running *lcgen*, a (.comp) file must be made listing the comparison stars with their apparent magnitudes and error. The PEGA website provides finding charts with links to the magnitudes of comparison stars for all of the blazars in the PEGA monitoring program. When running *lcgen* from IDL, all of the following steps happen without interruption.

The first step is converting the information into a usable format. The data are converted from one line of information per object per frame (as described in Section 2.2.2) to one line containing all the information for each frame. The previous script for this action was *pegasort*. The one line of the new (.txt) file contains: image number, filter, Julian date, exposure time, aperture, and object type specific information such as FWHM, photon counts, and instrumental magnitude.

Next, the instrumental magnitude is converted to the actual magnitude using the previous script *pegacalib*. To do this the overall sky brightness must be removed and a correction made for the Earth's atmospheric transmission. For differential photometry this is easily done. Given

$$V_o = V_{io} - kX \tag{2.3}$$

where $V_o$ is the magnitude of the object outside of the Earth's atmosphere, $V_{io}$ is the instur-mental magnitude, k is the extinction coefficent, and X is the airmass during observation. This relationship is true for any object in the field.

$$V_c = V_{ic} - kX \tag{2.4}$$

where $V_c$ is the magnitude of the comparison star outside of the atmosphere. Since neither airmass nor extinction change across the frame, it can be written

$$V_o - V_c = V_{io} - V_{ic} \tag{2.5}$$

An important point this relationship makes is the difference in instrumental magnitude is equal to the difference in apparent magnitude. Thus,

$$V_o = V_c + V_{io} - V_{ic} \tag{2.6}$$

A third term in (2.3) includes color difference as a function of airmass. Carini (1990) confirmed the work by Hardie (1962) stating that, in most cases, this term can be neglected.

The error measurements for the actual apparent magnitudes are calculated using the scaling factor method presented in Section 2.3.

### 2.3 The Dataset

The data for 3C279 come from the PEGA archive, Pica et al. (1980), and unpublished data belonging to H. Richard Miller. The earliest observations begin in 1971. Almost all of the PEGA archival data were taken in the R-filter and are listed in Table 2.2. There

were two data points omitted from this table. Both were from March 2008 with one point indicating an extreme increase in brightness (R magnitude=8) and the other indicating an impossible decrease in brightness (R magnitude=90). Neither had a second point to verify the possibility of such an excursion. The data obtained from Pica et al. (1980) were primarily photographic data and required conversion to R magnitudes as discussed in Section 3.1.1. The magnitudes pertaining to the data belonging to Miller were V magnitudes and their conversion is also discussed in the same section. The epoch is given in column 1, the nightly average R magnitude is given in column 2, and the range in R magnitude for the night is given in column 3.

TABLE 2.2: Long-Term Data for 3C279 in R-Filter

| **UT Date** | **Average Magnitude** | **Magnitude Range** |
|---|---|---|
| 26 May 71 | 16.93 | 16.93-16.93 |
| 10 Mar. 72 | 16.52 | 16.52-16.52 |
| 13 Mar. 72 | 16.36 | 16.36-16.36 |
| 11 Apr. 72 | 16.71 | 16.71-16.71 |
| 10 Jun. 72 | 16.35 | 16.35-16.35 |
| 10 Mar. 73 | 16.13 | 16.13-16.13 |
| 14 Apr. 74 | 15.95 | 15.95-15.95 |
| 19 Apr. 74 | 15.94 | 15.94-15.94 |
| 17 Apr. 75 | 16.45 | 16.45-16.45 |
| 29 Mar. 76 | 15.29 | 15.29-15.29 |
| 28 Jan. 77 | 16.68 | 16.68-16.68 |
| 29 Mar. 77 | 17.30 | 17.17-17.42 |
| 15 Apr. 77 | 17.75 | 17.62-17.88 |
| 08 Jun. 77 | 17.38 | 17.38-17.38 |
| 19 Jun. 77 | 17.39 | 17.19-17.59 |
| 20 Jun. 77 | 17.64 | 17.64-17.64 |
| 21 Jun. 77 | 17.45 | 17.28-17.62 |
| 12 Feb. 78 | 17.40 | 17.40-17.40 |

Continued on Next Page...

TABLE 2.2 – Continued

| UT Date | Average Magnitude | Magnitude Range |
|---|---|---|
| 15 Feb. 78 | 17.55 | 17.55-17.55 |
| 12 Apr. 78 | 17.71 | 17.71-17.71 |
| 28 Apr. 78 | 17.40 | 17.40-17.40 |
| 29 May 78 | 16.81 | 16.81-16.81 |
| 11 Dec. 78 | 16.69 | 16.69-16.69 |
| 28 Feb. 79 | 17.17 | 17.17-17.17 |
| 21 Mar. 79 | 17.32 | 17.32-17.32 |
| 30 Mar. 79 | 17.56 | 17.56-17.56 |
| 21 Apr. 79 | 17.15 | 17.15-17.15 |
| 30 May 79 | 17.34 | 17.34-17.34 |
| 17 Jan. 80 | 16.04 | 16.04-16.04 |
| 22 Feb. 80 | 15.95 | 15.95-15.95 |
| 15 May 80 | 16.15 | 16.15-16.15 |
| 17 May 80 | 16.26 | 16.26-16.26 |
| 21 May 80 | 16.20 | 16.20-16.20 |
| 06 Jan. 81 | 15.54 | 15.54-15.54 |
| 23 Jan. 83 | 14.95 | 14.95-14.95 |
| 11 May 83 | 15.97 | 15.97-15.97 |
| 13 May 83 | 16.05 | 16.05-16.05 |
| 03 Feb. 84 | 16.64 | 16.64-16.64 |
| 07 Apr. 84 | 16.97 | 16.97-16.97 |
| 13 Feb. 85 | 16.05 | 16.05-16.05 |
| 12 Jan. 86 | 16.23 | 16.23-16.23 |
| 22 Feb. 87 | 15.66 | 15.66-15.66 |
| 27 Apr. 96 | 15.24 | 15.23-15.24 |
| 08 Mar. 98 | 14.18 | 14.02-14.29 |
| 09 Mar. 98 | 14.54 | 14.46-14.58 |
| 10 Mar. 98 | 14.69 | 14.62-14.77 |
| 15 May 98 | 13.67 | 13.63-13.71 |
| 17 May 98 | 13.71 | 13.71-13.71 |
| 18 May 98 | 14.20 | 14.17-14.23 |
| 19 May 98 | 14.67 | 14.67-14.68 |
| 23 Jan. 99 | 14.57 | 14.52-14.62 |
| 17 Feb. 99 | 14.02 | 13.99-14.06 |
| 18 Feb. 99 | 13.98 | 13.96-14.00 |
| 19 Feb. 99 | 13.96 | 13.92-13.99 |
| 20 Feb. 99 | 14.18 | 14.16-14.20 |
| 21 Feb. 99 | 14.33 | 14.23-14.38 |

Continued on Next Page...

TABLE 2.2 – Continued

| UT Date | Average Magnitude | Magnitude Range |
|---|---|---|
| 01 Feb. 00 | 14.37 | 14.36-14.39 |
| 03 Feb. 00 | 14.43 | 14.41-14.44 |
| 13 Apr. 00 | 14.65 | 14.64-14.67 |
| 14 Apr. 00 | 14.66 | 14.64-14.69 |
| 15 Apr. 00 | 14.57 | 13.81-14.64 |
| 17 Apr. 01 | 14.24 | 14.04-14.65 |
| 21 May 01 | 14.01 | 13.98-14.07 |
| 22 May 01 | 14.16 | 14.11-14.25 |
| 23 May 01 | 14.16 | 13.86-14.21 |
| 24 May 01 | 14.08 | 13.91-14.11 |
| 16 Jun. 01 | 13.48 | 13.44-13.53 |
| 07 Dec. 01 | 14.35 | 14.35-14.36 |
| 19 May 02 | 14.34 | 14.33-14.34 |
| 06 Mar. 03 | 16.74 | 16.74-16.75 |
| 07 Mar. 03 | 16.76 | 16.75-16.77 |
| 08 Mar. 03 | 16.84 | 16.83-16.84 |
| 10 Mar. 03 | 16.85 | 16.85-16.86 |
| 24 Apr. 03 | 16.48 | 16.47-16.49 |
| 25 Apr. 03 | 16.89 | 16.88-16.89 |
| 26 Apr. 03 | 16.94 | 16.94-16.94 |
| 27 Apr. 03 | 16.99 | 16.98-16.99 |
| 23 Apr. 04 | 15.66 | 15.63-15.68 |
| 26 Apr. 04 | 15.58 | 15.57-15.58 |
| 22 May 04 | 15.09 | 15.08-15.09 |
| 08 May 05 | 15.16 | 15.15-15.17 |
| 09 May 05 | 15.19 | 15.18-15.20 |
| 10 May 05 | 15.27 | 15.25-15.29 |
| 11 May 05 | 15.17 | 15.16-15.17 |
| 19 Feb. 06 | 14.23 | 14.22-14.23 |
| 23 Apr. 06 | 14.75 | 14.75-14.75 |
| 12 Dec. 06 | 13.63 | 13.63-13.63 |
| 23 Apr. 07 | 15.90 | 15.86-15.92 |
| 25 Apr. 07 | 15.95 | 15.91-16.01 |
| 27 Apr. 07 | 15.82 | 15.80-15.84 |
| 07 Jun. 07 | 15.11 | 15.07-15.15 |
| 08 Jun. 07 | 14.89 | 14.88-14.89 |
| 10 Jun. 07 | 14.83 | 14.81-14.86 |
| 19 Nov. 07 | 15.27 | 15.27-15.27 |

Continued on Next Page...

TABLE 2.2 – Continued

| UT Date | Average Magnitude | Magnitude Range |
|---|---|---|
| 25 Feb. 08 | 16.46 | 16.45-16.47 |
| 26 Feb. 08 | 16.41 | 16.38-16.48 |
| 27 Feb. 08 | 16.46 | 16.44-16.49 |
| 28 Feb. 08 | 16.37 | 16.35-16.39 |
| 29 Feb. 08 | 16.45 | 16.41-16.47 |
| 13 Mar. 08 | 16.43 | 16.41-16.45 |
| 14 Mar. 08 | 16.43 | 16.43-16.44 |
| 15 Mar. 08 | 16.47 | 16.47-16.48 |
| 26 Apr. 08 | 17.34 | 16.33-16.35 |
| 29 Mar. 09 | 16.20 | 16.20-16.20 |
| 16 May 09 | 17.86 | 18.85-17.86 |
| 18 Feb. 10 | 17.19 | 17.13-17.31 |
| 16 Mar. 10 | 17.12 | 17.12-17.13 |
| 17 Mar. 10 | 17.15 | 17.10-17.22 |
| 10 Apr. 10 | 17.22 | 17.18-17.26 |
| 11 Apr. 10 | 17.14 | 17.06-17.21 |
| 12 Apr. 10 | 17.23 | 17.07-17.34 |
| 14 Apr. 10 | 17.57 | 17.53-17.65 |
| 15 Apr. 10 | 17.57 | 17.51-17.61 |

During the week of 10 April through 15 April 2010, 3C279 was observed simultaneously with the 31" and the 42" telescopes at Lowell Observatory with R-, V-, and B-filter coverage. The R- and V-filter data have been smoothed using the IDL function TS_SMOOTH. This function performs a moving average of the data, averaging three data points at a time. This was done to reduce the noise of the data further, which will help confirm microvariabilty with even more certainty. There were two data points in the V-filter that were removed from the sample, one on 10 April and one on 15 April. In both instances the points indicated an increase in brightness of several magnitudes and were uncorroborated by any other points or trend in the data. The information for this observing run has been tabulated separately

in Table 2.3 and Table 2.4. In Table 2.3, the reduced Julian date is given in column 1, smoothed R-filter magnitude in column 2, and error in column 3. In Table 2.4, the reduced Julian date is given in column 1, smoothed V-filter magnitude in column 2, error in column 3, and B-V color when available in column 4.

TABLE 2.3: Data from 10 April to 15 April 2010 for 3C279 R-Filter

| **Reduced JD** | **R Magnitude** | **Error** |
|---|---|---|
| 296.64213 | 17.24 | 0.006 |
| 296.64570 | 17.25 | 0.009 |
| 296.64928 | 17.23 | 0.008 |
| 296.65285 | 17.22 | 0.007 |
| 296.65642 | 17.20 | 0.009 |
| 296.65999 | 17.21 | 0.007 |
| 296.66356 | 17.21 | 0.008 |
| 296.66963 | 17.22 | 0.014 |
| 296.67320 | 17.23 | 0.014 |
| 296.67677 | 17.22 | 0.013 |
| 296.68034 | 17.21 | 0.008 |
| 296.68392 | 17.20 | 0.012 |
| 296.68749 | 17.22 | 0.011 |
| 296.69106 | 17.22 | 0.010 |
| 296.69463 | 17.23 | 0.010 |
| 296.69820 | 17.23 | 0.016 |
| 296.70177 | 17.23 | 0.012 |
| 296.70534 | 17.23 | 0.011 |
| 296.70892 | 17.23 | 0.009 |
| 296.71249 | 17.23 | 0.010 |
| 296.71606 | 17.22 | 0.011 |
| 296.71963 | 17.21 | 0.011 |
| 296.72514 | 17.22 | 0.009 |
| 296.72871 | 17.22 | 0.009 |
| 296.73229 | 17.21 | 0.008 |
| 296.73586 | 17.21 | 0.008 |
| 296.73943 | 17.20 | 0.007 |
| 296.74300 | 17.20 | 0.008 |

Continued on Next Page...

TABLE 2.3 – Continued

| Reduced JD | R Magnitude | Error |
|---|---|---|
| 296.74657 | 17.19 | 0.008 |
| 296.75014 | 17.20 | 0.008 |
| 296.75371 | 17.20 | 0.007 |
| 296.75728 | 17.19 | 0.006 |
| 296.76085 | 17.19 | 0.008 |
| 296.76442 | 17.20 | 0.006 |
| 296.76800 | 17.20 | 0.006 |
| 296.77157 | 17.20 | 0.008 |
| 296.77514 | 17.20 | 0.011 |
| 296.78065 | 17.21 | 0.011 |
| 296.78422 | 17.22 | 0.007 |
| 296.78780 | 17.23 | 0.006 |
| 296.79137 | 17.23 | 0.010 |
| 296.79494 | 17.22 | 0.010 |
| 296.79851 | 17.24 | 0.008 |
| 296.80208 | 17.24 | 0.008 |
| 296.80565 | 17.25 | 0.009 |
| 296.80922 | 17.24 | 0.008 |
| 296.81279 | 17.26 | 0.008 |
| 296.81636 | 17.24 | 0.008 |
| 296.81993 | 17.23 | 0.007 |
| 296.82350 | 17.23 | 0.008 |
| 296.82708 | 17.22 | 0.008 |
| 296.83064 | 17.24 | 0.006 |
| 296.83702 | 17.24 | 0.008 |
| 296.84059 | 17.24 | 0.008 |
| 296.84416 | 17.22 | 0.007 |
| 296.84774 | 17.23 | 0.007 |
| 296.85131 | 17.23 | 0.009 |
| 296.85488 | 17.24 | 0.008 |
| 296.85845 | 17.24 | 0.009 |
| 296.86202 | 17.24 | 0.008 |
| 296.86559 | 17.24 | 0.007 |
| 296.86917 | 17.23 | 0.008 |
| 296.87274 | 17.21 | 0.007 |
| 296.87631 | 17.20 | 0.007 |
| 296.87988 | 17.20 | 0.008 |
| 296.88345 | 17.21 | 0.008 |

Continued on Next Page...

TABLE 2.3 – Continued

| Reduced JD | R Magnitude | Error |
|---|---|---|
| 296.88702 | 17.21 | 0.008 |
| 296.89253 | 17.21 | 0.008 |
| 296.89611 | 17.21 | 0.009 |
| 296.89968 | 17.21 | 0.007 |
| 296.90325 | 17.21 | 0.009 |
| 296.90682 | 17.20 | 0.007 |
| 296.91039 | 17.18 | 0.007 |
| 296.91396 | 17.19 | 0.007 |
| 296.91753 | 17.19 | 0.007 |
| 296.92111 | 17.19 | 0.007 |
| 296.92468 | 17.19 | 0.007 |
| 296.92825 | 17.19 | 0.006 |
| 296.93183 | 17.20 | 0.008 |
| 296.93540 | 17.23 | 0.008 |
| 296.93897 | 17.25 | 0.010 |
| 296.94254 | 17.25 | 0.007 |
| 296.95200 | 17.24 | 0.008 |
| 296.95558 | 17.23 | 0.008 |
| 296.95915 | 17.24 | 0.011 |
| 296.96272 | 17.25 | 0.007 |
| 296.96629 | 17.24 | 0.008 |
| 296.96986 | 17.23 | 0.010 |
| 296.97343 | 17.24 | 0.008 |
| 296.97700 | 17.26 | 0.009 |
| 296.98057 | 17.26 | 0.011 |
| 297.69468 | 17.21 | 0.015 |
| 297.69825 | 17.20 | 0.011 |
| 297.70182 | 17.18 | 0.013 |
| 297.70539 | 17.19 | 0.014 |
| 297.70896 | 17.20 | 0.010 |
| 297.71253 | 17.19 | 0.010 |
| 297.71611 | 17.17 | 0.012 |
| 297.71968 | 17.16 | 0.014 |
| 297.72519 | 17.16 | 0.012 |
| 297.72876 | 17.16 | 0.012 |
| 297.73233 | 17.16 | 0.013 |
| 297.73590 | 17.14 | 0.012 |
| 297.73947 | 17.13 | 0.013 |

Continued on Next Page...

TABLE 2.3 – Continued

| Reduced JD | R Magnitude | Error |
|---|---|---|
| 297.74305 | 17.12 | 0.012 |
| 297.74662 | 17.13 | 0.012 |
| 297.75019 | 17.15 | 0.012 |
| 297.75376 | 17.15 | 0.013 |
| 297.75733 | 17.15 | 0.014 |
| 297.76090 | 17.15 | 0.013 |
| 297.76447 | 17.16 | 0.012 |
| 297.76804 | 17.16 | 0.012 |
| 297.77161 | 17.16 | 0.013 |
| 297.77518 | 17.14 | 0.011 |
| 297.78071 | 17.11 | 0.012 |
| 297.78767 | 17.09 | 0.015 |
| 297.79124 | 17.06 | 0.010 |
| 297.79481 | 17.07 | 0.013 |
| 297.79838 | 17.07 | 0.012 |
| 297.80196 | 17.08 | 0.010 |
| 297.80553 | 17.07 | 0.011 |
| 297.80911 | 17.07 | 0.012 |
| 297.81268 | 17.08 | 0.012 |
| 297.81624 | 17.09 | 0.011 |
| 297.81982 | 17.10 | 0.012 |
| 297.82339 | 17.10 | 0.011 |
| 297.82696 | 17.09 | 0.012 |
| 297.83053 | 17.09 | 0.011 |
| 297.83605 | 17.09 | 0.011 |
| 297.83962 | 17.10 | 0.012 |
| 297.84319 | 17.11 | 0.012 |
| 297.84676 | 17.11 | 0.011 |
| 297.85034 | 17.12 | 0.012 |
| 297.85391 | 17.11 | 0.011 |
| 297.85748 | 17.11 | 0.012 |
| 297.86106 | 17.12 | 0.011 |
| 297.86463 | 17.13 | 0.013 |
| 297.86820 | 17.15 | 0.012 |
| 297.87177 | 17.13 | 0.015 |
| 297.87534 | 17.13 | 0.015 |
| 297.87891 | 17.13 | 0.014 |
| 297.88248 | 17.14 | 0.013 |

Continued on Next Page...

TABLE 2.3 – Continued

| Reduced JD | R Magnitude | Error |
|---|---|---|
| 297.88606 | 17.15 | 0.013 |
| 297.89156 | 17.17 | 0.012 |
| 297.89514 | 17.19 | 0.010 |
| 297.89871 | 17.20 | 0.011 |
| 297.90228 | 17.19 | 0.011 |
| 297.90585 | 17.18 | 0.011 |
| 297.90942 | 17.19 | 0.011 |
| 297.91299 | 17.17 | 0.013 |
| 297.91656 | 17.18 | 0.014 |
| 297.92013 | 17.17 | 0.011 |
| 297.92370 | 17.18 | 0.011 |
| 297.92727 | 17.14 | 0.013 |
| 297.93085 | 17.11 | 0.011 |
| 297.93441 | 17.10 | 0.012 |
| 297.93799 | 17.12 | 0.013 |
| 297.94156 | 17.15 | 0.011 |
| 297.95083 | 17.17 | 0.010 |
| 297.95440 | 17.19 | 0.012 |
| 297.96135 | 17.18 | 0.010 |
| 297.96492 | 17.17 | 0.015 |
| 297.97189 | 17.15 | 0.011 |
| 297.97546 | 17.14 | 0.013 |
| 297.97903 | 17.15 | 0.012 |
| 298.64183 | 17.08 | 0.009 |
| 298.64540 | 17.08 | 0.009 |
| 298.64897 | 17.07 | 0.009 |
| 298.65254 | 17.09 | 0.009 |
| 298.65611 | 17.11 | 0.008 |
| 298.65968 | 17.12 | 0.008 |
| 298.66326 | 17.13 | 0.008 |
| 298.66935 | 17.13 | 0.010 |
| 298.67631 | 17.16 | 0.011 |
| 298.67987 | 17.16 | 0.010 |
| 298.68684 | 17.14 | 0.011 |
| 298.69041 | 17.13 | 0.008 |
| 298.69398 | 17.12 | 0.016 |
| 298.70094 | 17.13 | 0.012 |
| 298.70451 | 17.13 | 0.010 |

Continued on Next Page...

TABLE 2.3 – Continued

| Reduced JD | R Magnitude | Error |
|---|---|---|
| 298.71147 | 17.12 | 0.010 |
| 298.71504 | 17.14 | 0.010 |
| 298.71861 | 17.16 | 0.009 |
| 298.72447 | 17.19 | 0.008 |
| 298.72804 | 17.20 | 0.009 |
| 298.73161 | 17.21 | 0.009 |
| 298.73858 | 17.21 | 0.009 |
| 298.74216 | 17.22 | 0.009 |
| 298.74573 | 17.21 | 0.009 |
| 298.74930 | 17.20 | 0.009 |
| 298.75287 | 17.20 | 0.007 |
| 298.75644 | 17.20 | 0.009 |
| 298.76001 | 17.19 | 0.009 |
| 298.76358 | 17.19 | 0.007 |
| 298.76715 | 17.20 | 0.007 |
| 298.77072 | 17.21 | 0.008 |
| 298.77430 | 17.22 | 0.007 |
| 298.78067 | 17.23 | 0.008 |
| 298.78424 | 17.24 | 0.007 |
| 298.78782 | 17.25 | 0.008 |
| 298.79139 | 17.30 | 0.010 |
| 298.79496 | 17.30 | 0.009 |
| 298.79853 | 17.29 | 0.009 |
| 298.80210 | 17.26 | 0.008 |
| 298.80567 | 17.25 | 0.008 |
| 298.80924 | 17.25 | 0.009 |
| 298.81282 | 17.25 | 0.006 |
| 298.81639 | 17.28 | 0.009 |
| 298.81996 | 17.29 | 0.011 |
| 298.82353 | 17.31 | 0.009 |
| 298.82710 | 17.30 | 0.009 |
| 298.83067 | 17.32 | 0.009 |
| 298.83618 | 17.33 | 0.011 |
| 298.83975 | 17.34 | 0.013 |
| 298.84332 | 17.33 | 0.009 |
| 298.84690 | 17.30 | 0.007 |
| 298.85047 | 17.31 | 0.007 |
| 298.85404 | 17.31 | 0.008 |

Continued on Next Page...

TABLE 2.3 – Continued

| Reduced JD | R Magnitude | Error |
|---|---|---|
| 298.85761 | 17.31 | 0.009 |
| 298.86118 | 17.30 | 0.009 |
| 298.86475 | 17.29 | 0.010 |
| 298.86832 | 17.29 | 0.007 |
| 298.87189 | 17.29 | 0.007 |
| 298.87547 | 17.28 | 0.008 |
| 298.87904 | 17.27 | 0.008 |
| 298.88261 | 17.28 | 0.009 |
| 298.88618 | 17.28 | 0.008 |
| 298.89167 | 17.31 | 0.007 |
| 298.89524 | 17.31 | 0.008 |
| 298.90220 | 17.34 | 0.008 |
| 298.90577 | 17.33 | 0.006 |
| 298.90934 | 17.31 | 0.006 |
| 298.91291 | 17.29 | 0.006 |
| 298.91648 | 17.29 | 0.008 |
| 298.92006 | 17.29 | 0.009 |
| 298.92702 | 17.27 | 0.008 |
| 298.93059 | 17.24 | 0.008 |
| 298.93416 | 17.23 | 0.007 |
| 298.93773 | 17.23 | 0.006 |
| 298.94131 | 17.26 | 0.008 |
| 298.94753 | 17.26 | 0.012 |
| 298.95110 | 17.27 | 0.007 |
| 298.95468 | 17.24 | 0.007 |
| 298.95825 | 17.23 | 0.008 |
| 298.96182 | 17.21 | 0.009 |
| 298.96539 | 17.20 | 0.008 |
| 300.64169 | 17.65 | 0.018 |
| 300.64526 | 17.61 | 0.016 |
| 300.64883 | 17.55 | 0.018 |
| 300.65240 | 17.53 | 0.016 |
| 300.65597 | 17.55 | 0.017 |
| 300.65954 | 17.58 | 0.017 |
| 300.66311 | 17.57 | 0.018 |
| 300.66917 | 17.57 | 0.010 |
| 300.67274 | 17.56 | 0.012 |
| 300.67631 | 17.55 | 0.012 |

Continued on Next Page...

TABLE 2.3 – Continued

| Reduced JD | R Magnitude | Error |
|---|---|---|
| 300.67989 | 17.55 | 0.012 |
| 300.68346 | 17.55 | 0.012 |
| 300.68703 | 17.56 | 0.013 |
| 300.69061 | 17.56 | 0.012 |
| 300.69417 | 17.55 | 0.012 |
| 300.69775 | 17.55 | 0.013 |
| 300.70132 | 17.56 | 0.013 |
| 300.70489 | 17.56 | 0.012 |
| 300.70846 | 17.56 | 0.012 |
| 300.71203 | 17.55 | 0.012 |
| 300.71560 | 17.56 | 0.014 |
| 300.71918 | 17.57 | 0.012 |
| 300.72472 | 17.57 | 0.013 |
| 300.72829 | 17.58 | 0.011 |
| 300.73186 | 17.58 | 0.014 |
| 300.73543 | 17.59 | 0.012 |
| 300.73900 | 17.58 | 0.012 |
| 300.74257 | 17.57 | 0.011 |
| 300.74614 | 17.57 | 0.011 |
| 300.74971 | 17.58 | 0.012 |
| 300.75328 | 17.60 | 0.013 |
| 300.75685 | 17.59 | 0.012 |
| 300.76042 | 17.59 | 0.012 |
| 300.76399 | 17.56 | 0.013 |
| 300.76757 | 17.57 | 0.012 |
| 300.77114 | 17.57 | 0.012 |
| 300.77471 | 17.58 | 0.011 |
| 300.78021 | 17.57 | 0.011 |
| 300.78379 | 17.57 | 0.013 |
| 300.78736 | 17.55 | 0.017 |
| 300.79093 | 17.56 | 0.012 |
| 300.79450 | 17.55 | 0.012 |
| 300.79807 | 17.56 | 0.014 |
| 300.80164 | 17.55 | 0.013 |
| 300.80522 | 17.55 | 0.013 |
| 300.80879 | 17.57 | 0.014 |
| 300.81236 | 17.57 | 0.013 |
| 300.81593 | 17.57 | 0.014 |

Continued on Next Page...

TABLE 2.3 – Continued

| Reduced JD | R Magnitude | Error |
|---|---|---|
| 300.81950 | 17.56 | 0.013 |
| 300.82307 | 17.56 | 0.014 |
| 300.82664 | 17.55 | 0.014 |
| 300.83022 | 17.56 | 0.015 |
| 300.83569 | 17.56 | 0.012 |
| 300.83926 | 17.57 | 0.011 |
| 300.84283 | 17.56 | 0.011 |
| 300.84640 | 17.57 | 0.011 |
| 300.84997 | 17.57 | 0.010 |
| 300.85355 | 17.58 | 0.011 |
| 300.85711 | 17.57 | 0.012 |
| 300.86068 | 17.58 | 0.010 |
| 300.86426 | 17.58 | 0.011 |
| 300.86783 | 17.58 | 0.011 |
| 300.87140 | 17.57 | 0.011 |
| 300.87497 | 17.58 | 0.011 |
| 300.87854 | 17.58 | 0.012 |
| 300.88210 | 17.60 | 0.011 |
| 300.88568 | 17.60 | 0.012 |
| 300.89458 | 17.58 | 0.011 |
| 300.89815 | 17.57 | 0.011 |
| 300.90510 | 17.58 | 0.011 |
| 300.90867 | 17.59 | 0.011 |
| 300.91564 | 17.60 | 0.011 |
| 300.91921 | 17.61 | 0.009 |
| 300.92278 | 17.60 | 0.010 |
| 300.92635 | 17.60 | 0.011 |
| 300.92992 | 17.58 | 0.011 |
| 300.93349 | 17.58 | 0.011 |
| 300.93706 | 17.57 | 0.011 |
| 300.94666 | 17.58 | 0.012 |
| 300.95023 | 17.58 | 0.013 |
| 300.95380 | 17.58 | 0.011 |
| 300.96076 | 17.58 | 0.013 |
| 300.96433 | 17.58 | 0.010 |
| 301.76387 | 17.57 | 0.012 |
| 301.76744 | 17.57 | 0.013 |
| 301.77101 | 17.60 | 0.012 |

Continued on Next Page...

TABLE 2.3 – Continued

| Reduced JD | R Magnitude | Error |
|---|---|---|
| 301.77458 | 17.59 | 0.011 |
| 301.77815 | 17.57 | 0.015 |
| 301.78368 | 17.59 | 0.012 |
| 301.78725 | 17.60 | 0.012 |
| 301.79082 | 17.60 | 0.012 |
| 301.79439 | 17.57 | 0.013 |
| 301.79796 | 17.56 | 0.012 |
| 301.80153 | 17.57 | 0.011 |
| 301.80510 | 17.57 | 0.012 |
| 301.80867 | 17.59 | 0.012 |
| 301.81224 | 17.58 | 0.014 |
| 301.81582 | 17.58 | 0.011 |
| 301.81939 | 17.55 | 0.012 |
| 301.82296 | 17.58 | 0.013 |
| 301.82653 | 17.58 | 0.012 |
| 301.83350 | 17.57 | 0.011 |
| 301.84242 | 17.55 | 0.015 |
| 301.84599 | 17.56 | 0.014 |
| 301.85296 | 17.58 | 0.012 |
| 301.85653 | 17.60 | 0.011 |
| 301.86010 | 17.60 | 0.010 |
| 301.86367 | 17.57 | 0.018 |
| 301.86724 | 17.51 | 0.012 |
| 301.87081 | 17.53 | 0.014 |
| 301.87438 | 17.54 | 0.015 |
| 301.87796 | 17.58 | 0.020 |
| 301.88867 | 17.56 | 0.019 |
| 301.89502 | 17.56 | 0.013 |
| 301.89859 | 17.56 | 0.015 |
| 301.90216 | 17.57 | 0.011 |
| 301.90572 | 17.58 | 0.014 |
| 301.90929 | 17.57 | 0.013 |
| 301.91287 | 17.56 | 0.012 |
| 301.91644 | 17.60 | 0.015 |
| 301.92000 | 17.60 | 0.011 |
| 301.92358 | 17.61 | 0.015 |
| 301.92715 | 17.57 | 0.015 |
| 301.93072 | 17.57 | 0.014 |

Continued on Next Page...

TABLE 2.3 – Continued

| Reduced JD | R Magnitude | Error |
|---|---|---|
| 301.93429 | 17.58 | 0.013 |
| 301.93786 | 17.57 | 0.016 |
| 301.94143 | 17.58 | 0.014 |
| 301.94500 | 17.58 | 0.016 |
| 301.95208 | 17.58 | 0.012 |
| 301.95565 | 17.57 | 0.013 |
| 301.95922 | 17.56 | 0.012 |
| 301.96279 | 17.57 | 0.012 |
| 301.96637 | 17.55 | 0.010 |
| 301.96993 | 17.56 | 0.007 |

TABLE 2.4: Data from 10 April to 15 April 2010 for 3C279 V-Filter

| Reduced JD | V Magnitude | Error | B-V |
|---|---|---|---|
| 296.64756 | 17.79 | 0.012 | |
| 296.65120 | 17.77 | 0.014 | |
| 296.65485 | 17.75 | 0.021 | |
| 296.65849 | 17.74 | 0.014 | |
| 296.66214 | 17.75 | 0.020 | |
| 296.66578 | 17.75 | 0.010 | |
| 296.66943 | 17.72 | 0.011 | |
| 296.67307 | 17.70 | 0.017 | |
| 296.67672 | 17.71 | 0.013 | 0.54 |
| 296.68036 | 17.74 | 0.013 | 0.54 |
| 296.70410 | 17.76 | 0.018 | |
| 296.70775 | 17.77 | 0.021 | |
| 296.71139 | 17.75 | 0.015 | |
| 296.71504 | 17.72 | 0.026 | |
| 296.71868 | 17.70 | 0.027 | |
| 296.72233 | 17.71 | 0.025 | |
| 296.72597 | 17.75 | 0.021 | |
| 296.72962 | 17.73 | 0.027 | |
| 296.73326 | 17.75 | 0.019 | |
| 296.73691 | 17.73 | 0.019 | 0.52 |
| 296.75970 | 17.74 | 0.028 | 0.46 |

Continued on Next Page...

TABLE 2.4 – Continued

| Reduced JD | V Magnitude | Error | B-V |
|---|---|---|---|
| 296.76334 | 17.75 | 0.016 | |
| 296.76699 | 17.75 | 0.016 | |
| 296.77063 | 17.73 | 0.014 | |
| 296.77428 | 17.73 | 0.016 | |
| 296.77792 | 17.73 | 0.016 | |
| 296.78157 | 17.75 | 0.016 | |
| 296.78521 | 17.72 | 0.017 | |
| 296.78886 | 17.73 | 0.016 | 0.45 |
| 296.80853 | 17.76 | 0.013 | 0.53 |
| 296.81217 | 17.76 | 0.018 | |
| 296.81581 | 17.76 | 0.019 | |
| 296.81946 | 17.76 | 0.020 | |
| 296.82311 | 17.78 | 0.019 | |
| 296.82675 | 17.76 | 0.020 | |
| 296.83039 | 17.75 | 0.018 | |
| 296.83404 | 17.75 | 0.020 | |
| 296.83768 | 17.77 | 0.020 | |
| 296.84133 | 17.77 | 0.020 | 0.53 |
| 296.86140 | 17.79 | 0.020 | 0.49 |
| 296.86504 | 17.81 | 0.022 | |
| 296.86869 | 17.80 | 0.023 | |
| 296.87233 | 17.78 | 0.026 | |
| 296.87598 | 17.77 | 0.023 | |
| 296.87962 | 17.76 | 0.024 | |
| 296.88327 | 17.75 | 0.021 | |
| 296.88692 | 17.74 | 0.022 | |
| 296.89057 | 17.75 | 0.020 | |
| 296.89421 | 17.73 | 0.020 | 0.57 |
| 296.91306 | 17.71 | 0.020 | 0.54 |
| 296.91670 | 17.68 | 0.017 | |
| 296.92035 | 17.68 | 0.019 | |
| 296.92399 | 17.67 | 0.018 | |
| 296.92764 | 17.69 | 0.019 | |
| 296.93128 | 17.70 | 0.016 | |
| 296.93493 | 17.74 | 0.019 | |
| 296.93857 | 17.76 | 0.018 | |
| 296.94222 | 17.78 | 0.020 | |
| 296.94587 | 17.76 | 0.018 | 0.54 |

Continued on Next Page...

TABLE 2.4 – Continued

| Reduced JD | V Magnitude | Error | B-V |
|---|---|---|---|
| 296.96588 | 17.76 | 0.017 | 0.53 |
| 296.96952 | 17.76 | 0.022 | |
| 296.97317 | 17.78 | 0.017 | |
| 296.97681 | 17.79 | 0.013 | |
| 296.98046 | 17.80 | 0.023 | |
| 297.71487 | 17.71 | 0.018 | |
| 297.71852 | 17.70 | 0.017 | |
| 297.72216 | 17.70 | 0.019 | |
| 297.72580 | 17.73 | 0.019 | |
| 297.72945 | 17.69 | 0.026 | |
| 297.73310 | 17.67 | 0.015 | |
| 297.73674 | 17.67 | 0.016 | |
| 297.74039 | 17.70 | 0.026 | |
| 297.74403 | 17.69 | 0.017 | |
| 297.74768 | 17.67 | 0.023 | 0.53 |
| 297.76805 | 17.69 | 0.032 | 0.48 |
| 297.77169 | 17.68 | 0.020 | |
| 297.77534 | 17.68 | 0.022 | |
| 297.77899 | 17.62 | 0.017 | |
| 297.78263 | 17.61 | 0.015 | |
| 297.78628 | 17.60 | 0.032 | |
| 297.78992 | 17.59 | 0.022 | |
| 297.79356 | 17.59 | 0.021 | |
| 297.79721 | 17.58 | 0.021 | |
| 297.80085 | 17.58 | 0.017 | 0.52 |
| 297.81938 | 17.59 | 0.014 | 0.51 |
| 297.82302 | 17.59 | 0.018 | |
| 297.82666 | 17.61 | 0.025 | |
| 297.83031 | 17.60 | 0.020 | |
| 297.83395 | 17.60 | 0.024 | |
| 297.83760 | 17.61 | 0.027 | |
| 297.84124 | 17.62 | 0.027 | |
| 297.84489 | 17.62 | 0.027 | |
| 297.84853 | 17.61 | 0.027 | |
| 297.85218 | 17.62 | 0.020 | 0.51 |
| 297.87087 | 17.62 | 0.020 | 0.53 |
| 297.87451 | 17.64 | 0.018 | |
| 297.87815 | 17.65 | 0.019 | |

Continued on Next Page...

TABLE 2.4 – Continued

| Reduced JD | V Magnitude | Error | B-V |
|---|---|---|---|
| 297.88179 | 17.66 | 0.017 | |
| 297.88544 | 17.68 | 0.019 | |
| 297.88908 | 17.70 | 0.011 | |
| 297.89272 | 17.72 | 0.016 | |
| 297.89637 | 17.72 | 0.018 | |
| 297.90002 | 17.72 | 0.017 | |
| 297.90367 | 17.72 | 0.017 | 0.54 |
| 297.92785 | 17.70 | 0.016 | 0.61 |
| 297.93149 | 17.67 | 0.021 | |
| 297.93514 | 17.65 | 0.015 | |
| 297.93878 | 17.66 | 0.021 | |
| 297.94242 | 17.68 | 0.020 | |
| 297.94638 | 17.69 | 0.023 | |
| 297.95002 | 17.71 | 0.021 | |
| 297.95367 | 17.70 | 0.019 | |
| 297.95731 | 17.70 | 0.014 | |
| 297.96096 | 17.70 | 0.013 | |
| 298.63830 | 17.59 | 0.010 | |
| 298.64194 | 17.60 | 0.013 | |
| 298.64558 | 17.61 | 0.016 | |
| 298.64923 | 17.61 | 0.014 | |
| 298.65287 | 17.62 | 0.021 | |
| 298.65652 | 17.59 | 0.018 | |
| 298.66016 | 17.64 | 0.019 | |
| 298.66381 | 17.65 | 0.020 | |
| 298.66746 | 17.70 | 0.019 | |
| 298.67111 | 17.68 | 0.018 | 0.55 |
| 298.69298 | 17.67 | 0.017 | 0.57 |
| 298.69778 | 17.68 | 0.018 | |
| 298.70258 | 17.68 | 0.019 | |
| 298.70738 | 17.70 | 0.022 | |
| 298.71218 | 17.71 | 0.019 | |
| 298.71762 | 17.74 | 0.022 | |
| 298.72242 | 17.80 | 0.024 | |
| 298.72723 | 17.78 | 0.023 | |
| 298.73203 | 17.81 | 0.027 | |
| 298.73684 | 17.76 | 0.021 | 0.52 |
| 298.76150 | 17.74 | 0.015 | 0.53 |

Continued on Next Page...

TABLE 2.4 – Continued

| Reduced JD | V Magnitude | Error | B-V |
|---|---|---|---|
| 298.76515 | 17.69 | 0.014 | |
| 298.76879 | 17.71 | 0.015 | |
| 298.77244 | 17.71 | 0.011 | |
| 298.77609 | 17.72 | 0.014 | |
| 298.78030 | 17.75 | 0.019 | |
| 298.78394 | 17.78 | 0.034 | |
| 298.78759 | 17.82 | 0.021 | |
| 298.79123 | 17.82 | 0.017 | |
| 298.79488 | 17.83 | 0.026 | 0.52 |
| 298.81472 | 17.84 | 0.030 | 0.52 |
| 298.81871 | 17.85 | 0.034 | |
| 298.82270 | 17.91 | 0.028 | |
| 298.82670 | 17.93 | 0.028 | |
| 298.83069 | 17.94 | 0.031 | |
| 298.84677 | 17.89 | 0.035 | |
| 298.85157 | 17.86 | 0.028 | |
| 298.85637 | 17.85 | 0.023 | |
| 298.86118 | 17.86 | 0.023 | |
| 298.86598 | 17.85 | 0.022 | 0.54 |
| 298.89035 | 17.84 | 0.019 | 0.51 |
| 298.89399 | 17.83 | 0.019 | |
| 298.89764 | 17.83 | 0.017 | |
| 298.90128 | 17.84 | 0.013 | |
| 298.90493 | 17.83 | 0.014 | |
| 298.90857 | 17.83 | 0.015 | |
| 298.91222 | 17.83 | 0.014 | |
| 298.91586 | 17.85 | 0.013 | |
| 298.91951 | 17.85 | 0.015 | |
| 298.92315 | 17.84 | 0.014 | 0.54 |
| 298.94146 | 17.82 | 0.016 | 0.59 |
| 298.94510 | 17.82 | 0.014 | |
| 298.94874 | 17.82 | 0.014 | |
| 298.95238 | 17.81 | 0.016 | |
| 298.95603 | 17.80 | 0.021 | |
| 298.95967 | 17.77 | 0.018 | |
| 298.96331 | 17.78 | 0.015 | |
| 298.96695 | 17.75 | 0.016 | |
| 298.97060 | 17.76 | 0.013 | |

Continued on Next Page...

TABLE 2.4 – Continued

| Reduced JD | V Magnitude | Error | B-V |
|---|---|---|---|
| 298.97424 | 17.73 | 0.016 | |
| 300.62799 | 18.17 | 0.013 | |
| 300.63163 | 18.15 | 0.014 | |
| 300.63528 | 18.15 | 0.017 | |
| 300.63892 | 18.15 | 0.015 | |
| 300.64256 | 18.18 | 0.017 | |
| 300.64621 | 18.16 | 0.017 | |
| 300.64985 | 18.13 | 0.020 | |
| 300.65350 | 18.10 | 0.017 | |
| 300.65714 | 18.08 | 0.020 | |
| 300.66079 | 18.09 | 0.015 | 0.53 |
| 300.67975 | 18.09 | 0.014 | 0.54 |
| 300.68374 | 18.10 | 0.028 | |
| 300.68774 | 18.10 | 0.035 | |
| 300.69173 | 18.11 | 0.032 | |
| 300.69572 | 18.14 | 0.031 | |
| 300.69971 | 18.14 | 0.032 | |
| 300.70371 | 18.13 | 0.022 | |
| 300.70770 | 18.11 | 0.022 | |
| 300.71169 | 18.14 | 0.023 | |
| 300.71568 | 18.15 | 0.017 | 0.48 |
| 300.73650 | 18.14 | 0.026 | 0.53 |
| 300.74015 | 18.12 | 0.030 | |
| 300.74379 | 18.11 | 0.018 | |
| 300.74743 | 18.11 | 0.018 | |
| 300.75108 | 18.10 | 0.026 | |
| 300.75472 | 18.08 | 0.024 | |
| 300.75837 | 18.09 | 0.028 | |
| 300.76201 | 18.11 | 0.029 | |
| 300.76565 | 18.12 | 0.018 | |
| 300.76929 | 18.11 | 0.022 | 0.49 |
| 300.78918 | 18.10 | 0.030 | 0.48 |
| 300.79282 | 18.12 | 0.028 | |
| 300.79646 | 18.12 | 0.025 | |
| 300.80010 | 18.11 | 0.026 | |
| 300.80375 | 18.09 | 0.024 | |
| 300.80739 | 18.09 | 0.025 | |
| 300.81103 | 18.10 | 0.028 | |

Continued on Next Page...

TABLE 2.4 – Continued

| Reduced JD | V Magnitude | Error | B-V |
|---|---|---|---|
| 300.81468 | 18.10 | 0.025 | |
| 300.81832 | 18.11 | 0.030 | |
| 300.82197 | 18.12 | 0.033 | 0.48 |
| 300.84245 | 18.13 | 0.031 | 0.54 |
| 300.84609 | 18.12 | 0.035 | |
| 300.84974 | 18.12 | 0.031 | |
| 300.85338 | 18.11 | 0.032 | |
| 300.85703 | 18.10 | 0.034 | |
| 300.86067 | 18.10 | 0.035 | |
| 300.86432 | 18.10 | 0.031 | |
| 300.86796 | 18.10 | 0.031 | |
| 300.87160 | 18.10 | 0.028 | |
| 300.87525 | 18.09 | 0.021 | 0.55 |
| 300.89515 | 18.10 | 0.020 | 0.54 |
| 300.89880 | 18.11 | 0.020 | |
| 300.90245 | 18.13 | 0.024 | |
| 300.90609 | 18.13 | 0.020 | |
| 300.90974 | 18.12 | 0.020 | |
| 300.91339 | 18.10 | 0.014 | |
| 300.91703 | 18.09 | 0.018 | |
| 300.92067 | 18.09 | 0.015 | |
| 300.92431 | 18.11 | 0.015 | |
| 300.92795 | 18.13 | 0.015 | 0.54 |
| 300.94654 | 18.15 | 0.025 | 0.61 |
| 300.95019 | 18.17 | 0.020 | |
| 300.95383 | 18.14 | 0.014 | |
| 300.95747 | 18.14 | 0.017 | |
| 300.96111 | 18.12 | 0.021 | |
| 300.96689 | 18.12 | 0.017 | |
| 301.62799 | 18.11 | 0.036 | |
| 301.63164 | 18.21 | 0.024 | |
| 301.63529 | 18.57 | 0.027 | |
| 301.64966 | 18.16 | 0.022 | 0.55 |
| 301.69088 | 18.12 | 0.033 | 0.43 |
| 301.69487 | 18.16 | 0.017 | |
| 301.69886 | 18.12 | 0.035 | |
| 301.70512 | 18.22 | 0.035 | |
| 301.70992 | 18.17 | 0.033 | |

Continued on Next Page...

TABLE 2.4 – Continued

| Reduced JD | V Magnitude | Error | B-V |
|---|---|---|---|
| 301.71472 | 18.28 | 0.038 | |
| 301.71952 | 18.15 | 0.025 | |
| 301.72435 | 18.28 | 0.029 | |
| 301.72916 | 18.11 | 0.044 | |
| 301.73876 | 18.11 | 0.036 | |
| 301.74357 | 18.12 | 0.024 | |
| 301.76975 | 18.17 | 0.027 | 0.45 |
| 301.78384 | 18.18 | 0.022 | |
| 301.78981 | 18.16 | 0.033 | |
| 301.79577 | 18.15 | 0.017 | |
| 301.80172 | 18.15 | 0.035 | |
| 301.80774 | 18.14 | 0.035 | |
| 301.81370 | 18.16 | 0.033 | |
| 301.81965 | 18.14 | 0.038 | |
| 301.82562 | 18.14 | 0.025 | |
| 301.83158 | 18.13 | 0.029 | 0.55 |
| 301.85803 | 18.12 | 0.044 | 0.54 |
| 301.86283 | 18.09 | 0.023 | |
| 301.86763 | 18.04 | 0.034 | |
| 301.87243 | 18.04 | 0.029 | |
| 301.87723 | 18.17 | 0.024 | |
| 301.88204 | 18.19 | 0.025 | |
| 301.88685 | 18.20 | 0.024 | |
| 301.89165 | 18.11 | 0.022 | |
| 301.89646 | 18.13 | 0.019 | |
| 301.90126 | 18.15 | 0.016 | 0.51 |
| 301.93513 | 18.14 | 0.017 | 0.51 |
| 301.93993 | 18.14 | 0.017 | |
| 301.94473 | 18.15 | 0.020 | |
| 301.94954 | 18.14 | 0.021 | |
| 301.95434 | 18.13 | 0.025 | |
| 301.95914 | 18.12 | 0.025 | |
| 301.96400 | 18.12 | 0.024 | |

# – 3 –

# Results & Analysis

## 3.1 Results

Data from the PEGA archives, Pica et al. (1980), and data from H. Richard Miller were used to create the long-term light curve for 3C279. The tabular version of these data can be viewed in Table 2.2. For the most recent high temporal resolution observations, nightly light curves are constructed for visual microvariability analysis. Only the nights with confirmed microvariability are presented in this section. The light curves for the other nights are given in the appendicies. Two panels are shown for each night. The top panel shows the difference in magnitude of the object and one comparison star. The bottom panel shows the difference between the comparison star used above and another comparison star in the frame. The comparison stars used for analysis are clearly labeled along the y-axis. The top panel shows the object's variability relative to a comparison star whereas the bottom panel shows the difference of the two comparison stars. The scatter of these two stars can be used to determine the photometric precision of the measurements. Notable events have been marked with a capital letter for easy comparison between filters for a given night. A positive detection of microvariability will be confirmed (99.5% confidence) by any change in magnitude greater than $3\sigma$, as discussed by Carini (1990).

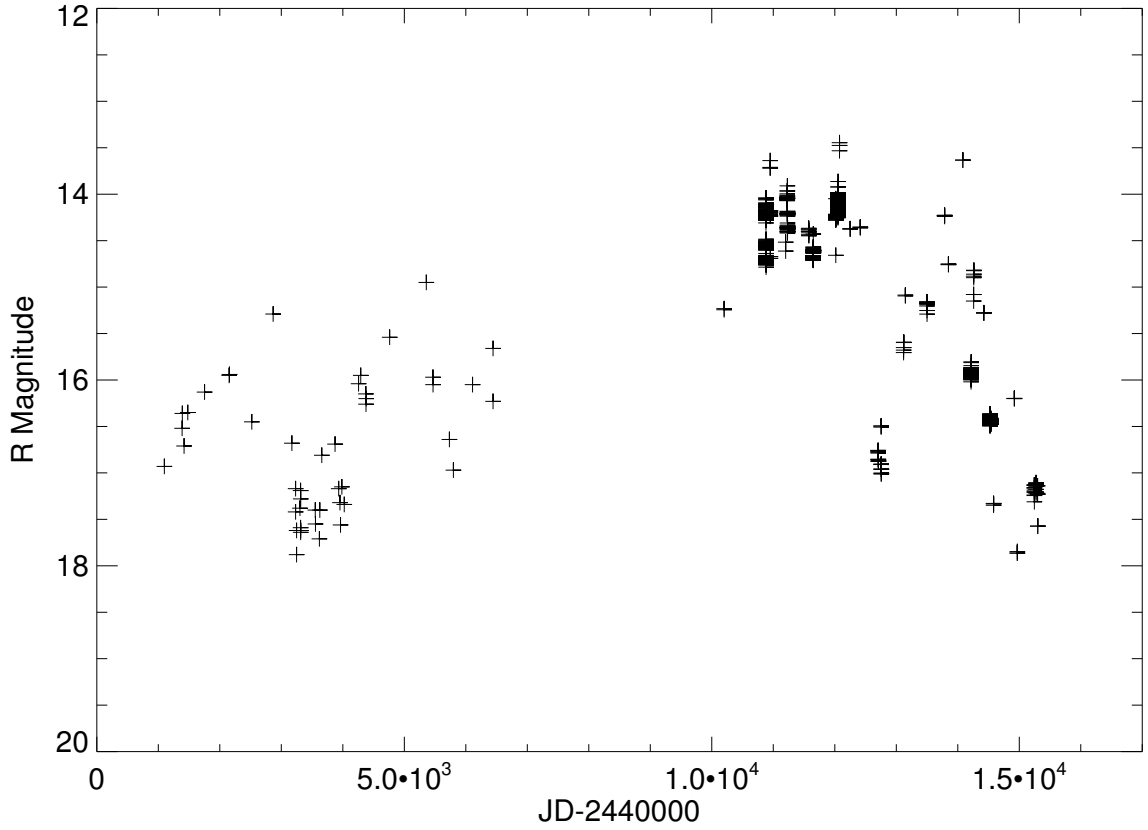


FIGURE 3.1: Light Curve of 3C279 spanning 1971 to 2010.

### 3.1.1 Long-Term Light Curve

The long-term light curve for 3C279 presented here spans 39 years, from 1971 to 2010. All of the observations taken from the PEGA archive were made using the R-filter. The data used from Pica et al. (1980) were taken using photographic plates and have been converted to R magnitudes by using values given in Larionov et al. (2008). Although the data presented in Section 3.2.3 indicate a color dependence, a constant value was used here and does not have a large effect on the magnitude values in the long-term light curve. The primary observations obtained from private communication with H. Richard Miller were the averaged magnitudes

observed in V-band for a given night and were converted to R magnitudes using Larionov et al. (2008) as well. Error bars were omitted because their size compared to the size of the data point is small. This light curve shows a range of ∼4.6 magnitudes. Values published by Eachus & Liller (1975) state an apparent R magnitude of 11.10 on 12 April 1937 (maximum brightness) and a minimum brightness of 17.84 in March 1965 giving 3C279 a total range of ∼6.7 magnitudes. The most recent data for 3C279 show it to be in one of the faintest states observed in at least 73 years. This provides a unique opportunity to test the variability of this blazar in an extreme low state. Confirmed microvariability detections in this low state will be the first ever observed for this object.

### 3.1.2 Recent Light Curves

The data for the entire observation run in April 2010 are shown in the top section of Figure 3.2. The data for the comparison stars are given in the bottom panel. The night to night variability is clearly seen while the comaprison stars show no change in magnitude. Between 10, 11, and 12 April there is very little change observed in the average magnitude. There is a large drop of ∼0.4 magnitudes from the 12 to the 14 April. There were no data taken 13 April due to inclement weather. There is no change in average magnitude observed between 14 and 15 April.

The observations for the night of 10 April 2010 are shown in Figure 3.3 and Figure 3.4. In Figure 3.3, the V-band observations for 10 April 2010 show an increase of ∼0.1 mag in ∼40 min early in the night followed by a decrease of a similar amplitude and timespan shortly thereafter. This event is labeled A. Towards the end of the night there is an event labeled C

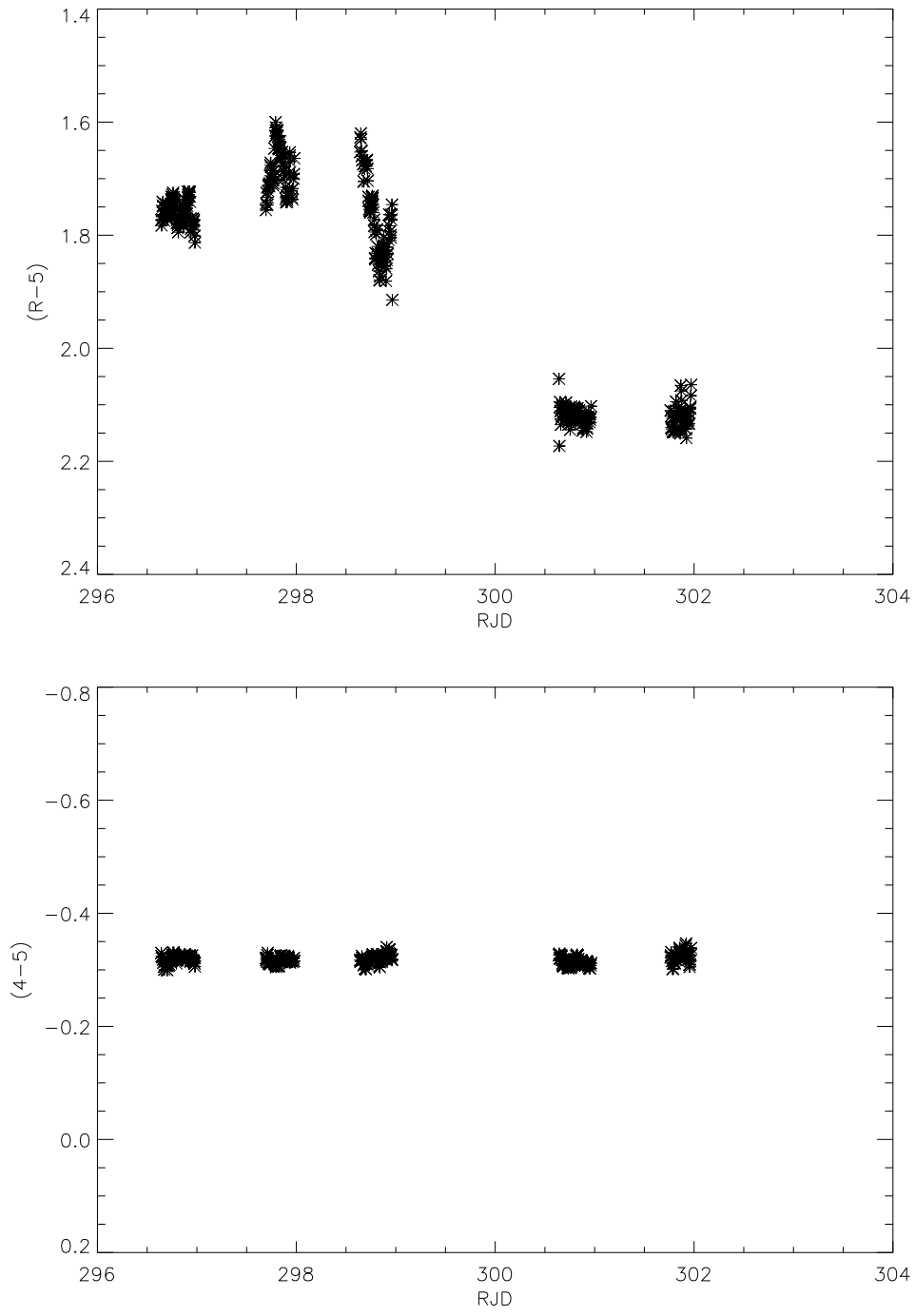


FIGURE 3.2: Light Curve of 3C279 for the week of 10-15 April 2010. *Top* Object light curve. *Bottom* Check 4-Check 5 light curve. Data taken with the Lowell 31" telescope.

which shows another increase in brightness with a change of ∼0.13 mag in ∼1.5 hours with a subsequent decline of ∼0.11 mag over ∼40 min. These represent 3.5, 4.5, and 3.8$\sigma$ change respectively.

Figure 3.4 displays the R-band observations for the same night. There are several short time scale events that are at the 99% confidence (2.8$\sigma$) level. The night begins with an increase of ∼0.05 mag in ∼30 min (2.8$\sigma$) labeled A, followed by a more gradual increase of ∼0.05 mag spanning ∼1.5 hours. A gradual decrease of 3.9$\sigma$ is observed over the same length of time. These two events together are labeled B. Two more 30 min events (labeled C) occur at the 2.8$\sigma$ and 3.9$\sigma$ levels respectively before the end of the night.

By combining the information in both light curves, from two different telescopes, together with the precision measurements in the bottom panels, each event can be further confirmed. It is important to note that the V-band data will show a similar event with a larger amplitude. The event labeled A in both light curves for 10 April was barely under the 3$\sigma$ level in the R-band. Its clear presence in the V-band confirms the variability in the R-band. The inclusion of the event labeled B was to show that not all events are consistently reproduced. The poor S/N in V-band, evident from the bottom panel, combined with the longer exposure times resulted in an event that was not verified by the data in the other filter. The final event, C, is apparent in both filters with the hint of a "shoulder" being reproduced at the very end of the night. Even though the amplitude of the "shoulder" is below the 3$\sigma$ level, its reproduction in both filters gives credibility to its reality.

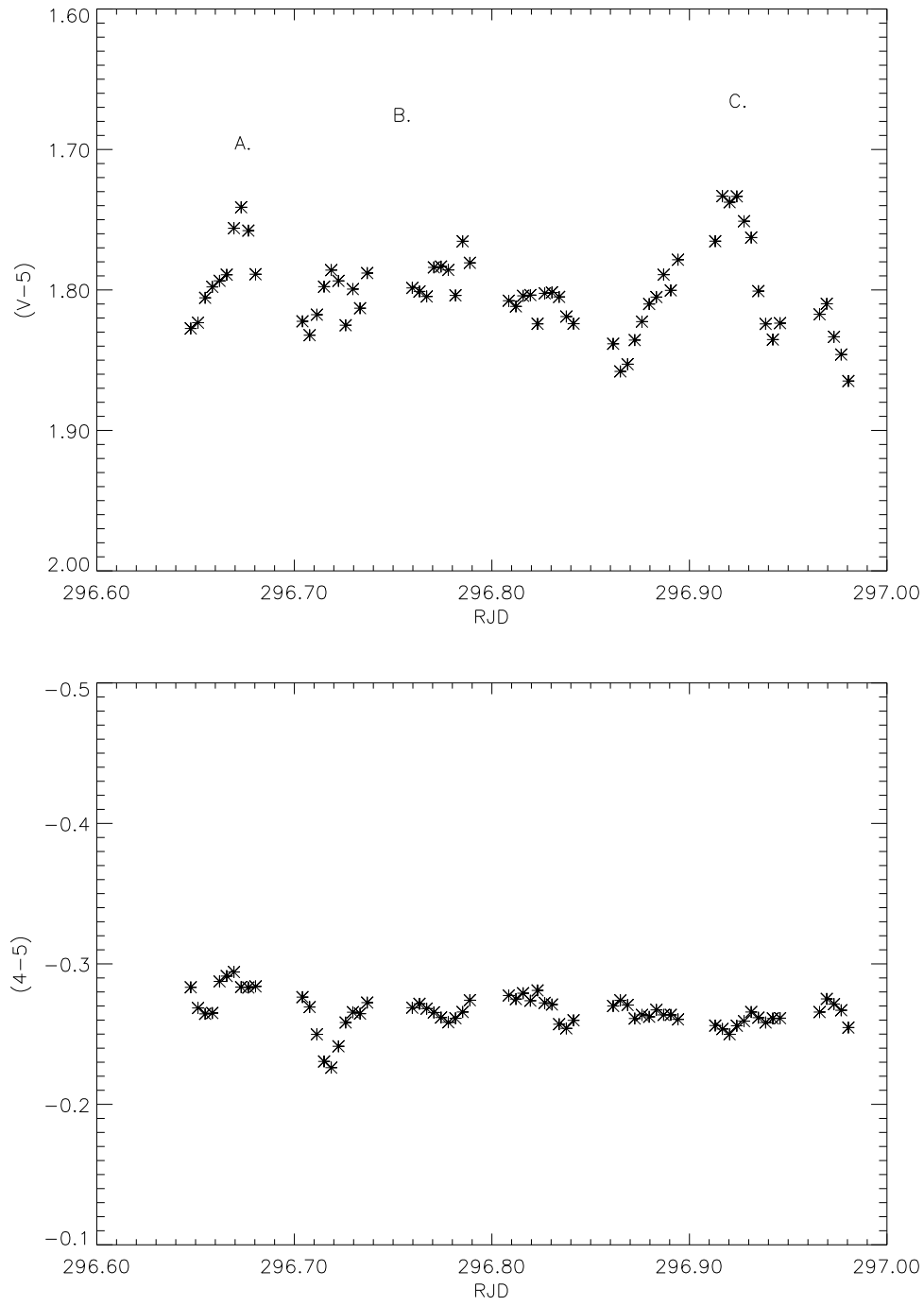


FIGURE 3.3: Observations from 10 April 2010. *Top* Object light curve. *Bottom* Check 4-Check 5 light curve. Data taken with the Lowell 42" telescope.

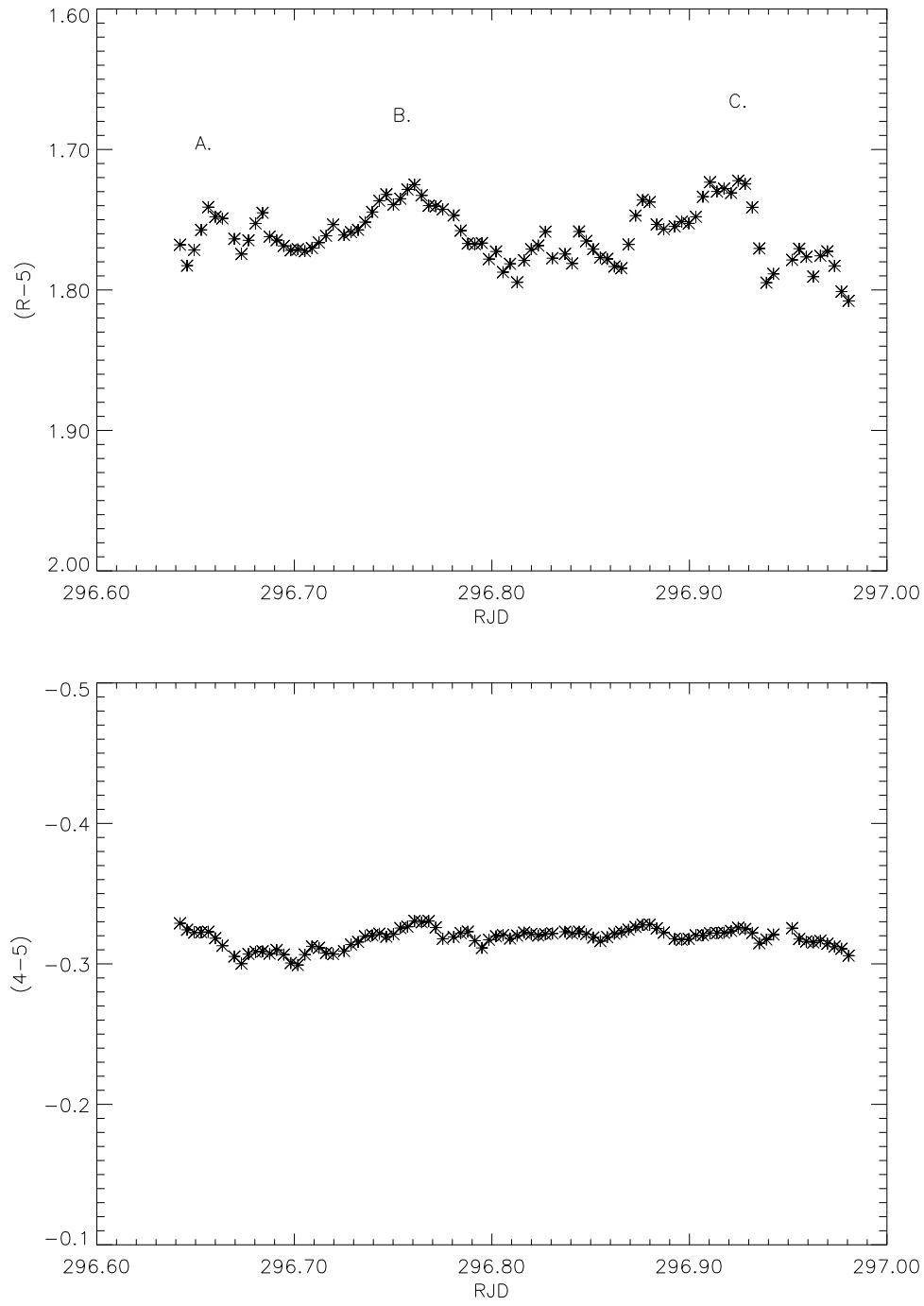


FIGURE 3.4: Observations from 10 April 2010. *Top* Object light curve. *Bottom* Check 4-Check 5 light curve. Data taken with the Lowell 31" telescope.

The V-band data for 11 April 2010 given in Figure 3.5 begin $\sim$0.1 mag brighter than the night before and displays several examples of microvariability that are well above the $3\sigma$ detection level. There is a large ($4.5\sigma$) increase in brightness followed by a decrease of $\sim 3\sigma$ with a total event time of $\sim$1.7 hours. It is quickly followed by another decrease in brightness of $\sim$0.11 mag ($3.5\sigma$) lasting $\sim$40 min. These three changes in brightness make up the event labeled B. There is a recovery in magnitude of $\sim$0.08 that falls just short of the 99.5% confidence level at $2.6\sigma$ (labeled C).

The excellent S/N observations in R-band allow almost continuous confirmation of microvariable events for 11 April 2010 as seen in Figure 3.6. One positive detection after another begins to hint at the possibility of oscillatory behavior superimposed on a gradual increase and decrease in brightness. Each change in magnitude greater than 0.04 is a microvariability detection at the 99.5% confidence level. The general increase in brightness (from the beginning of the night through A to the beginning of B) is $\sim$0.18 mag spanning the first $\sim$2.5 hours of the night and the later decline (all of B up to C) is $\sim$0.15 mag lasting a similar amount of time. These correspond to a $12.9\sigma$ change for the former and a $10.7\sigma$ change for the latter! The final event labeled C shows an equal increase and decrease in brightness of $\sim$0.09 with a total event time of $\sim$1 hour.

The poor S/N in the V-band does not allow the $3\sigma$ confirmation of the event labeled A, however, the clear reproduction of this event in R-band where the S/N is high does suggest that A is a real detection of microvariability. The extended event labeled B shows the beginning of the oscillatory behavior overlaying a general decrease in brightness. Again,

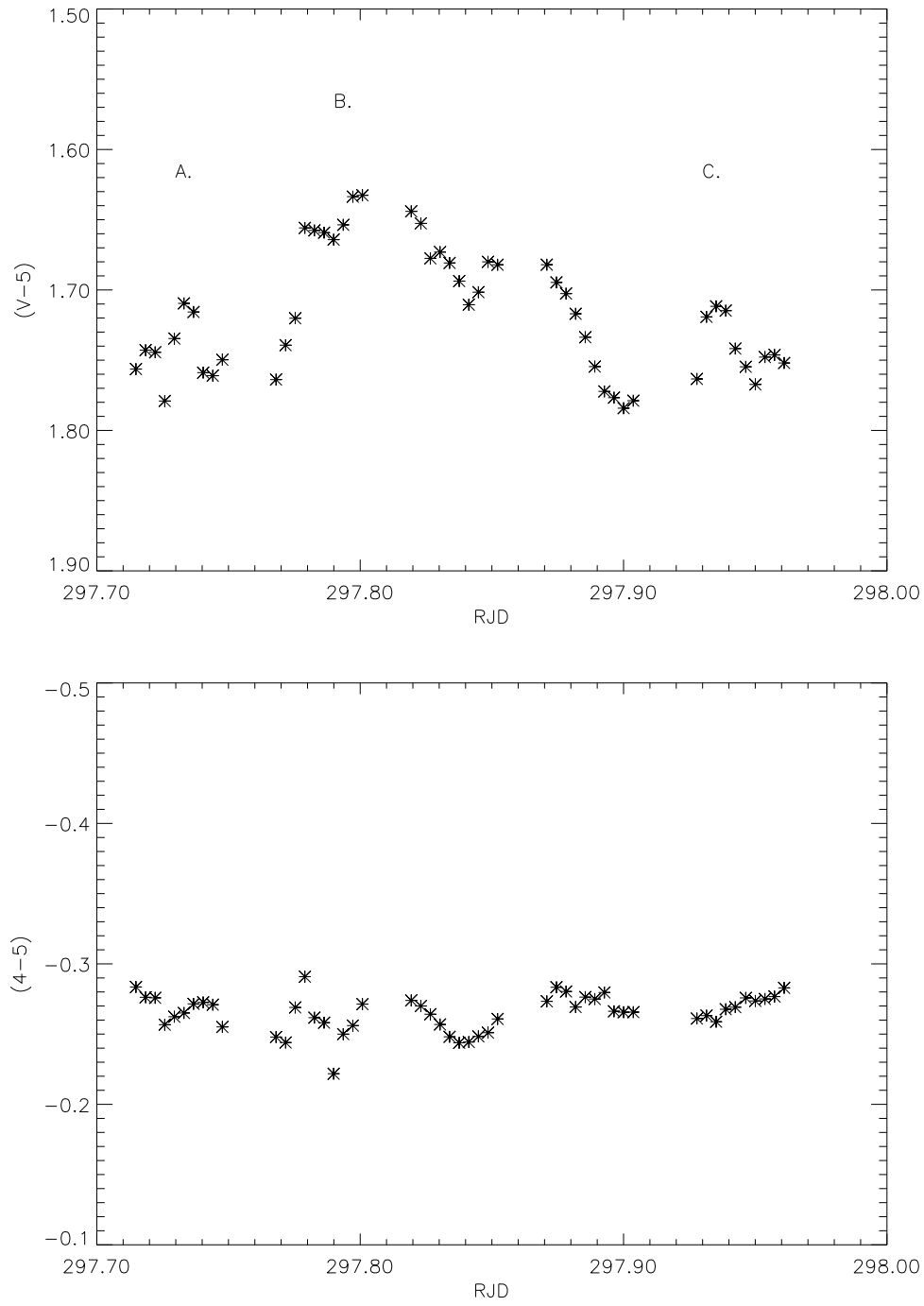


FIGURE 3.5: Observations from 11 April 2010. *Top* Object light curve. *Bottom* Check 4-Check 5 light curve. Data taken with the Lowell 42" telescope.

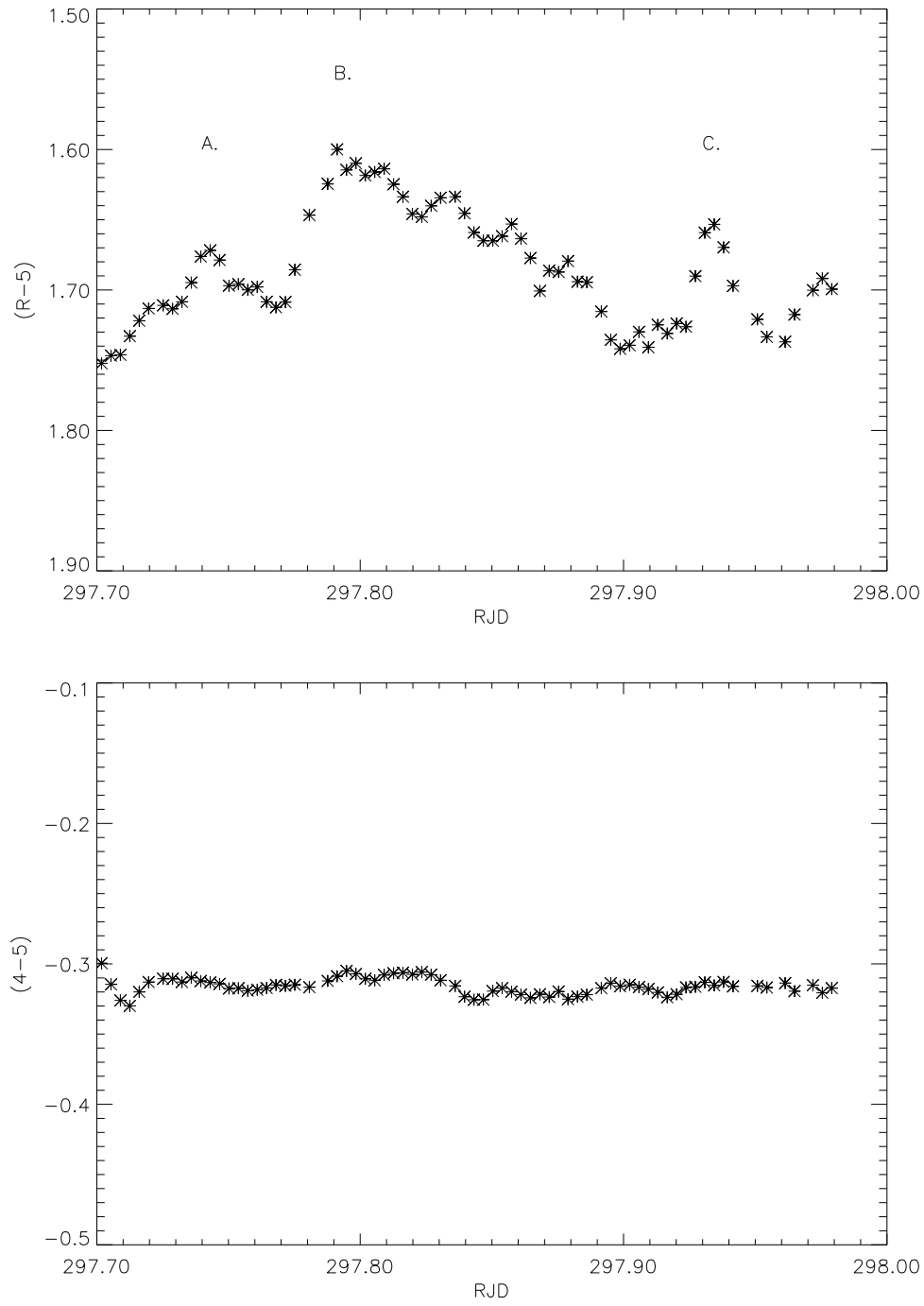


FIGURE 3.6: Observations from 11 April 2010. *Top* Object light curve. *Bottom* Check 4-Check 5 light curve. Data taken with the Lowell 31" telescope.

the R-band has the better S/N and sampling rate as seen in the bottom panel. The possible periodicity or quasi-periodicity for these data will be discussed in Section 3.2. The last event, labeled C, is just below the 99.5% confidence level in V-band, but is well above this level in R-band ($6.4\sigma$) thus the event is real.

Dramatic variability was observed the night of 12 April 2010 in both V- and R-band as seen in Figure 3.7 and Figure 3.8 respectively. In the V-band, the night begins $\sim$0.15 mag brighter than the previous night and in the first 4.6 hours shows a decline of $\sim$0.36 mag ($11.1\sigma$). Superimposed on that decline is four seperate positive detections of microvariability (event A through C). A general increase of $\sim$0.20 mag was observed over the next 3.6 hours ($6.2\sigma$) with two more confirmations of microvariabilty overlayed (event labeled D). Again, the possibility of periodic behavior is evident as discussed in Section 3.2.

The R-band observations in Figure 3.8 begin $\sim$0.1 mag brighter than the end of the previous night and emulate the same general trends that the V-band data present. There is a decrease in brightness of $\sim$0.26 mag for the first 4.6 hours with five superimposed microvariability detections (beginning of the night through C). The next $\sim$3.1 hours are characterized by a general increase in brightness of $\sim$0.15 mag and four embedded mircrovariability detections (event labeled D). The observations for this night make the most persuasive arguement for periodicity which will be discussed in Section 3.2.

The events labeled A, B, and C occur with high enough S/N in both filters to stand alone without the need for confirmation from the other telescope. The event labeled D stretches across the last half of the night. In the V-band, the first portion of D is not sampled at a

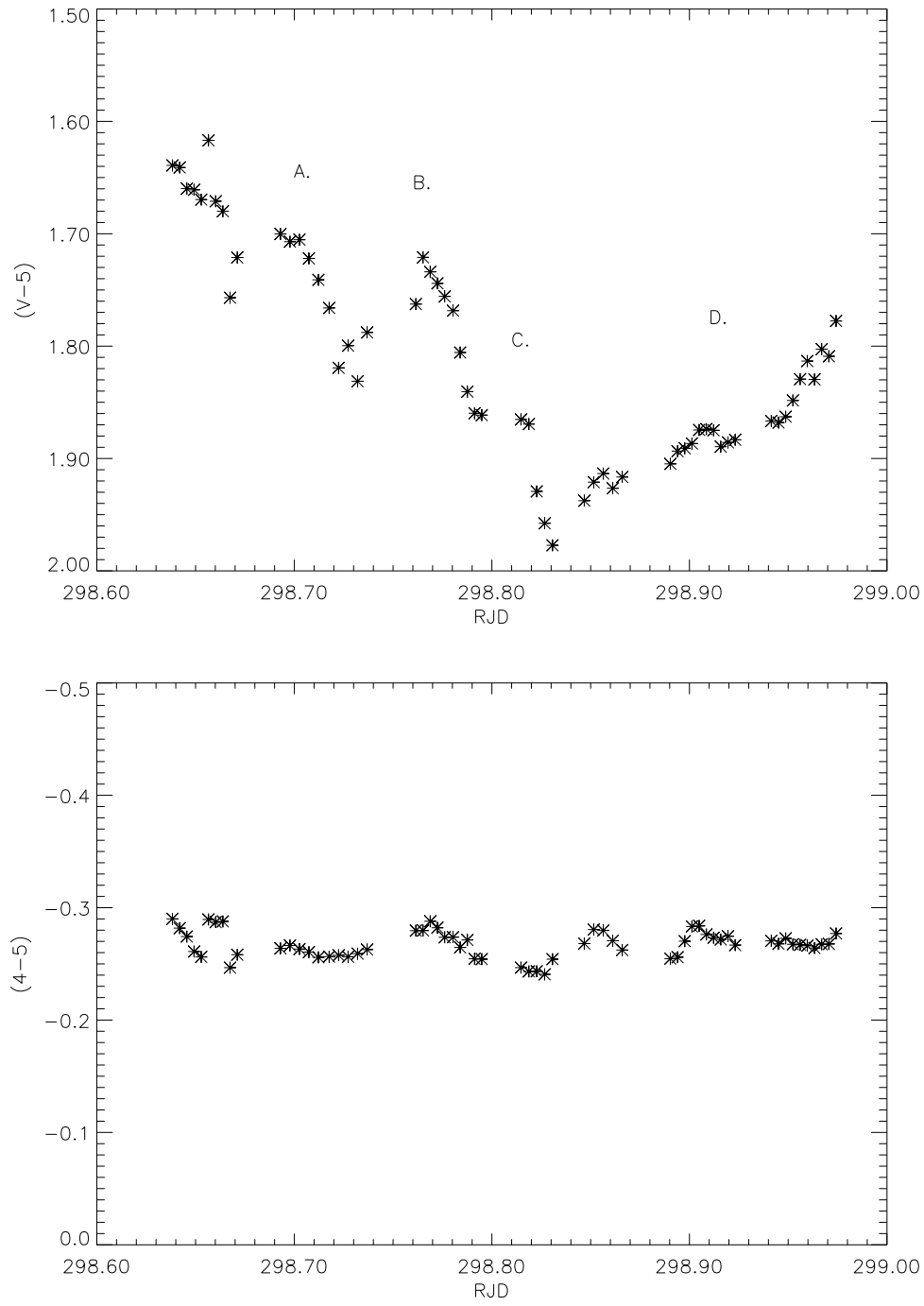


FIGURE 3.7: Observations from 12 April 2010. *Top* Object light curve. *Bottom* Check 4-Check 5 light curve. Data taken with the Lowell 42" telescope.

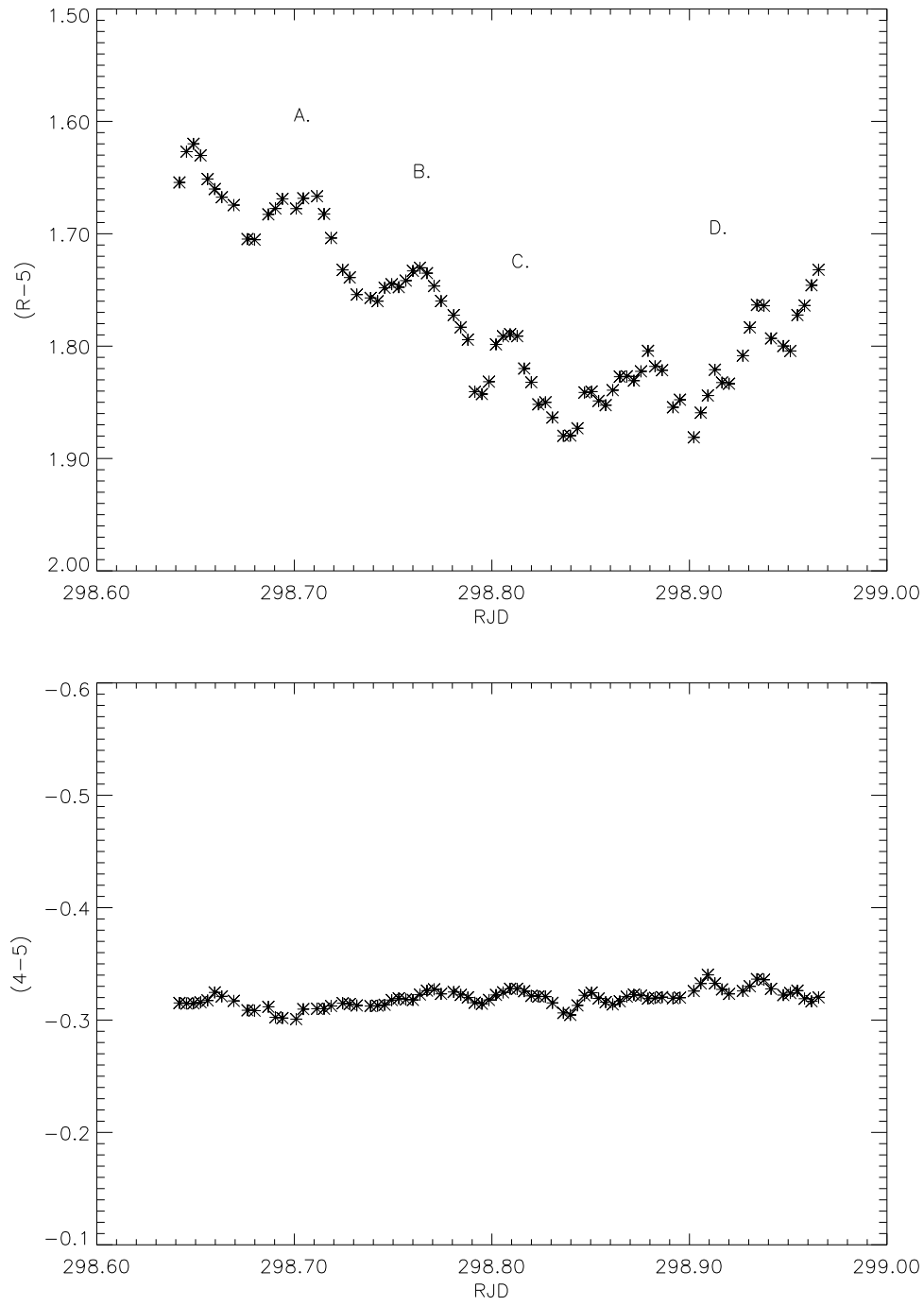


FIGURE 3.8: Observations from 12 April 2010. *Top* Object light curve. *Bottom* Check 4-Check 5 light curve. Data taken with the Lowell 31" telescope.

high enough resolution to produce the structure seen in the R-band. In the R-band, there is a peak seen in the second portion of D that appears to be real, but when compared with the variation in the bottom panel and the lack of reproduction in the V-band, it must be dismissed.

### 3.2 Analysis

Two methods of analysis are used in this study to determine the nature of the observed variability: visual inspection and cross-correlation analysis. Visual inspection was used in the discussions in Section 3.1.2 to determine events that were above the 99.5% confidence level and/or whether they were reproduced by the other telescope. Cross correlation functions are used in Section 3.2.1 to examine any lags or leads that may exist between simultaneous observations in different filters.

The cross correlation coefficient was computed by correlating the R- and V-filter light curves. This was done for each night and then for parts of each night. To do this, both filters must have the same number of data points to correlate. A linear interpolation was performed on each filter for each night to ensure equal data set sizes. The cross correlation functions (CCF) for each night are displayed in the top panel with the auto correlation function (ACF) for each filter plotted below. The nights with confirmed microvariability are shown here. The data for the other nights of observations are given in the appendices. The ACF are the CCF of each filter with itself. By definition the ACF will always have a maximum value of 1 with 0 lag.

### 3.2.1 Cross Correlation Function

The CCF for the entire night of 10 April 2010 shows no lag between the R- and V-filter with a notable correlation as seen in the top portion of Figure 3.9. The "wings" that extend past ±0.1 should be ignored. The increase in correlation seen is due to the effects of very few points being correlated when the lag is large. The R- and V-filter ACF are displayed respectively below the CCF.

Figure 3.10 plots the CCF for portions of the night. The data train was divided into three smaller data sets of ∼0.1 of a day with some overlap. The purpose is to provide yet another confirmation of small amplitude variations. Since small portions of the night are being analyzed, the "wings" extending past ±0.05 should be ignored due to the few data points that are being correlated. The first portion of the night does not show a strong correlation, but this was expected from the discussion of the 10 April light curves in Section 3.1.2. The second and third portions of the night have strong peaks with correlation coefficients larger than the overall coefficient for the entire night. The third portion of the night has the highest correlation giving another confirmation of the reality of the "shoulder" mentioned in Section 3.1.2. There is no lag observed for any portions of the night.

The CCF for 11 April 2010, shown in the top panel of Figure 3.11, shows a strong correlation coefficient centered at 0 lag. Again the "wings" extending past ±0.1 should be ignored since only a small number of points are being correlated at this lag. The ACF for the R- and V-filter are displayed below.

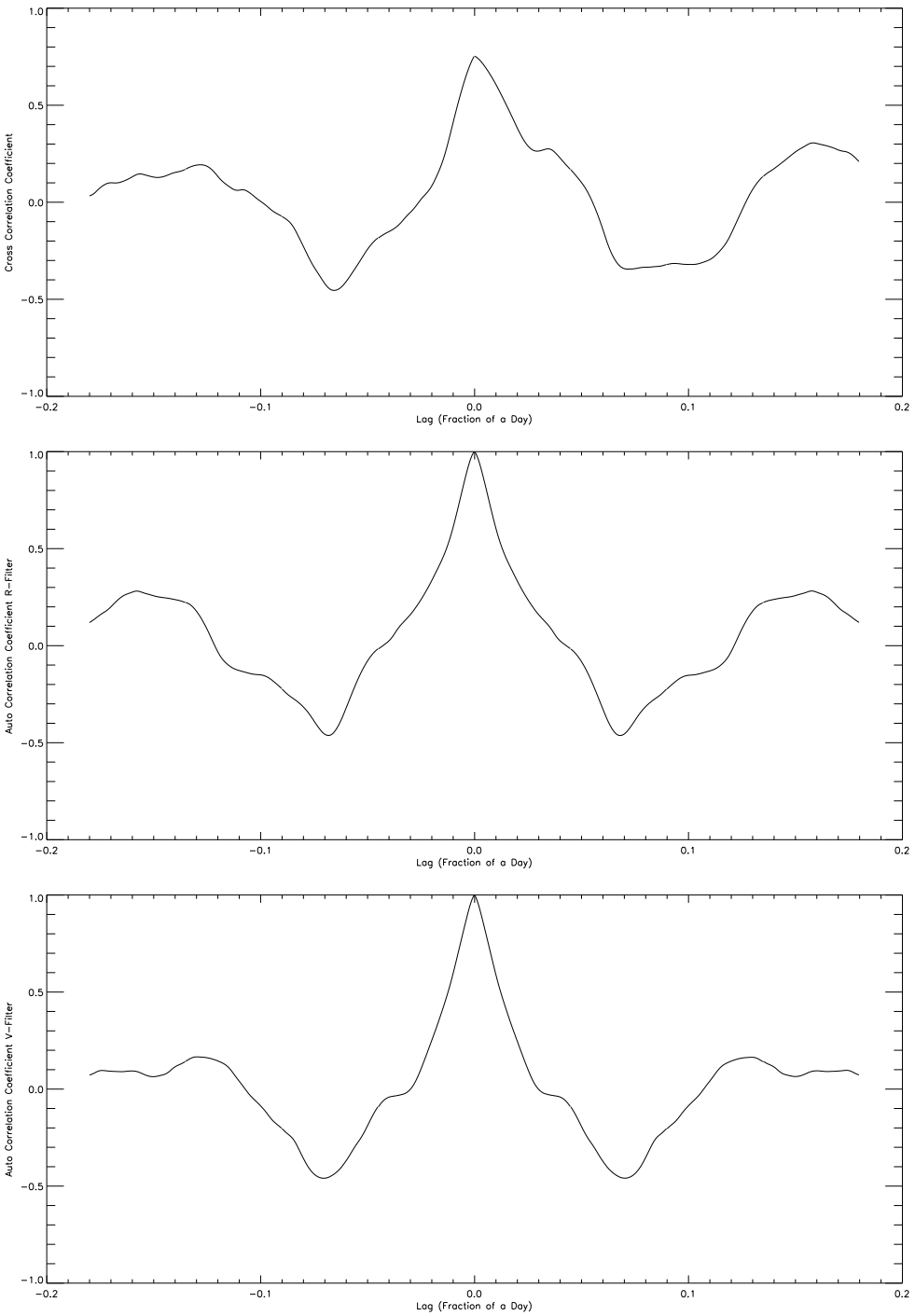


FIGURE 3.9: *Top* Cross Correlation Function for 10 April 2010. *Center* Auto Correlation for R-Filter. *Bottom* Auto Correlation for V-Filter.

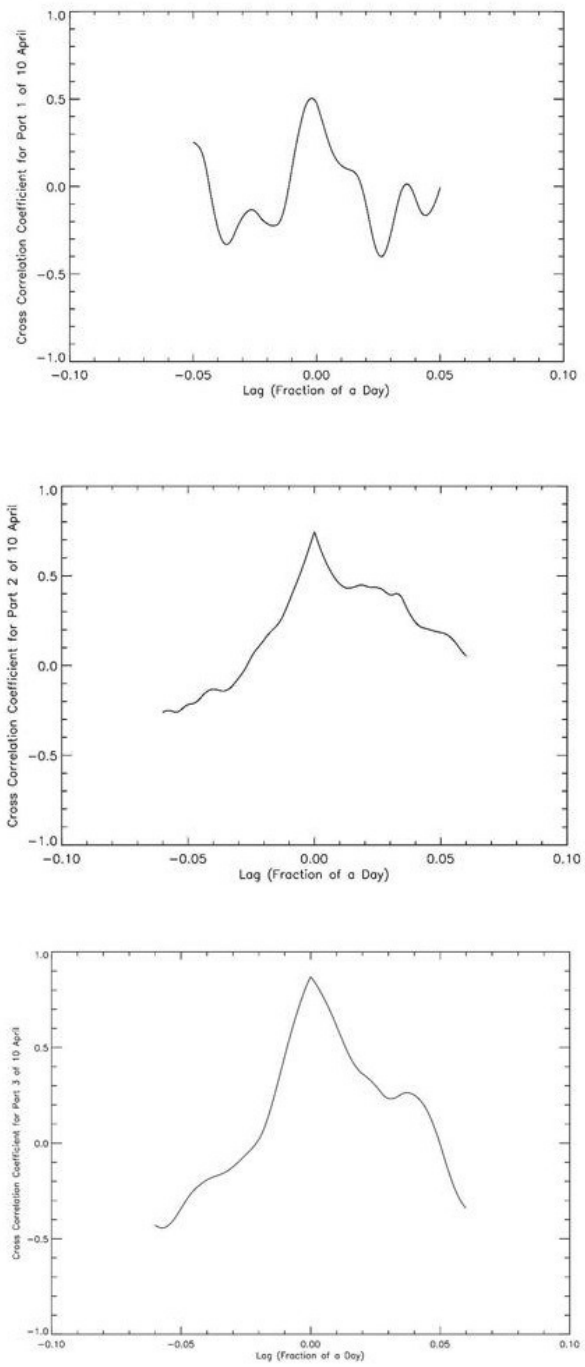


FIGURE 3.10: *Top* Cross Correlation Function for First Part of 10 April 2010. *Center* Cross Correlation Function for Second Part of 10 April 2010. *Bottom* Cross Correlation Function for Third Part of 10 April 2010.

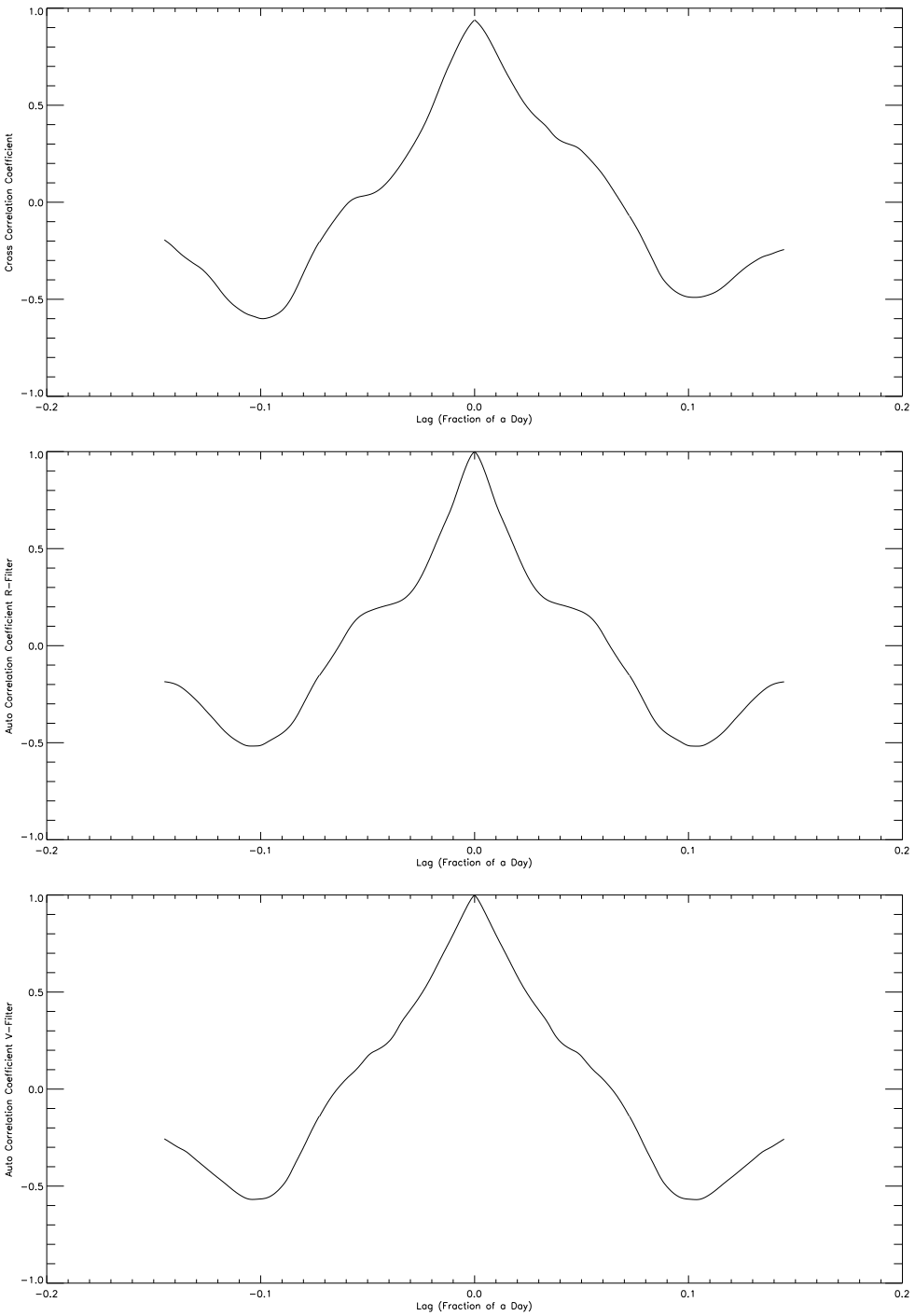


FIGURE 3.11: *Top* Cross Correlation Function for 11 April 2010. *Center* Auto Correlation for R-Filter. *Bottom* Auto Correlation for V-Filter.

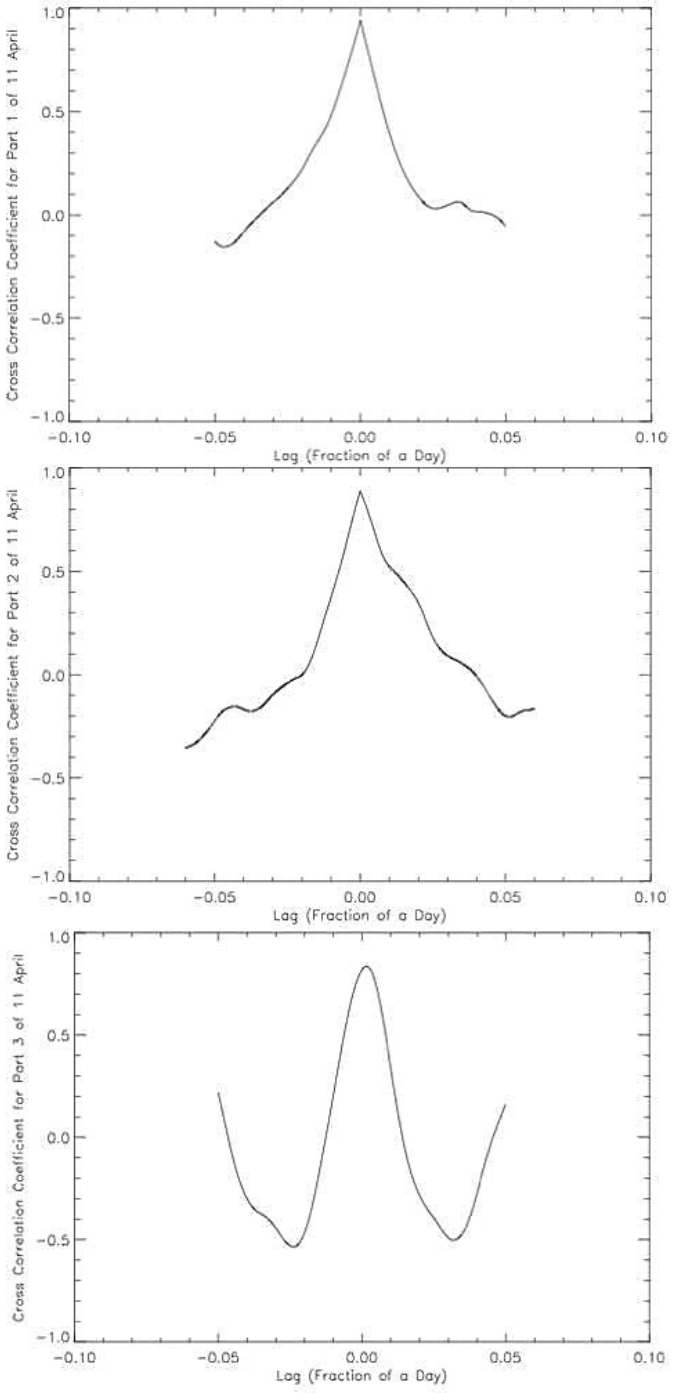


FIGURE 3.12: *Top* Cross Correlation Function for First Part of 11 April 2010. *Center* Cross Correlation Function for Second Part of 11 April 2010. *Bottom* Cross Correlation Function for Third Part of 11 April 2010.

The night of 11 April was also divided into three overlapping portions seen in Figure 3.12. Again the "wings" extending past ±0.05 should be ignored due to too few data points for accurate cross correlation analysis. Each CCF shows a strong correlation with 0 lag. Only the first portion of the night shows a larger correlation coefficient than the CCF for the entire night, but the second and third portions are not much less. The strong correlation for the first portion of the night indicates the event labeled A is indeed a real detection of microvariability.

Figure 3.13 shows the peaked CCF centered at 0 lag and the ACF's for 12 April. The "wings" extending past ±0.1 should be ignored for the reason previously stated. Of the three nights presented in this section, 12 April has the largest correlation coefficient. The FWHM is noticeably larger than the previous nights.

The night of 12 April 2010 was also divided into three overlapping portions as seen in Figure 3.14. Again the "wings" extending past ±0.05 should be ignored due to too few data points. This division was choosen to examine the "decline", "valley", and "incline" independently of each other. The correlation coefficient of the entire night was greater than any of the individual portions. However, the first and second portions of the night had a correlation coefficient within 3% of the coefficient for the entire night. A lower coefficient was expected for the third portion of the night due to the reasons discussed in Section 3.1.2.

### 3.2.2 Possible Periodicity

From visual inspection oscillatory behavior is clearly seen in the light curves for 12 April and possibly 11 April. To analyze the data for possible periodicity a Lomb Normalized

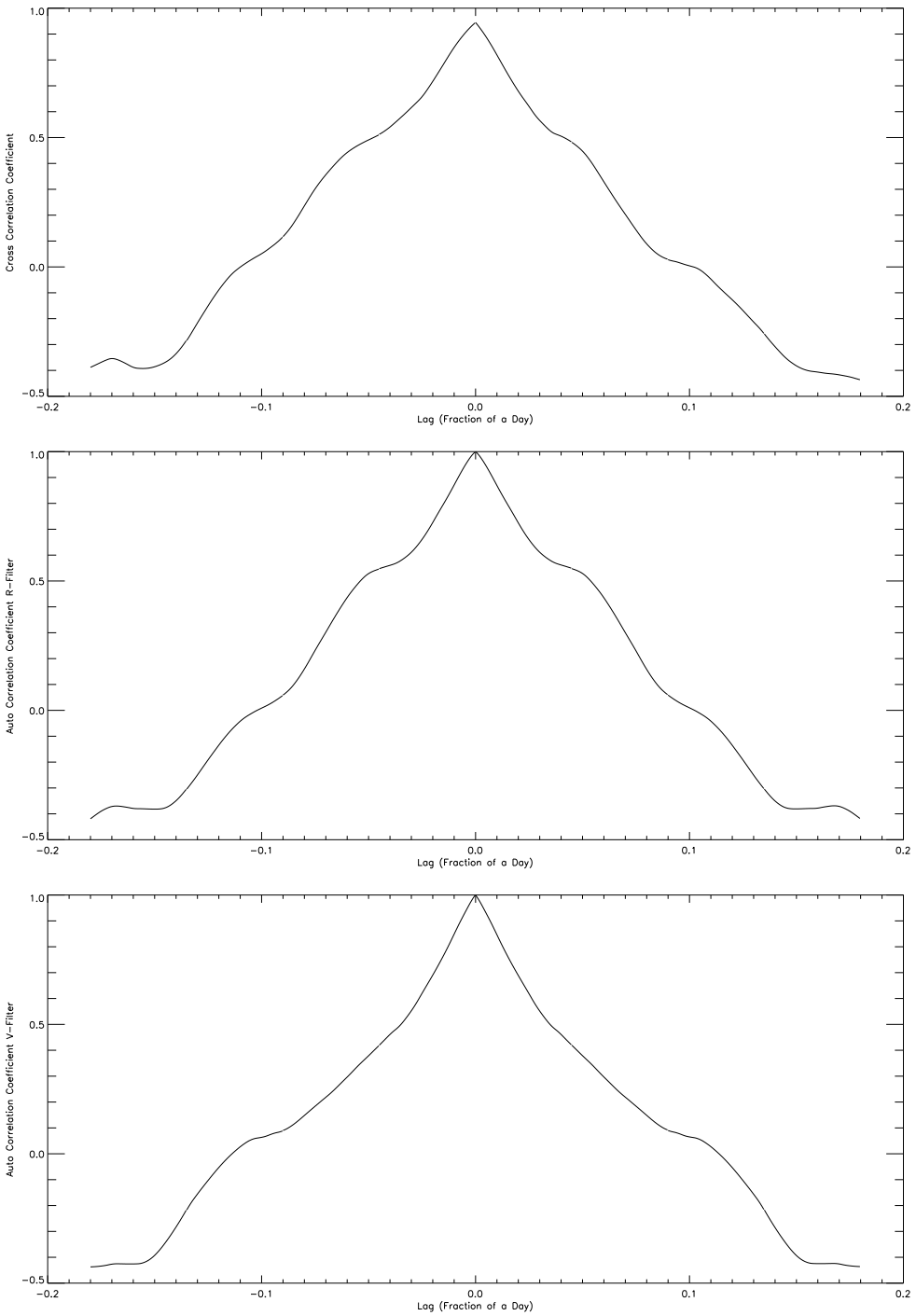


FIGURE 3.13: *Top* Cross Correlation Function for 12 April 2010. *Center* Auto Correlation for R-Filter. *Bottom* Auto Correlation for V-Filter.

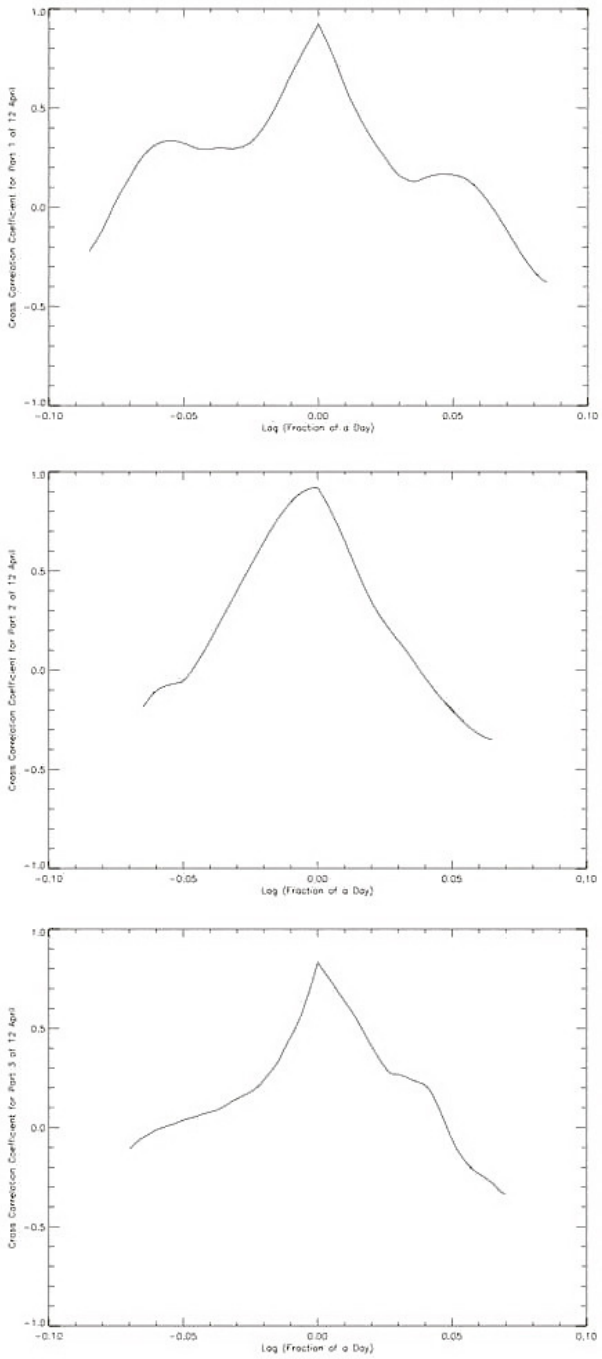


FIGURE 3.14: *Top* Cross Correlation Function for First Part of 12 April 2010. *Bottom* Cross Correlation Function for Second Part of 12 April 2010.

Periodogram (LNP) program was utilized in IDL. Created by Lomb in 1976 and refined by Scargle in 1982, this period searching program is useful for data that are unevenly sampled. A false alarm probability (FAP) can be calculated by

$$P(> z) = 1 - (1 - e^{-z})^M \tag{3.1}$$

This equation states that if M frequencies are scanned for periodicity, the probability that none of them give a value larger than z is P. In general the value chosen for M is twice the number of data points.

**Throughout the rest of this section, the term "period" will refer to the time scale of oscillation for a portion of data. This "period" may change from night to night or cease to persist completely.**

The strongest data set to suggest possible periodicity is the R-band observations taken on 12 April. These data have a high sampling rate combined with the best S/N. By visual inspection the period appears to be between 0.05 and 0.07 days. To isolate the smaller amplitude variability, the larger trend was removed by fitting a sine curve to the data, removing the general decrease and increase in brightness as seen in Figure 3.15 represented by the dotted line.

The LNP program was used to analyze the result of the detrended data and found a period of $0.056 \pm 0.004$ days with a FAP of $10^{-6}$. The periodogram is given in Figure 3.16.

In Figure 3.17 the data set is phased to the period of 0.056 days found by the LNP test to inspect the overall agreement level of the data with this period. A sinusoidal shape is seen in the figure indicating the reality of the period.

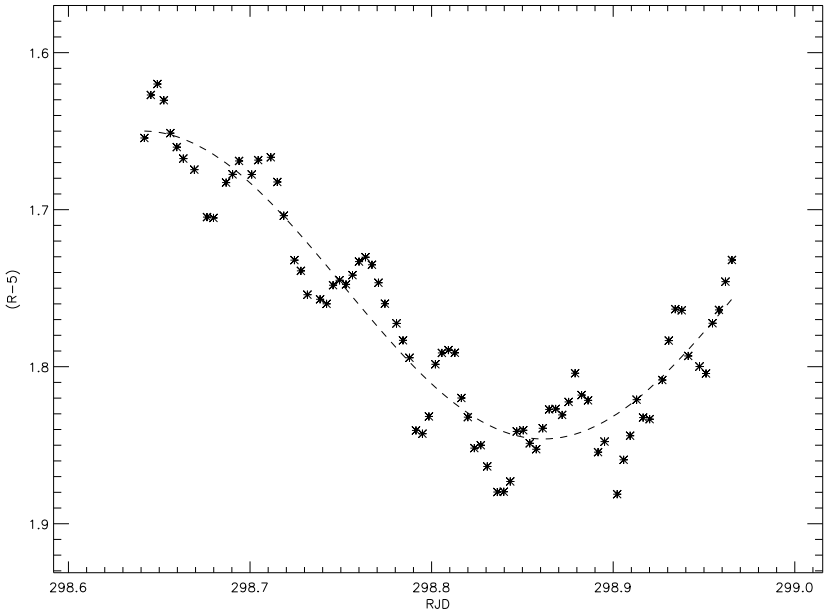


FIGURE 3.15: The dotted line represents the detrend performed on the R-filter observations taken on 12 April 2010.

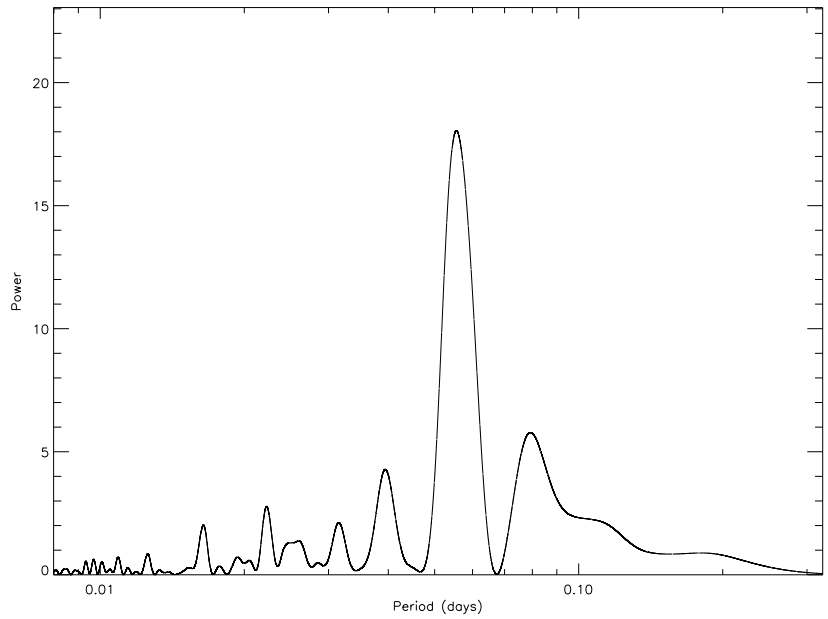


FIGURE 3.16: Periodogram for the detrended R-filter observations taken on 12 April 2010.

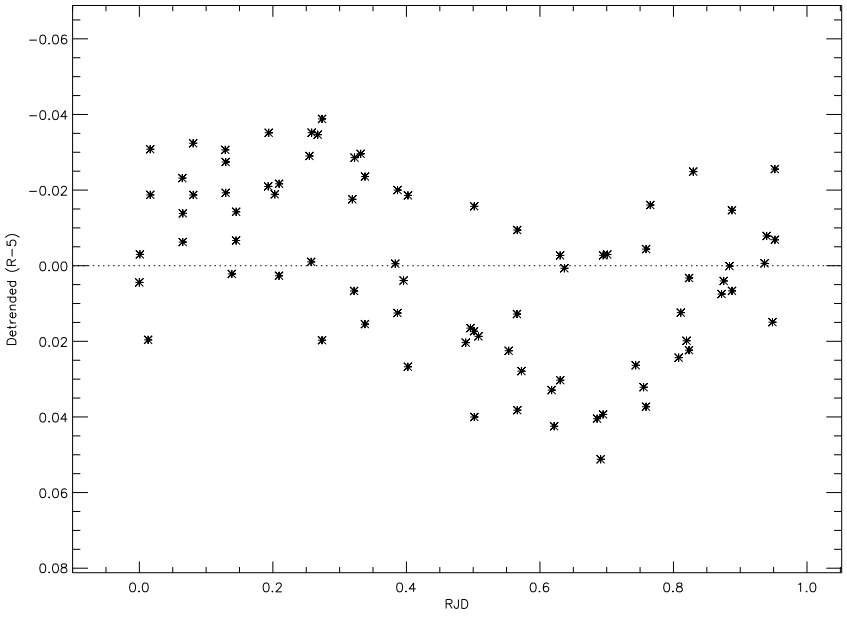


FIGURE 3.17: The data phased to the period found from the periodogram for the R-filter observations taken on 12 April 2010.

In order to confirm the periodicity seen in the R-filter, the V-filter data for the 12 April are analyzed in the same manner. The larger trend is removed from the V-filter data by fitting it to a sine curve, represented by the dotted line in Figure 3.18. The fit to these data is not as tight because of the larger amplitude of variations.

Using the LNP program, the data were analyzed for periodicity. Since the fit of the sine curve was not as good for these data, the LNP was unable to provide as accurate a result as it did for the R-filter data. The period found here is 0.108±0.050 days with a FAP of 0.01. The large error keeps this period within permissable range of a positive confirmation of periodic behavior.

The detrended data have been phased to the period of 0.108 days found by the LNP. The inability to provide a better sine curve fit to these data forced the larger scatter seen

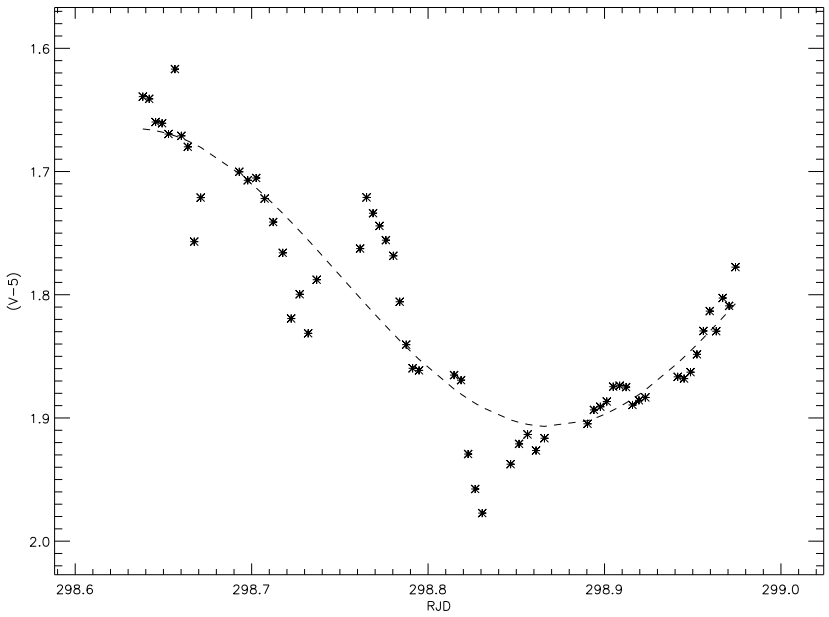


FIGURE 3.18: The dotted line represents the detrend performed on the V-filter observations taken on 12 April 2010.

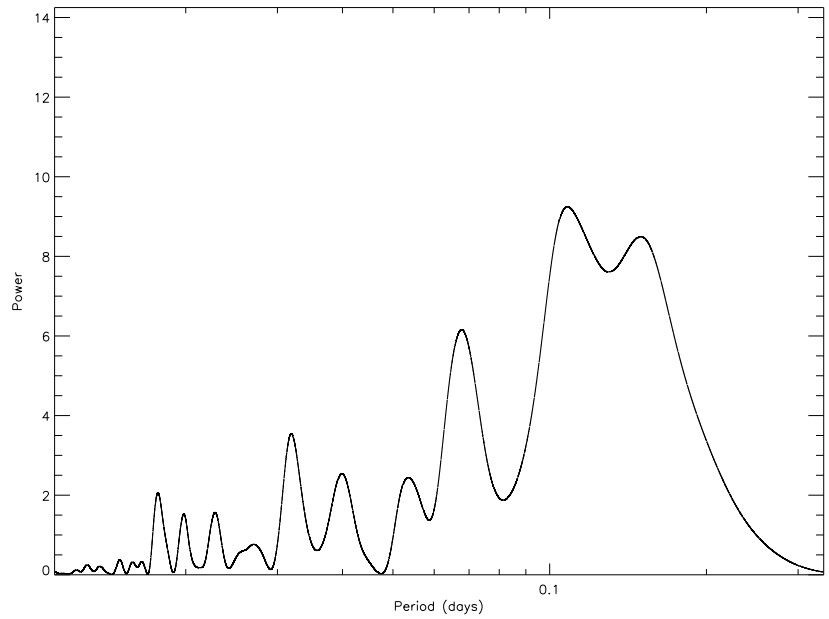


FIGURE 3.19: Periodogram for the detrended V-filter observations taken on 12 April 2010.

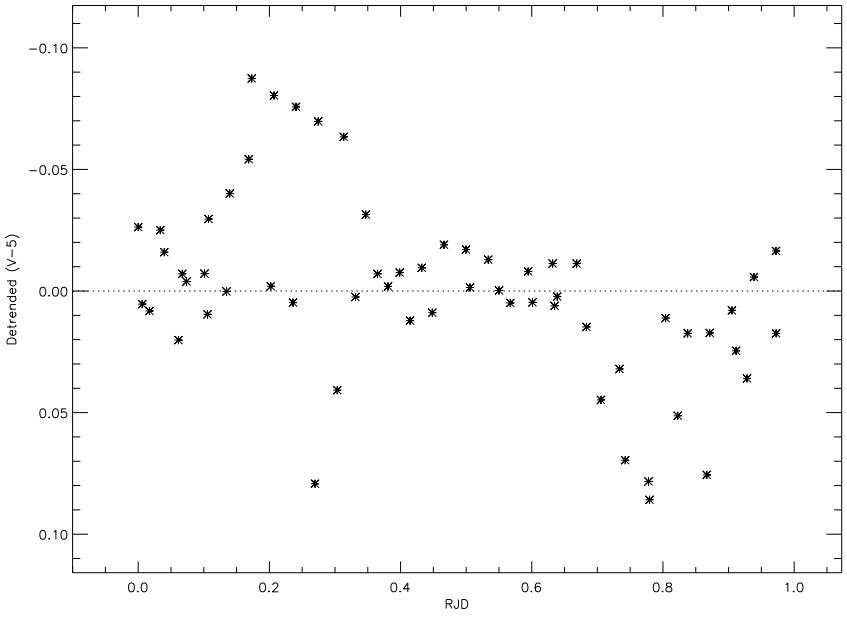


FIGURE 3.20: The data phased to the period found from the periodogram for the V-filter observations taken on 12 April 2010.

in Figure 3.20, however, the sinusoidal shape is still present. The data suggest this is a real detection of periodicity.

The data for 11 April have a distinctly different shape and required a different method of detrending. The R-band light curve for this night had only one major deviation labeled B in Figure 3.6. This larger event was removed using a linear fit in order to analyze the superimposed smaller amplitude oscillatory variations. The detrended portion is represented by the dotted line seen in Figure 3.21. Figure 3.22 shows the light curve after the linear trend has been removed.

The process of searching for a period for 11 April was different as well. The entire data set was analyzed by the LNP program for periodicity. The largest peak seen in Figure 3.23 (near $\sim$0.2 days) is a false detection. The program is most likely reading the first and

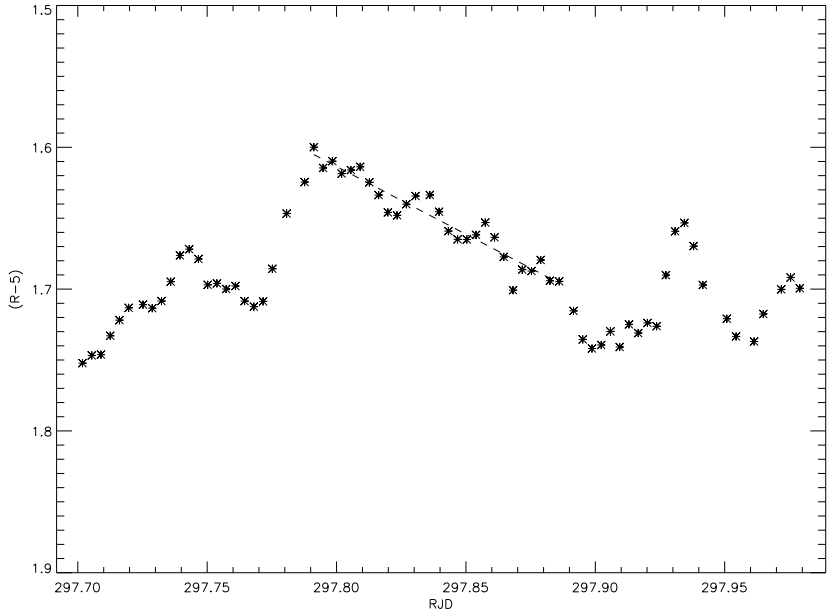


FIGURE 3.21: The dotted line represents the detrend performed on the R-filter observations taken on 11 April 2010.

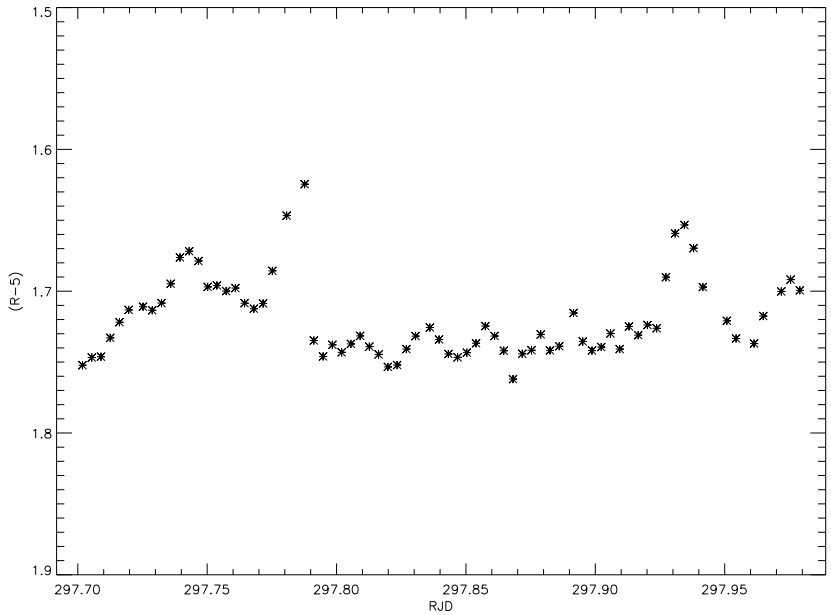


FIGURE 3.22: The data after the trend has been removed for the R-filter observations taken on 11 April 2010.

final events, labeled A and C in Figure 3.6, because of their larger amplitude. Another reason for disregarding this peak in the LNP is because only one period of this size can fit within the length of observations for this night (0.3 days). The second largest peak occurs at 0.049±0.003 days. This period appears to be a convolution of the two major events previously mentioned, residual data points from the detrending, and one of the smaller amplitude events.

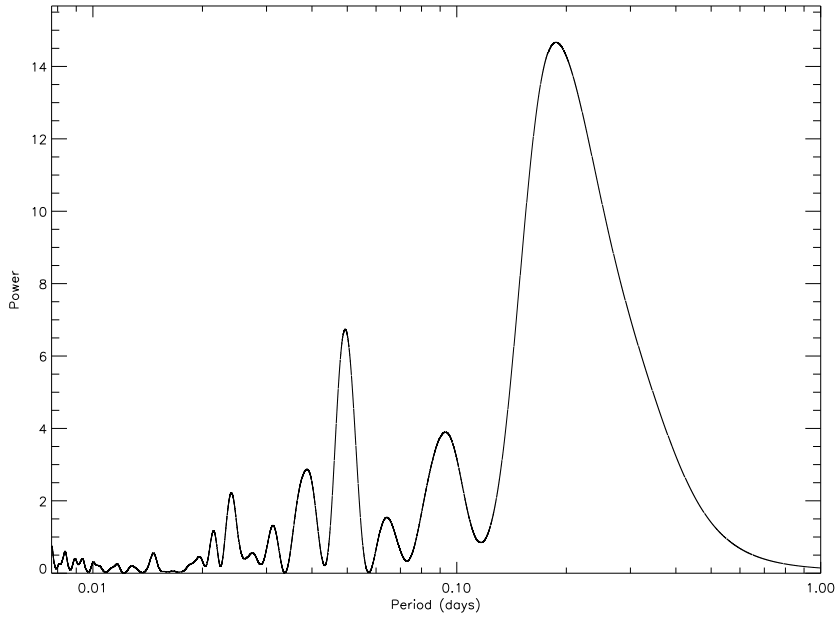


FIGURE 3.23: Periodogram for all of the detrended R-filter observations taken on 11 April 2010.

The larger amplitude events are overpowering the smaller changes in magnitude. In order to truely analyze the portion of the data that exhibit oscillatory behavior, only the detrended section of data were used in the LNP program. Figure 3.24 is the resulting periodogram showing a strong peak at 0.024±0.002 with a FAP of 0.03. Although this period differs from the one found for 12 April, it is visually consistent with the light curve.

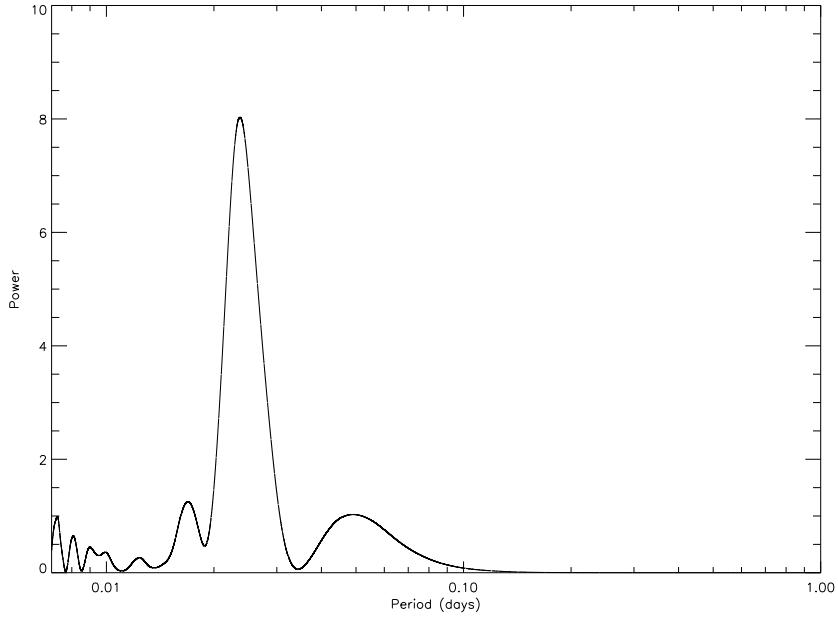


FIGURE 3.24: Periodogram for the detrended portion of R-filter observations taken on 11 April 2010.

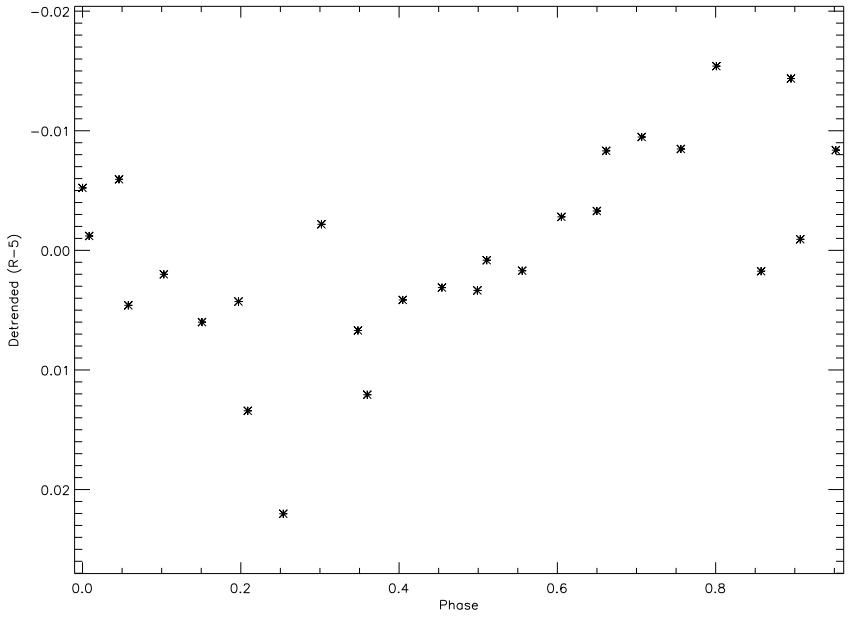


FIGURE 3.25: The detrended portion of the data phased to the period found from the periodogram for the R-filter observations taken on 11 April 2010.

To test the validity of the 0.024 day period, the data for the detrended portion were phased to that period as seen in Figure 3.25. There is a definite sinusoidal shape to the data meaning a valid period was found. As a test, the entire night's data were phased to the longer 0.049 day period, but there was no coherence to the folded light curve. The abscence of a trend in the data further proves 0.049 was a false period detection.

The V-band data were detrended in the same manner as the R-band data for 11 April. The portion to be detrended is seen as the dotted line in Figure 3.26. The resulting light curve to be analyzed is given in Figure 3.27. Due to poor S/N and sampling, visual inspection fails to immediately identify a clear period.

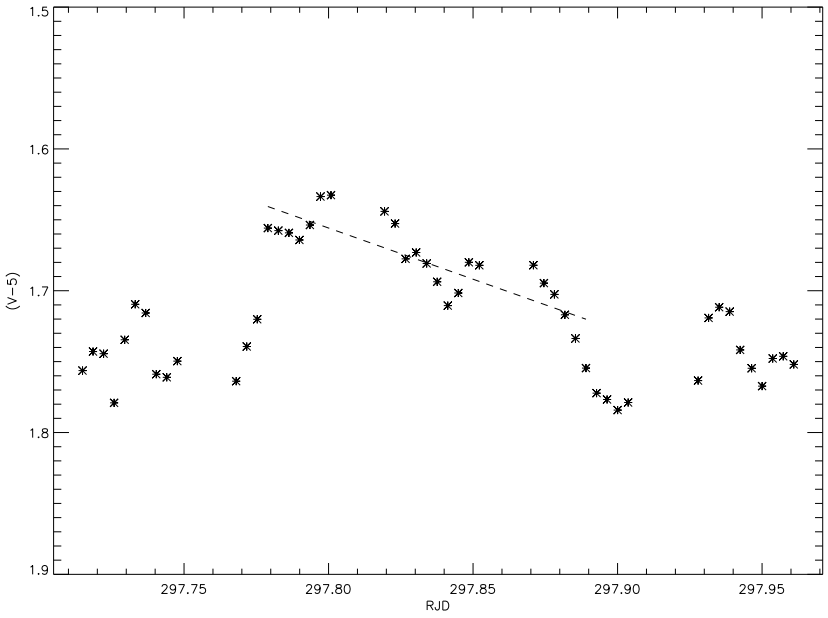


FIGURE 3.26: The dotted line represents the detrend performed on the V-filter observations taken on 11 April 2010.

The data for the entire night were analyzed using the LNP program. Figure 3.28 shows the resulting periodogram with two peaks having almost the same power. The detection of

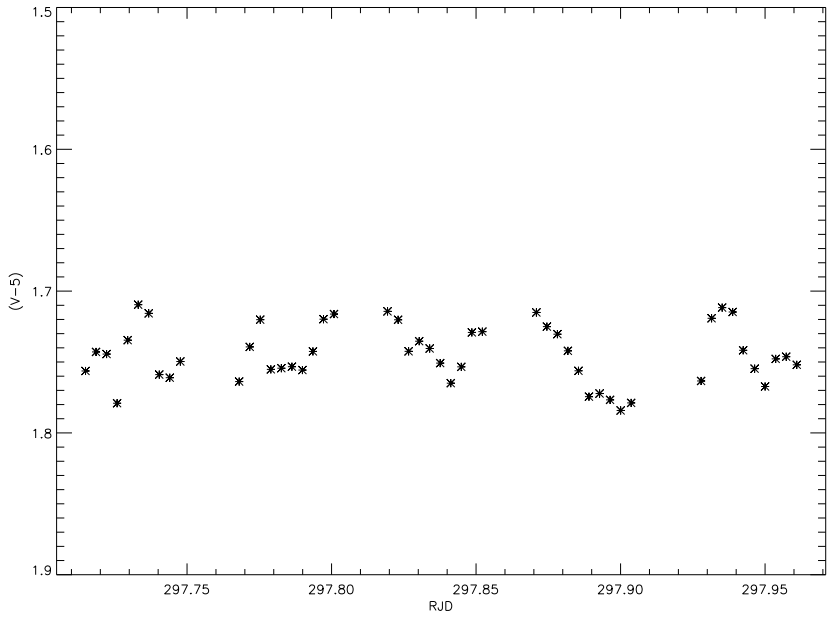


FIGURE 3.27: The data after the trend has beena removed for the V-filter observations taken on 11 April 2010.

a period of ∼0.06 days stems from the poor sampling mentioned previously as well as the overpowering of small amplitude events by larger ones. The second peak seen at a period of 0.029±0.001 days is consistent with the period found for the R-band data. There are several other noteworthy peaks occuring at periods of less than 0.025 days in this periodogram, but they are likely aliases of the first two peaks.

To be consistent between filters, only the detrended section of data were analyzed using the LNP. The periodogram, seen in Figure 3.29, has two prominent peaks as well. Their periods are slightly shorter than the period for the overall data. The peak seen at ∼0.06 days is a false detection for the reasons previously discussed. In addition, the inability to complete more than one period within the length of the data set is a valid reason to discard this period detection. The second peak occurs at a period of 0.026±0.002 with a FAP of 0.22.

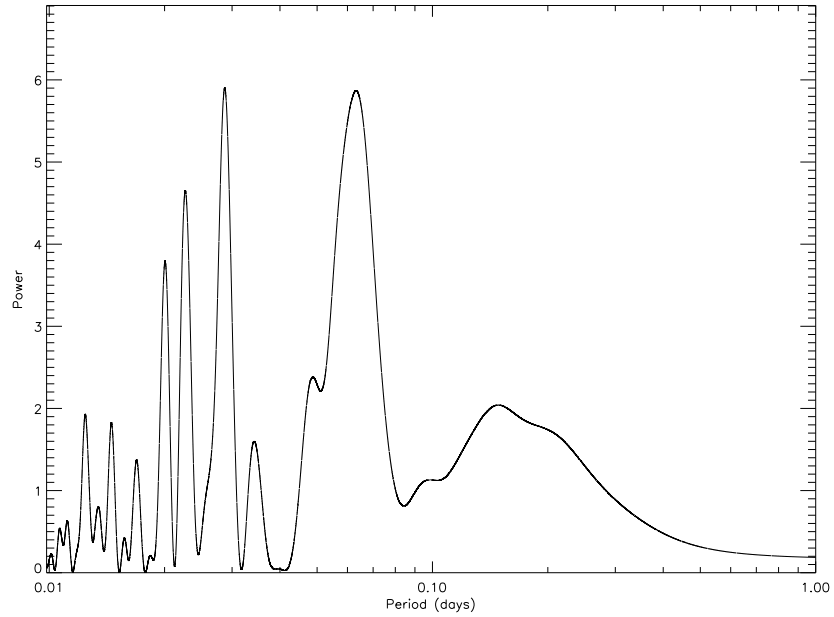


FIGURE 3.28: Periodogram for all of the detrended V-filter observations taken on 11 April 2010.

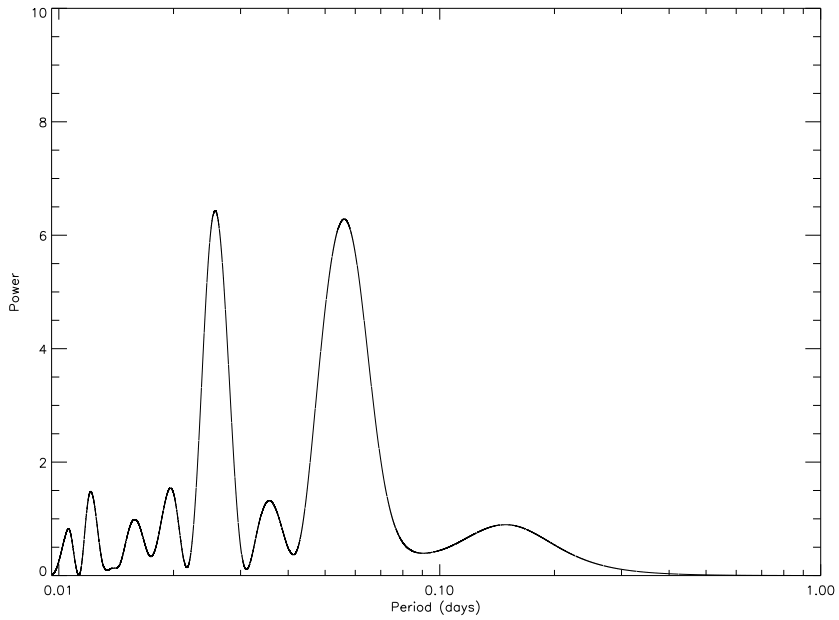


FIGURE 3.29: Periodogram for the detrended portion of V-filter observations taken on 11 April 2010.

The period found from the entire night of data and the period found from the detrended

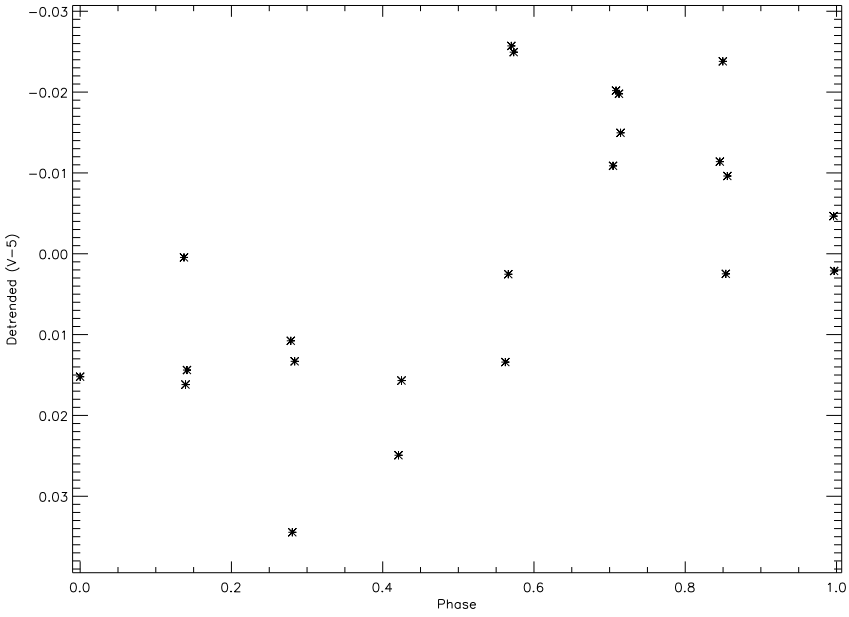


FIGURE 3.30: The detrended portion of the data phased to the period found from the periodogram for the V-filter observations taken on 11 April 2010.

portion of data are within the error bars of each other confirming the detection of periodic behavior.

To test the reality of the periods, the entire set of data and the detrended portion of data were phase to their respective peak periods. Both showed a strong sinusoidal shape in the folded light curves. Figure 3.30 shows the phased light curve for the detrended portion of data. Even though the FAP is higher for the 11 April V-band data, the R-band data show the same period. The data indicate this is a real detection of periodicity.

Much of the periodic work done for this thesis was completed in collaboration with J. Robert Parks.

### 3.2.3 Color Variability

Because data were taken in multiple filters, color information is available for analysis. Although no correlation was found in the variation of V-R over time, there is a strong correlation in color with respect to magnitude. Each point in Figure 3.31 is a nightly average. There is a linearly decreasing trend apparent. This indicates that as 3C279 became dimmer (increase in R magnitude) the blazar also got redder (increase in V-R).

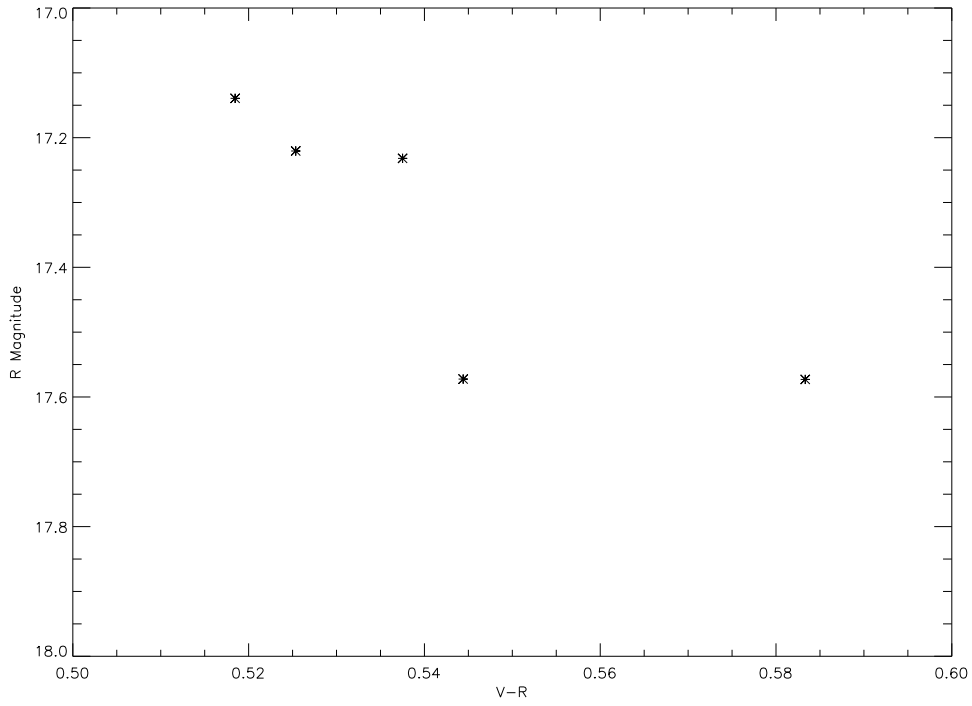


FIGURE 3.31: Each data point represents the average magnitude in V and R for each night. The linear decline is evident.

# – 4 –

# Conclusions & Future Work

## 4.1 Conclusions

As seen from Figure 3.1, 3C279 was in one of the faintest states observed in several decades, but certainly not a quiescent one. Throughout the week of 10-15 April 2010 intense observations of the object were made in V- and R-band showing a 0.4 mag change and a 0.3 mag change respectively. The reality of microvaribility events have been demonstrated using the simultaneous observations from the 31" and 42" telescopes and cross correlation analysis. No lag was seen for any night or portion of a night. The inability to observe confirmed microvariability the last two nights of observations could be due to the low S/N because of the dimness of the object or because the source of the microvariability was not present.

It is difficult to identify the source of microvariability without polarization measurements; however they are not absolutely necessary. An alternative way of connecting microvariability to either the jet or the accretion disk is to compare the amplitude of events in the low state with the amplitude of events in the high state. Because 3C279 is a radio loud object, it is reasonable to assume that the dominant source of radiation in the high state is the jet. It would also be reasonable to believe, in a low state, the next likely contributor to observed radiation would be the accretion disk (Noble & Miller 1996). However, if the amplitude (change in magnitude) of the observed event is independent of the luminosity state (i.e it "scales" with the luminosity) then the source of microvariability is most likely the jet. If the

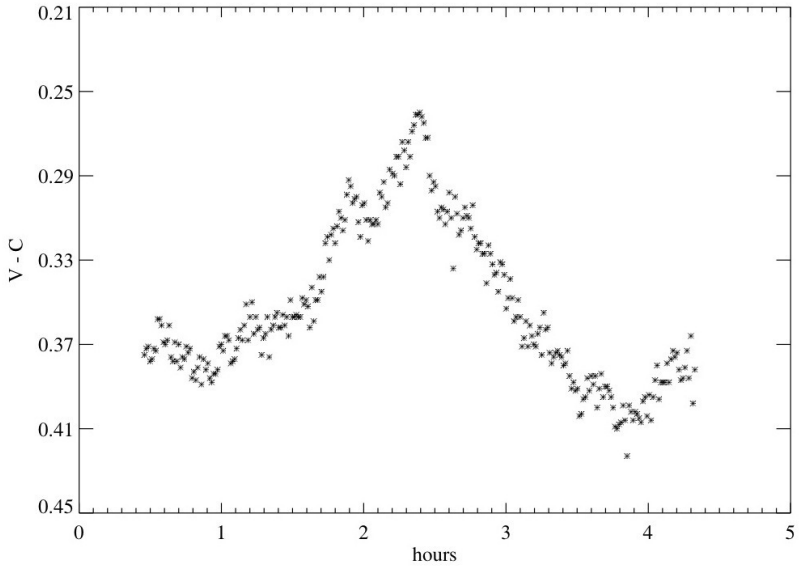


FIGURE 4.1: This event was observed in V-band 10 May 1989 while 3C279 was in a bright state. Figure adapted from Miller et al. (1996).

amplitude (change in magnitude) of variability is dependent upon state (i.e large amplitude in the low state, small amplitude in the high state) then the source is most likely the accretion disk (Miller 2006).

A study of 3C279 performed by Miller et al. (1996) found the object to be in a moderately bright state in May 1989 (V=15.2). Figure 4.1 shows a well sampled large amplitude event that was observed on 10 May 1989. By comparing the amplitude of this event with the amplitude of events from the April 2010 observations, it can be seen that they are of comparable size ($\sim$0.15 mag). This implies that the microvariations are not associated with the accretion disk. The next most likely candidate for the source of microvariability is the jet.

The reality of periodic behavior was tested for in two of the three nights microvariability was observed. The detection of transitory quasi-periodic oscillations in a blazar is similar to that seen by other observers for selected blazars. A likely candidate for the source of such behavior is shock propagation down the jet (Rani et al. 2010).

### 4.2 Future Work

This blazar being in such a low state gave a rare opportunity to study microvariability characteristics under extreme low state conditions. 3C279 exhibited confirmed microvariability three out of five nights, contrary to many studies done on blazar activity suggesting microvariability is a high state only phenomenon (Carini 1990). This study suggests a change be made in the choosing of objects to observe. Instead of searching archives for blazars in outbursts, one should look for those in a low state in order to observe their structure. Scanning the PEGA archive for recent observations of blazars in low states would provide a starting place for the investigation of low state blazar variability. Confirmation that 3C279 is not an anomoly in its class is necessary before completely disregarding the theory that microvariability occurs more frequently in the bright state.

Adding polarization measurements would greatly increase the constraints placed on the physical origin of the observed processes. These observations coupled with V- or R-filter observations could definitively connect the microvariability observed with the jet. More simultaneous observations are necessary. A world-wide collaboration would provide 24 hour

monitoring for these extremely variable objects which would connect the dots, so to speak. By filling in the gaps between observations caused by daylight, we may be enlightened.

## References

Blandford, R. D. 1990, in Active Galactic Nuclei, ed. R. D. Blandford, H. Netzer, L. Woltjer, T. J.-L. Courvoisier, & M. Mayor, 161–275

Carini, M. T. 1990, PhD thesis, Georgia State Univ., Atlanta.

Eachus, L. J., & Liller, W. 1975, ApJ, 200, L61+

Howell, S. B., Warnock, III, A., & Mitchell, K. J. 1988, AJ, 95, 247

Larionov, V. M. et al. 2008, A&A, 492, 389

Marscher, A. P. 1996, in Astronomical Society of the Pacific Conference Series, Vol. 110, Blazar Continuum Variability, ed. H. R. Miller, J. R. Webb, & J. C. Noble, 248–+

McFarland, J. P. 2005, PhD thesis, Georgia State University, United States – Georgia

Miller, H. R. 2006, in Astronomical Society of the Pacific Conference Series, Vol. 350, Blazar Variability Workshop II: Entering the GLAST Era, ed. H. R. Miller, K. Marshall, J. R. Webb, & M. F. Aller, 33–+

Miller, H. R., Webb, J. R., & Noble, J. C., eds. 1996, Astronomical Society of the Pacific Conference Series, Vol. 110, Blazar continuum variability

Noble, J. C., & Miller, H. R. 1996, in Astronomical Society of the Pacific Conference Series, Vol. 110, Blazar Continuum Variability, ed. H. R. Miller, J. R. Webb, & J. C. Noble, 30–+

Peterson, B. M. 1997, An Introduction to Active Galactic Nuclei, ed. Goméz de Castro, A. I. & Franqueira, M.

Pica, A. J., Pollock, J. T., Smith, A. G., Leacock, R. J., Edwards, P. L., & Scott, R. L. 1980,

AJ, 85, 1442

Raiteri, C. M., Villata, M., Lanteri, L., Cavallone, M., & Sobrito, G. 1998, A&AS, 130, 495

Rani, B., Gupta, A. C., Joshi, U. C., Ganesh, S., & Wiita, P. J. 2010, ApJ, 719, L153

Schmidt, M. 1968, Mitteilungen der Astronomischen Gesellschaft Hamburg, 25, 13

Urry, C. 2004, in Astronomical Society of the Pacific Conference Series, Vol. 311, AGN Physics with the Sloan Digital Sky Survey, ed. G. T. Richards & P. B. Hall, 49–+

Urry, C. M. 1999a, Astroparticle Physics, 11, 159

Urry, C. M., & Padovani, P. 1995, PASP, 107, 803

Urry, M. 1999b, in Astronomical Society of the Pacific Conference Series, Vol. 159, BL Lac Phenomenon, ed. L. O. Takalo & A. Sillanpää, 3–+

Urry, M. 2003, in Astronomical Society of the Pacific Conference Series, Vol. 290, Active Galactic Nuclei: From Central Engine to Host Galaxy, ed. S. Collin, F. Combes, & I. Shlosman, 3–+

# APPENDICES

# – A –

## Comparison Stars for 3C279.

The finder chart for 3C279 and the comparison stars used for this thesis are presented here. The table lists the characteristics of the comparisons stars. The identifier is given in column 1; right ascension and declination in degrees are given in columns 2 and 3 respectively; and the B, V, and R magnitudes are listed in columns 4, 5, and 6. The blazar is located between the solid lines near the center of the image. Each comparison star in the field is labeled clearly.

Table A.1: Comparison Star Information

| **ID** | **RA (deg)** | **Dec (deg)** | **B Mag** | **V Mag** | **R Mag** |
|---|---|---|---|---|---|
| 1 | 194.043023 | -5.837164 | 13.02(0.03) | 12.42(0.03) | 12.05(0.02) |
| 2 | 194.118637 | -5.739323 | 13.73(0.04) | 12.99(0.04) | 12.56(0.03) |
| 3 | 194.110812 | -5.756223 | 15.49(0.03) | 14.87(0.03) | 14.53(0.02) |
| 4 | 193.991812 | -5.738287 | 16.53(0.05) | 15.66(0.03) | 15.13(0.02) |
| 5 | 194.060423 | -5.779839 | 16.79(0.04) | 15.98(0.04) | 15.47(0.02) |

Reference: Raiteri et al. (1998).

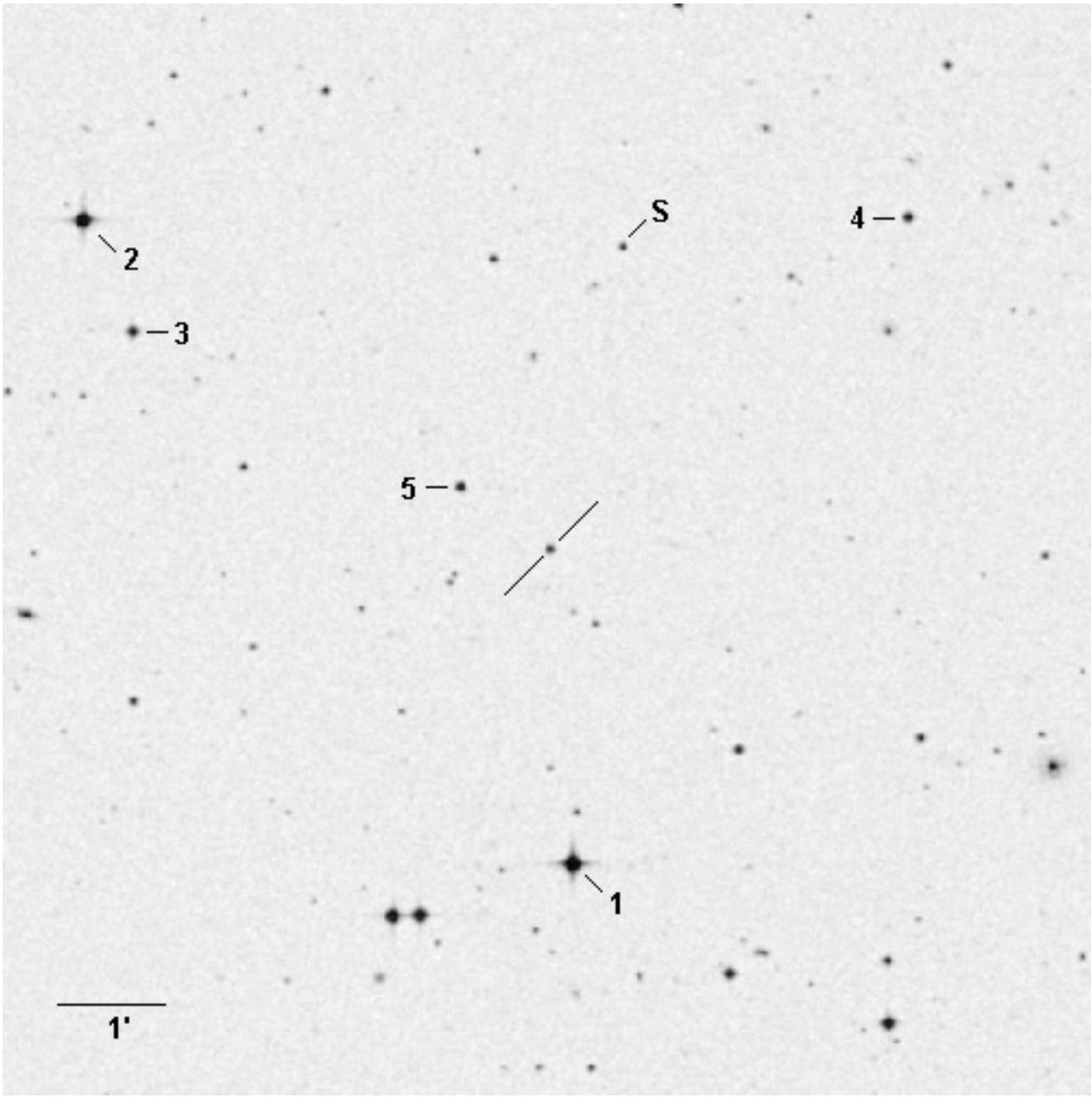


FIGURE A.1: Finding chart for 3C279 used for this thesis.

# – B –

## Light Curve for 14 April 2010.

The light curves for 14 April 2010 in V- and R-filter are shown here. Even though some variability over the $3\sigma$ level is present in the V-band, it is not reproduced in the R-band. Also the two spots where possible microvariability exists coincide with significant variation in the difference in comparison stars. Cross correlation analysis for the entire night and subsequent portions of the night are also presented and show very low cross correlation coefficients. Neither visual inspection nor cross correlation analysis could verify microvaribility for this night.

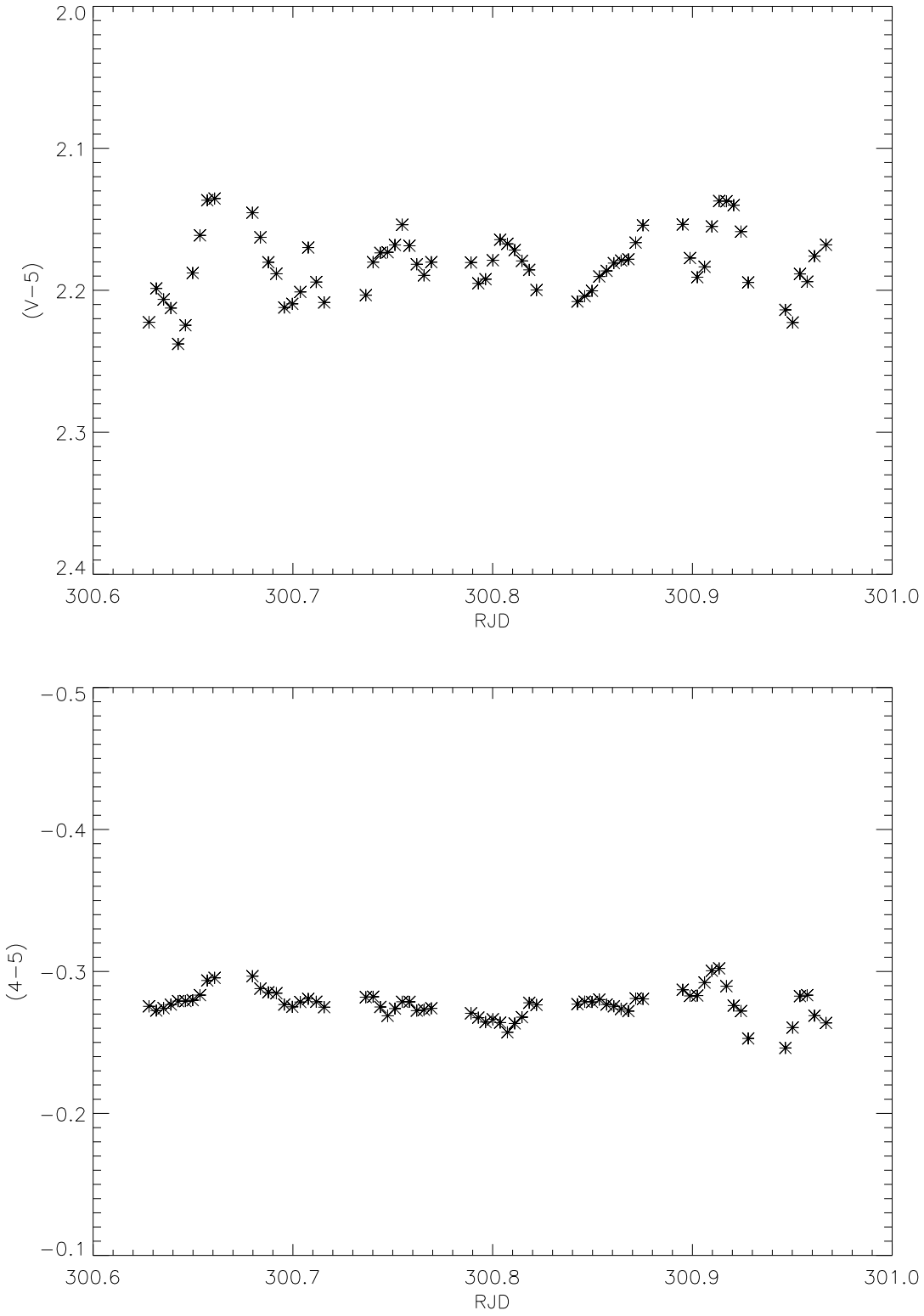


FIGURE B.1: Observations from 14 April 2010. *Top* Object light curve. *Bottom* Check 4-Check 5 light curve. Data taken with the Lowell 42" telescope.

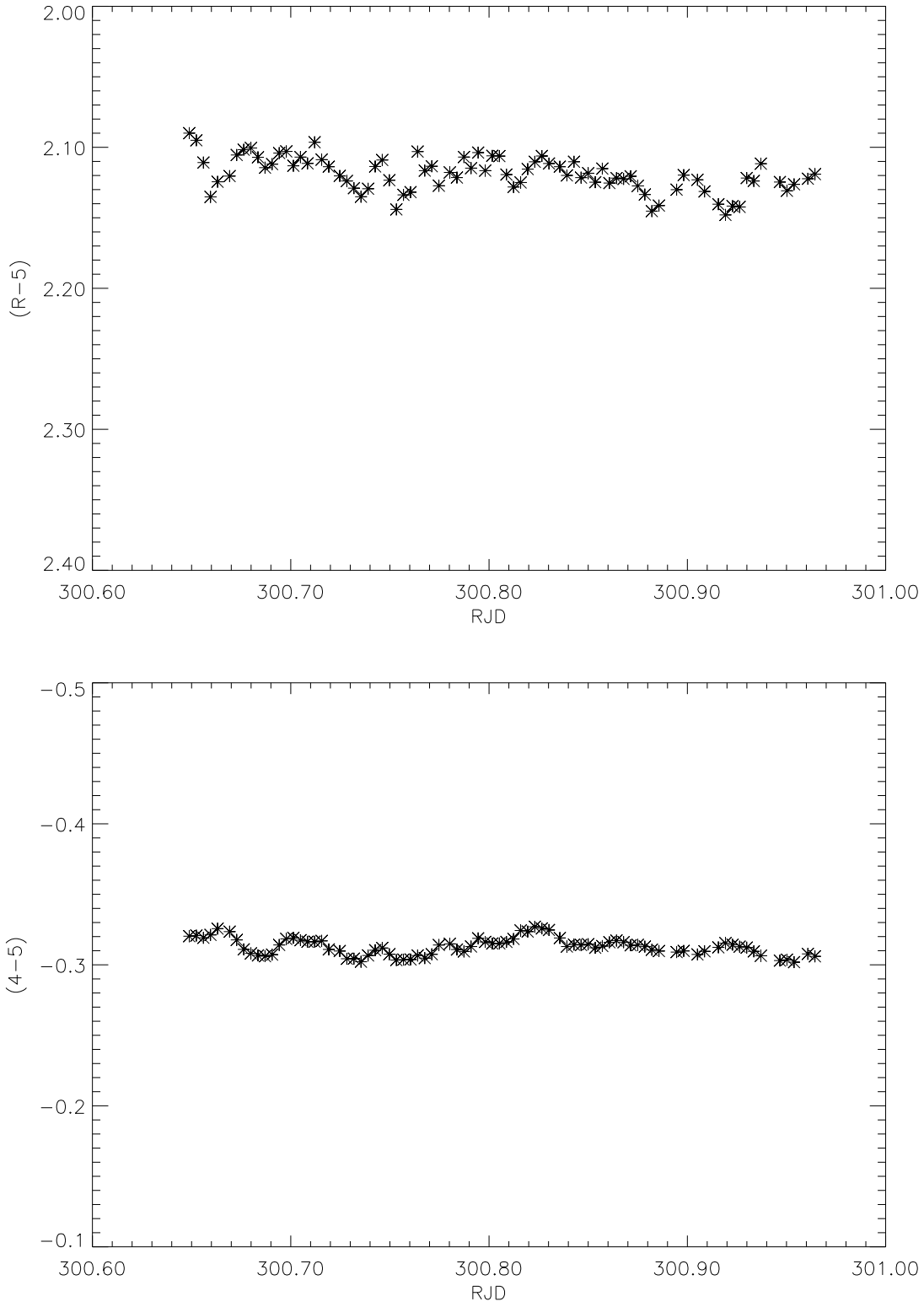


FIGURE B.2: Observations from 14 April 2010. *Top* Object light curve. *Bottom* Check 4-Check 5 light curve. Data taken with the Lowell 31" telescope.

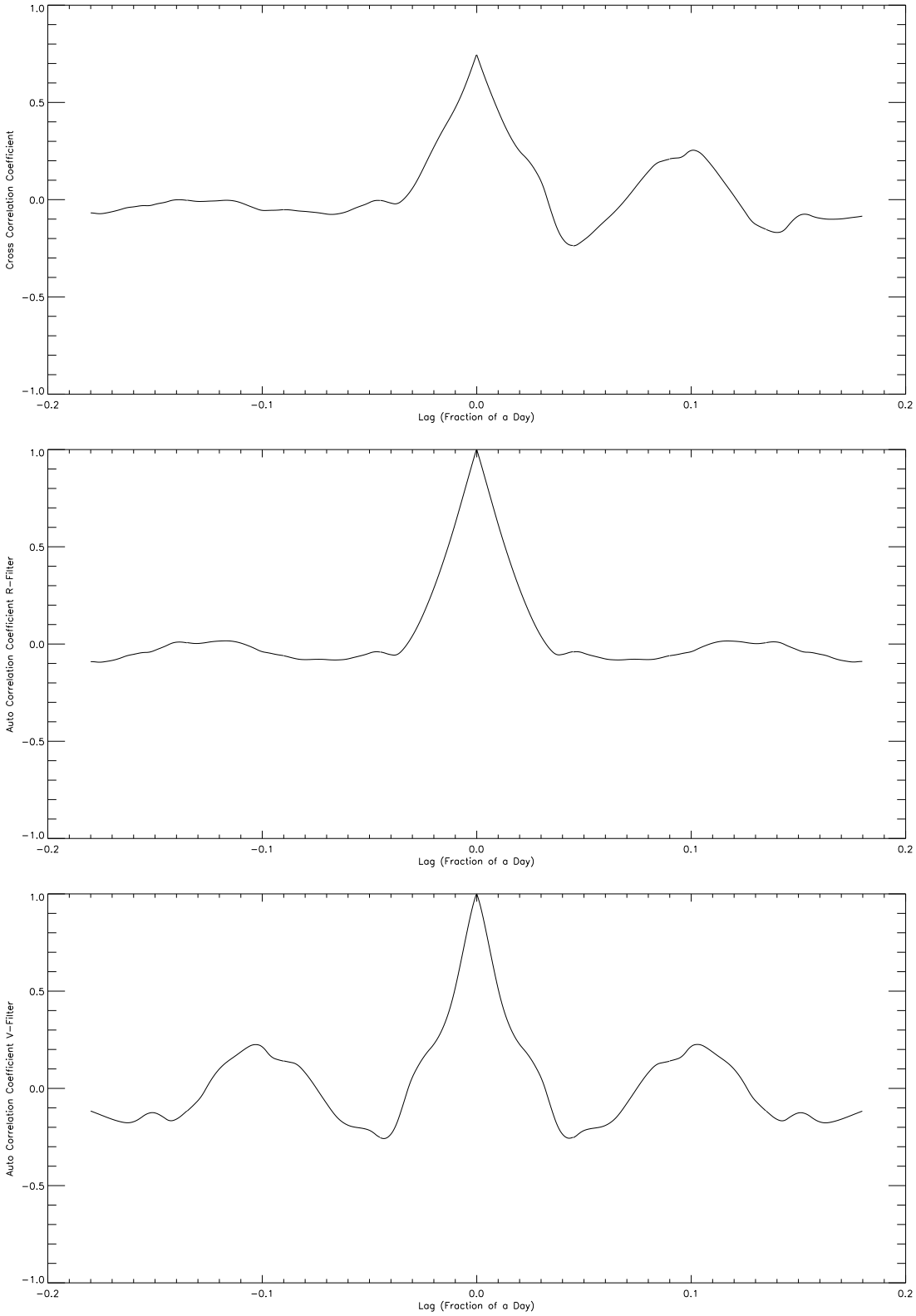


FIGURE B.3: *Top* Cross Correlation Function for 14 April 2010. *Center* Auto Correlation for R-Filter. *Bottom* Auto Correlation for V-Filter.

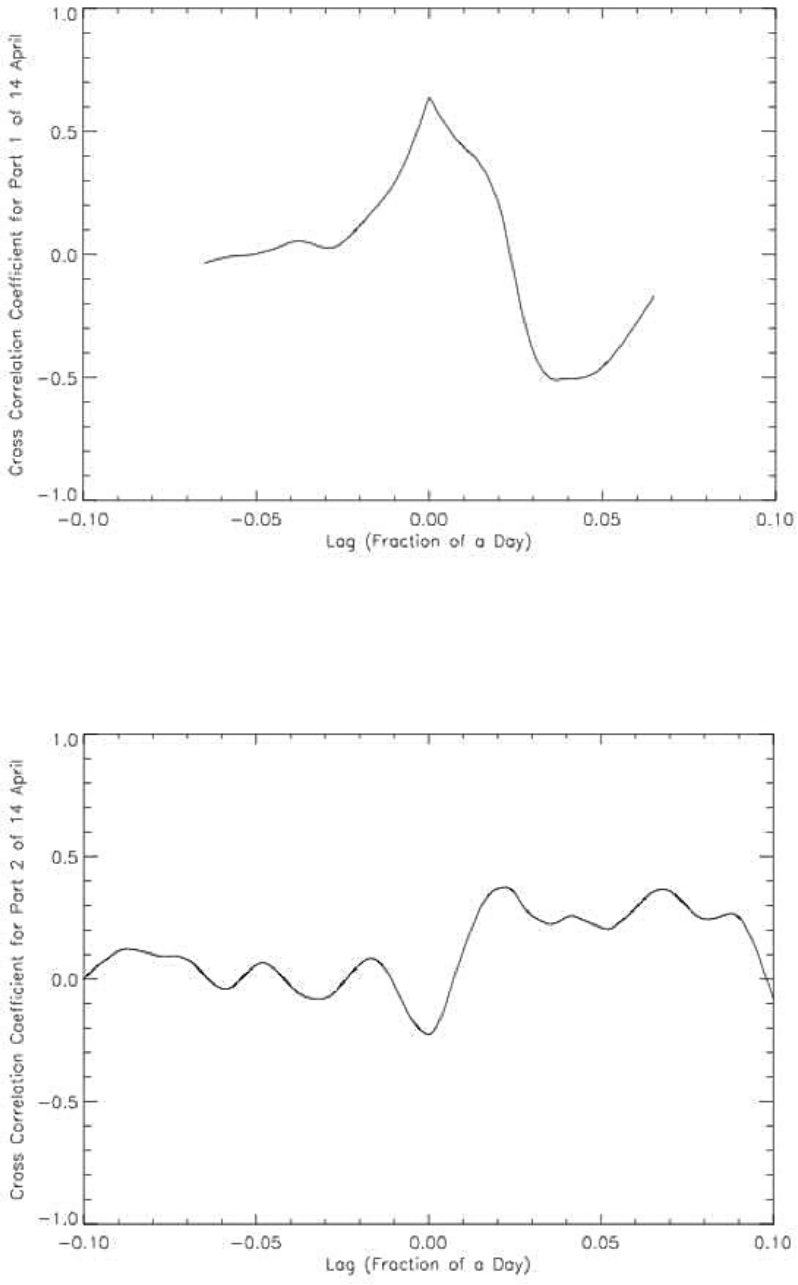


FIGURE B.4: *Top* Cross Correlation Function for First Part of 14 April 2010. *Bottom* Cross Correlation Function for Second Part of 14 April 2010.

# – C –

## Light Curve for 15 April 2010.

The light curves for 15 April 2010 in V- and R-filter are shown here. Even though some variability over the $3\sigma$ level is present in the V-band, it is not reproduced in the R-band. Also the events where possible microvariability exists coincide with significant variation in the difference in comparison stars. Cross correlation analysis for the entire night and subsequent portions of the night are also presented and show very low cross correlation coefficients. It would appear the second portion of the night has a non-negligible correlation coefficient, but upon closer inspection there are no events to correlate. The program is correlating noise in this case. Neither visual inspection nor cross correlation analysis could verify microvaribility for this night.

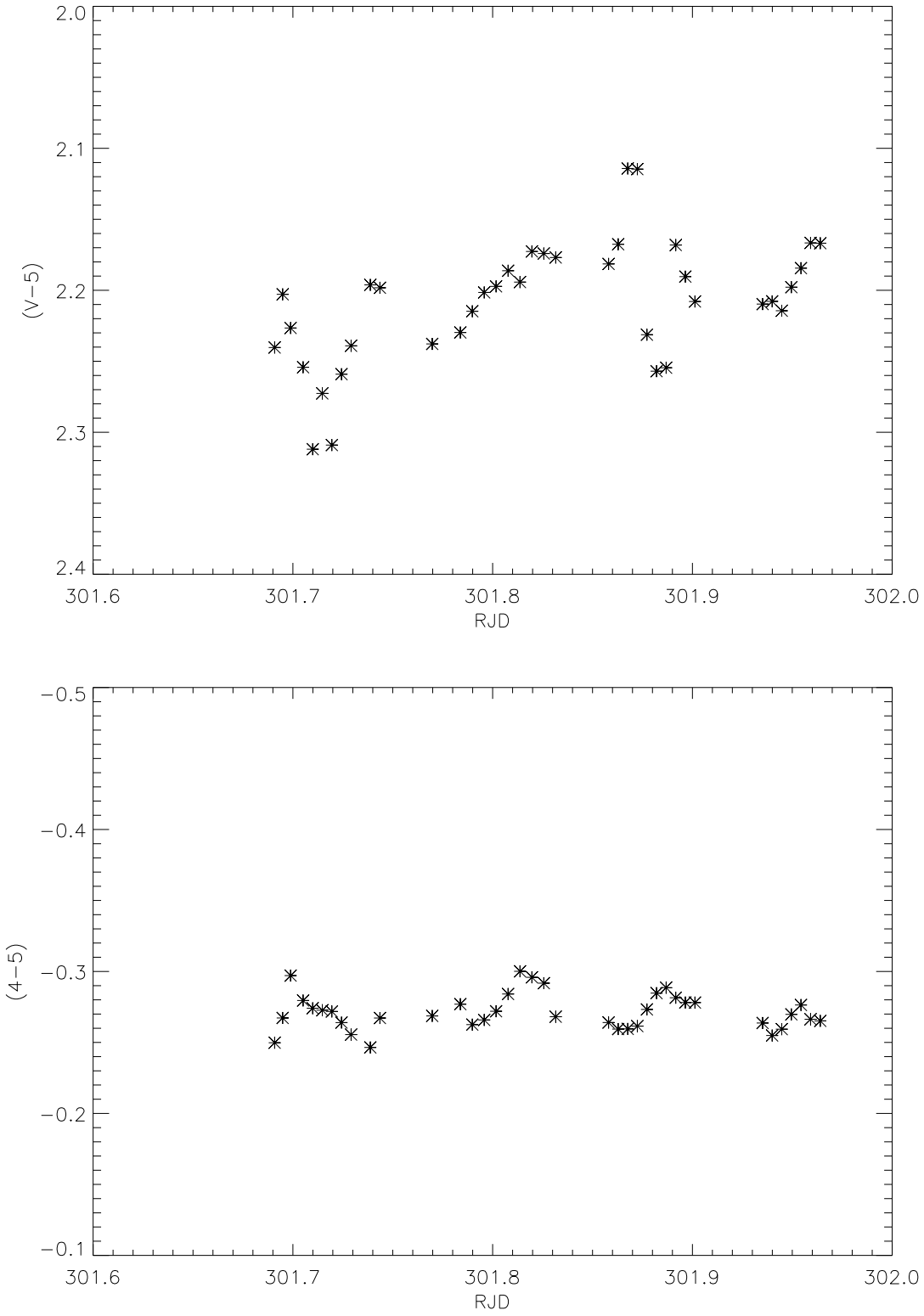


FIGURE C.1: Observations from 15 April 2010. *Top* Object light curve. *Bottom* Check 4-Check 5 light curve. Data taken with the Lowell 42" telescope.

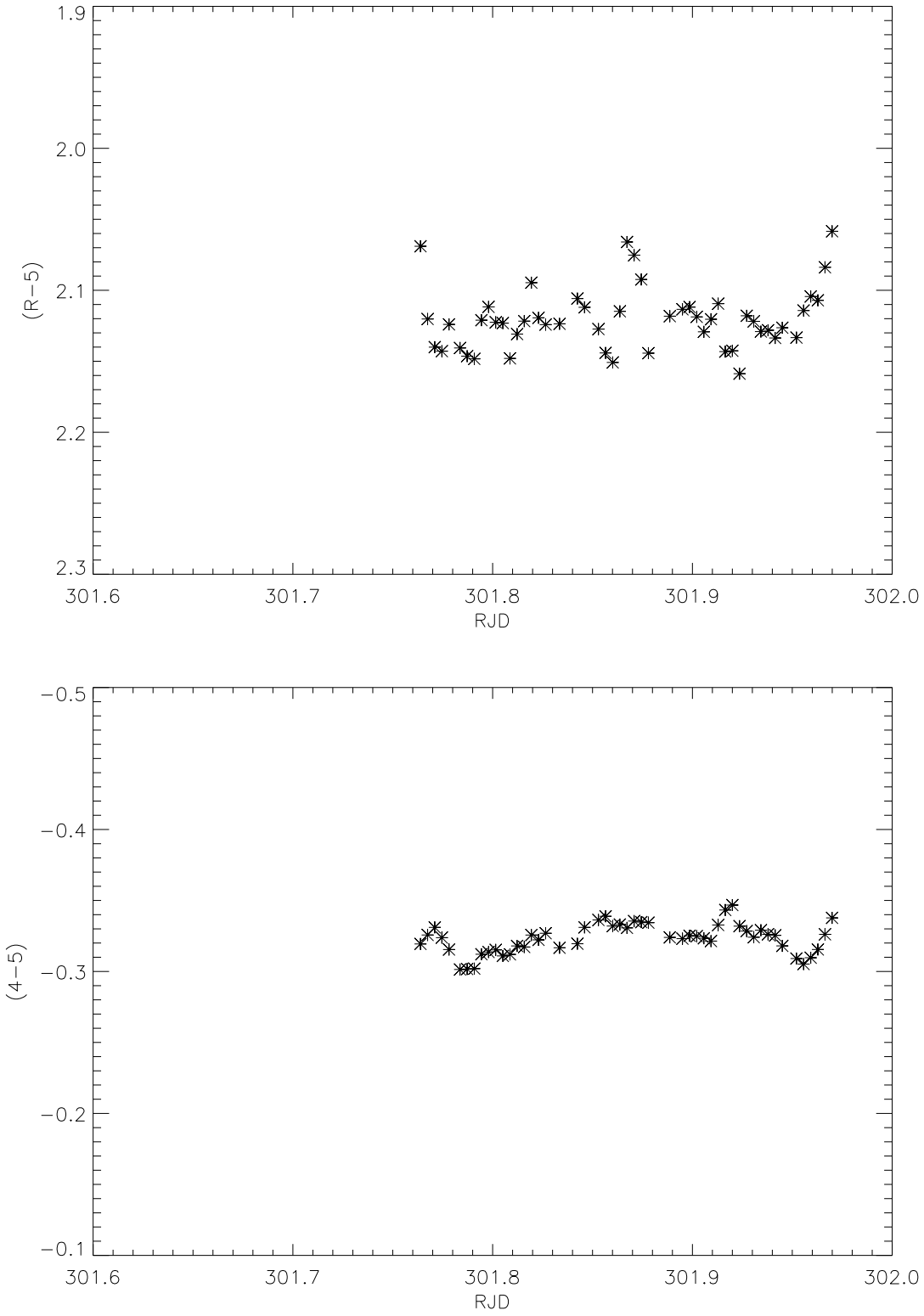


FIGURE C.2: Observations from 15 April 2010. *Top* Object light curve. *Bottom* Check 4-Check 5 light curve. Data taken with the Lowell 31" telescope.

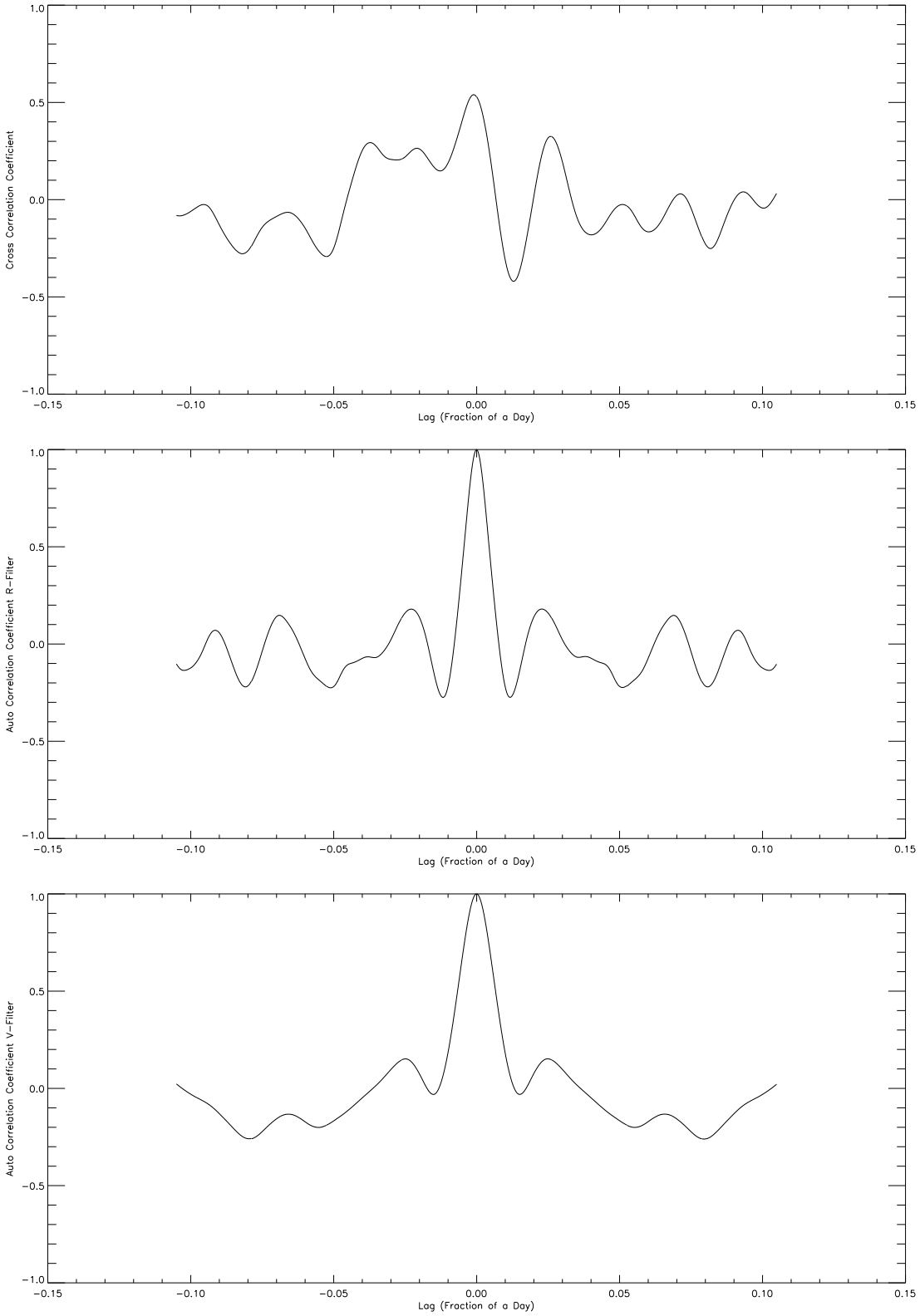


FIGURE C.3: *Top* Cross Correlation Function for 15 April 2010. *Center* Auto Correlation for R-Filter. *Bottom* Auto Correlation for V-Filter.

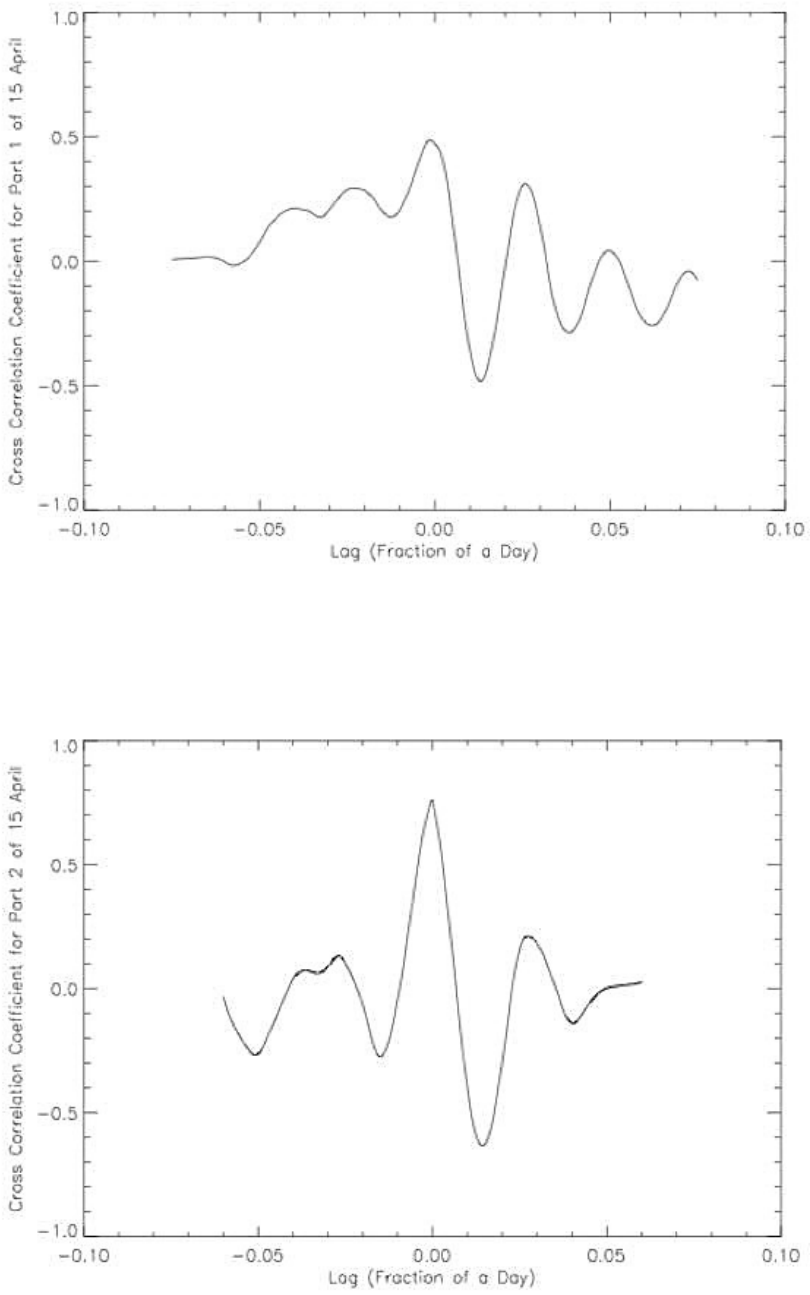


FIGURE C.4: *Top* Cross Correlation Function for First Part of 15 April 2010. *Bottom* Cross Correlation Function for Second Part of 15 April 2010.